



**Fakultät für Medizin**

**Institut für Molekulare Immunologie und Experimentelle Onkologie**

**Development of cytotoxic mRNAs as a new class of  
anti-cancer biotherapeutics**

**Kristin Hirschberger**

Vollständiger Abdruck der von der Fakultät für Medizin der Technischen Universität München  
zur Erlangung des akademischen Grades eines

**Doktor der Naturwissenschaften (Dr. rer. nat.)**

genehmigten Dissertation

**Vorsitzende:** Prof. Dr. Ulrike Protzer

**Prüfer der Dissertation:**

1. Prof. Dr. Percy A. Knolle

2. apl. Prof. Dr. Michael W. Pfaffl

Die Dissertation wurde am 01.02.2018 bei der Technischen Universität München eingereicht  
und durch die Fakultät für Medizin am 11.10.2018 angenommen.

## Table of contents

# Table of contents

Abbreviations .....	3
Figures .....	7
Tables .....	8
Summary .....	9
Zusammenfassung.....	11
<b>1 Introduction.....</b>	<b>13</b>
<b>1.1 mRNA in gene expression systems.....</b>	<b>13</b>
1.1.1 mRNA structure .....	13
1.1.2 Immunogenicity and stability of <i>in vitro</i> transcribed mRNA .....	14
1.1.3 mRNA transfection.....	15
1.1.4 Applications of mRNA in medicine .....	16
<b>1.2 Cancer treatment .....</b>	<b>16</b>
1.2.1 Conventional anti-cancer therapy and immunotoxins.....	16
1.2.2 DNA therapy in cancer treatment.....	17
1.2.3 Advantages of mRNA over DNA therapy.....	18
<b>1.3 Toxins.....</b>	<b>19</b>
1.3.1 Diphtheria Toxin.....	19
1.3.2 Subtilase cytotoxin .....	20
1.3.3 Abrin-a .....	21
<b>1.4 Apoptosis .....</b>	<b>23</b>
1.4.1 Initiation of apoptosis – Extrinsic and intrinsic pathway .....	23
1.4.2 Execution of apoptosis.....	24
1.4.3 Caspase-independent apoptosis .....	24
<b>1.5 The potential of microRNAs in therapy.....</b>	<b>24</b>
1.5.1 Approaches for tumor specificity .....	24
1.5.2 Concept of microRNAs .....	25
1.5.3 Applications of miRNAs and siRNAs in research and medicine .....	26
<b>1.6 Objectives .....</b>	<b>28</b>
<b>2 Material and Methods.....</b>	<b>29</b>
<b>2.1 Material .....</b>	<b>29</b>
2.1.1 Chemicals and Substances .....	29
2.1.2 Consumables.....	33
2.1.3 Equipment .....	34
2.1.4 Buffers and solutions .....	35

## Table of contents

<b>2.2 Methods</b> .....	35
2.2.1 Preparation of the buffers and solutions .....	35
2.2.2 Design of mRNA constructs.....	36
2.2.3 Cloning procedures and cmRNA production.....	37
2.2.4 Reticulocyte assay .....	40
2.2.5 Cell culture handling .....	40
2.2.6 Cell culture assays.....	41
2.2.7 miRNA expression analysis.....	48
2.2.8 Animal experiments.....	49
<b>2.3 Data analysis</b> .....	51
<b>3 Results</b> .....	52
<b>3.1 Cloning of toxin constructs and cmRNA production</b> .....	52
<b>3.2 HuH7 cells – A cell culture system for investigation of cell specific mRNA translation</b> .....	53
3.2.1 Transfection of HuH7 cells with toxin-encoding cmRNAs <i>in vitro</i> .....	53
3.2.2 HuH7 cells – Gaining cell specificity by exploiting miRNA expression profiles.....	69
<b>3.3 KB cells – Investigating <i>in vitro</i> and <i>in vivo</i> the effects of transfection with toxin-encoding cmRNAs</b> .....	71
3.3.1 Transfection of KB cells <i>in vitro</i> with toxin-encoding cmRNAs.....	71
3.3.2 Inhibition of KB tumor growth <i>in vivo</i> after transfection with AT cmRNA.....	81
<b>4 Discussion</b> .....	86
<b>4.1 Mechanisms of toxicity</b> .....	86
4.1.1 Nonfunctional and untranslatable control cmRNAs.....	86
4.1.2 Inhibition of protein synthesis .....	89
4.1.3 Cell death, influence on proliferation and on cell cycle.....	90
4.1.4 Apoptotic characteristics of induced cell death.....	91
4.1.5 Comparison of toxins .....	96
<b>4.2 Clinical application</b> .....	97
4.2.1 <i>In vivo</i> tumor experiments.....	97
4.2.2 Cell-specificity of cmRNA translation .....	99
4.2.3 Combination therapies and immunotherapy.....	100
<b>4.3 Conclusion and outlook</b> .....	102
<b>References</b> .....	103
<b>Supplements</b> .....	113
<b>Publication</b> .....	117
<b>Acknowledgements</b> .....	118

## Abbreviations

### Abbreviations

µg	Microgram
A	Alanine
AA	A-chain of arbin-a
ADP	Adenosine-5'-diphosphate
AF488	Alexa Fluor® 488
AIF	Apoptosis inducing factor
AN	Nonfunctional construct of AA
APAF-1	Apoptosis protease activating factor 1
Asp	Aspartic acid
Asp	Aspartic acid
AT	Toxin construct of AA
ATF6	Activating transcription factor 6
ATP	Adenosine-5'-triphosphate
AU	Untranslatable construct of AA
BCA	Bicinchoninic acid
Bcl-2	B-cell lymphoma 2
Bi-dist	Bi-distilled
BiP	Binding immunoglobulin protein, also GRP78
BL1	Blue laser 1
BL3	Blue laser 3
bp	Base pair
BSA	Bovine serum albumin
C	Luminescence of UT Cells at 46 h post transfection
CaCl <sub>2</sub>	Calcium chloride
CAD	Caspase activated DNase
CAS	Cellular Apoptosis Susceptibility
CD40	Cluster of differentiation 40
CD70	Cluster of differentiation 70
CD95	Cluster of differentiation 95
cDNA	complementary DNA
CHOP	C/EBP homologous protein
cmRNAs	Chemically modified mRNA
CO <sub>2</sub>	Carbon dioxide
Cq	Quantification cycle
CRM197	Cross reacting material 197
ctrl	Control
D	Aspartic acid
dATP	Deoxyadenosine-5'-triphosphate
DN	Nonfunctional construct of DT
DNA	Deoxyribonucleic acid
DT	Toxin construct of DTA
DTA	A-chain of diphtheria toxin
DU	Untranslatable construct of DTA
E	Glutamic acid
EDTA	Ethylenediaminetetraacetic acid
eEF-2	Eukaryotic elongation factor 2
Ef	Efficiency of amplification
EGF	Epidermal growth factor

## Abbreviations

EGFP	Enhanced green fluorescent protein
eIF	Eukaryotic translation initiation factors
ER	Endoplasmic reticulum
ERAD	ER-associated degradation
FADD	Fas-associated death domain-containing protein
FasR	Fas-receptor
FBS	Fetal bovine serum
FD	FastDigest
fig.	Figure
GADD	Growth Arrest and DNA Damage gene
GI	Growth inhibition
Glu	Glutamic acid
GRP78	78 kDa glucose-regulated protein
GTP	Guanosine-5'-triphosphate
h	hour
HCC	Hepatocellular carcinoma
HCl	Hydrochloric acid
HEPES	4-(2-hydroxyethyl)-1-piperazineethanesulfonic acid
His	Histidine
HRP	Horseradish peroxidase
Hsp70	70 kDa heat shock protein
HSV-TK	herpes simplex virus thymidine kinase
HUS	Hemolytic uremic syndrome
IC50	Half maximal inhibitory concentration
IL-6	Interleukin 6
IP-10	Interferon gamma-induced protein 10
IRE1 $\alpha$	Inositol-requiring enzyme 1
IVT	<i>In vitro</i> transcription
K	Lysine
kb	Kilo-base pair
kDa	Kilo dalton
l	Liter
L	Leucine
Leu	Leucine
lg	Common logarithm
LMP	Lysosomal Membrane Permeabilization
LPS	Lipopolysaccharide
luc	Firefly luciferase
Lys	Lysine
m <sup>7</sup> G	7-methylguanosine
MDR	Multidrug resistance
MFI	Mean fluorescence intensity
mg	Milligram
min	minutes
miRNA	microRNA
ml	Milliliter
mM	Millimolar
mm <sup>3</sup>	Cubic millimetre
mRNA	Messenger RNA
N	Nonfunctional control

## Abbreviations

n	Number of replicates
NaCl	Sodium chloride
NAD	Nicotinamide adenine dinucleotide
NCBI	National Center for Biotechnology Information
ng	Nanogram
NK cells	Natural killer cells
nt	Nucleotide
PABP	Poly(A)-binding protein
PBS	Phosphate buffered saline
PD-1	Programmed cell death protein 1
pDNA	Plasmid DNA
PERK	Protein kinase R (PKR)-like endoplasmic reticulum kinase
pg	Picogram
PI	Propidiumiodide
PKR	Protein kinase R
PS	Phosphatidylserine
Pseudouridine	5'-ribosyluracil
PVDF	Polyvinylidene fluoride
qPCR	Quantitative polymerase chain reaction
R	Arginine
Rcf	Relative centrifugal force
RE	Relative expression
RIG-I	Retinoic acid-inducible gene I
RIP	Ribosome inactivating protein
RISC	RNA induced silencing complex
RNA	Ribonucleic acid
RNAi	RNAinterference
ROS	Reactive oxygene species
rpm	Rounds per minute
rRNA	Ribosomal RNA
S	Svedberg
s	Second
SDS	Sodium dodecyl sulfate
SEM	Standard error of the mean
Ser	Serine
siRNA	Small interfering RNA
SN	Nonfunctional construct of SubA
ST	Toxin construct of SubA
STEC	Shiga toxigenic <i>Escherichia coli</i>
SU	Untranslatable construct of SubA
SubA	A-chain of subtilase cytotoxin
SubAB	Subtilase cytotoxin
T	Toxin
TAE	Tris base, acetic acid, EDTA
TGF $\beta$	Transforming growth factor $\beta$
Ti	Luminescence of sample at 48 h
TK/GCV	Herpes simplex virus-thymidine kinase/ganciclovir
TLR	Toll-like receptors
TNF	Tumor necrosis factor
TNFR	TNF-receptor

## Abbreviations

tRNA	Transfer RNA
Tz	Luminescence at 0 h
U	Untranslatable control
UPR	Unfolded protein response
UT	Untransfected control
UTR	Untranslated region

## Figures

### Figures

Figure 1: Structure of a mature eukaryotic mRNA .....	13
Figure 2: Circularization of mRNA during translation .....	14
Figure 3: Model of AB-toxin binding to and entry into the cell. ....	19
Figure 4: Induction of the unfolded protein response by the A-chain of subtilase cytotoxin (SubA).....	21
Figure 5: Translational silencing. ....	26
Figure 6: Agarose gel electrophoresis of SubA, DTA and AA toxin and control cmRNAs. ....	52
Figure 7: Inhibition of EGFP fluorescence in HuH7 cells by toxin-encoding cmRNAs.....	54
Figure 8: Inhibition of EGFP fluorescence in HuH7 cells – comparison of effectivity .....	56
Figure 9: Toxicity of toxin-encoding cmRNAs on HuH7 cells – dose-dependency.....	58
Figure 10: Toxicity of toxin-encoding cmRNAs on HuH7 cells – time-dependency .....	60
Figure 11: Inhibition of cell growth by toxin-encoding cmRNAs in HuH7 cells: Scratch Assay .	61
Figure 12: Cell cycle analysis of HuH7 cells after transfection with toxin-encoding cmRNAs...	63
Figure 13: Apoptotic characteristics of cell death induced by toxin-encoding cmRNAs on HuH7 cells.....	65
Figure 14: Bystander effect – Transfer of supernatants and lysates of HuH7 cells transfected with toxin-encoding cmRNAs.....	67
Figure 15: Bystander effect – Magnetofection of HuH7 cells with DT-encoding cmRNA .....	68
Figure 16: Exploiting miRNAs for cell-specific translation.....	70
Figure 17: Toxicity of toxin-encoding cmRNAs on KB cells – a comparison .....	73
Figure 18: Toxicity of AT cmRNA on KB cells.....	74
Figure 19: Detection of AA protein after transfection of KB cells with AT cmRNA by Western blot .....	75
Figure 20: Inhibition of protein synthesis by AT cmRNA.....	77
Figure 21: Apoptotic characteristics of cell death induced by AT cmRNA on KB cells.....	83
Figure 23: KB tumor histology after treatment with AT-LF132.....	85

## Tables

### Tables

Table 1: List of chemicals and substances and their providers.....	29
Table 2: List of consumables and their providers.....	33
Table 3: List of equipment and their providers.....	34
Table 4: List of utilized buffers and solutions. ....	35
Table 5: HuH7 cell culture assays. ....	42
Table 6: KB cell culture assays. ....	43
Table 7: Sum up of applied volumes per well. ....	43
Table 8: Primers utilized for miRNA expression analysis.....	49
Table 9: Process steps of the qPCR analysis.....	49
Table S 1: Toxin and control sequences ordered by GeneArt® .....	113
Table S 2: Sequence of the vector pVAX1-A120 .....	116

## Summary

### Summary

Transcript therapy implies the introduction of mRNAs encoding therapeutic proteins into cells. Interest herein has been vastly strengthening during the past decade as it provides several advantages over plasmid or viral gene therapy and over conventional protein therapy. In the field of anti-cancer therapy, new treatments to overcome the obstacles of conventional therapy are a permanent subject of investigation. The present study combined the benefits of transcript therapy with the principle of suicide cancer treatment by examining chemically modified mRNAs (cmRNAs) coding for the A-chains of two bacterial toxins (diphtheria toxin and subtilase cytotoxin) and of the plant toxin abrin-a.

The first part of the thesis analyzed the cytotoxicity of the three cmRNAs on the liver carcinoma cell line HuH7 *in vitro*. Inhibition of protein synthesis was established by EGFP co-expression experiments. Dose- and time-dependent reduction in cell viability and induction of cell death was demonstrated. The apoptotic characteristics of the induced cell death were investigated by determination of caspase-3/7 activity, phosphatidylserine exposure and DNA fragmentation. Potential follow-up studies include the protection of healthy liver and hematopoietic cells from toxin expression by virtue of differential microRNA expression patterns in healthy and tumor cells and inclusion of corresponding microRNA binding sites in the mRNA constructs. In respect thereof, qPCR experiments showed a suitable expression profile of three microRNAs in HuH7 cells and in three additional cell lines.

The subject of the second part of the thesis was to examine cytotoxicity of mRNA-encoded toxins on the cervix carcinoma cell line KB *in vitro* and *in vivo*. At the beginning, the three cmRNAs were compared regarding their potency to induce cytotoxicity and the best-performer abrin-a A-chain cmRNA was then investigated in detail. The successful expression of abrin-a protein after transfection of KB cells with abrin-a cmRNA was demonstrated by Western blot analysis. Experiments with firefly luciferase in reticulocyte lysates and co-transfection experiments with EGFP demonstrated the capability of abrin-a to inhibit protein synthesis. Its cytotoxic effect was quantified employing viability assays and propidium iodide staining. By studying caspase-3/7 activation, phosphatidylserine exposure and chromatin condensation with Hoechst33258 staining, apoptotic cell death could be confirmed. In mice, repeated intratumoral injections of complexed abrin-a cmRNA resulted in a significant reduction (89%) of KB tumor size compared to an untranslatable control cmRNA.

## Summary

In order to demonstrate that the observed toxicity is a toxin-generated and transfection unspecific effect, two control cmRNAs for each of the toxins were utilized. One control cmRNA was untranslatable while the other was designed to display none or diminished toxicity.

This is a first proof of concept study demonstrating the efficacy of “killer RNAs” as novel anti-tumor agents. Further studies with different tumor models will be highly valuable in determining the true potential of such mRNA-based therapeutics.

## Zusammenfassung

Der Ausdruck Transkripttherapie beschreibt das Einbringen von mRNAs, die für therapeutische Proteine kodieren, in Zellen. Das Interesse an dieser Methode nahm in den letzten Jahren stark zu, da sie vielfältige Vorteile gegenüber Plasmid- oder viraler Gentherapie sowie gegenüber konventioneller Proteintherapie birgt. Aufgrund der Schwierigkeiten konventioneller Therapien im Bereich der Krebsbehandlung ist die Entwicklung neuer Behandlungsmöglichkeiten ein permanentes Feld der Forschung. Ziel dieser Studie war die Verbundung der Vorteile der Transkripttherapie mit den Prinzipien der suizidalen Krebsbehandlung. Hierzu wurden chemisch modifizierte mRNAs (cmRNAs) untersucht, die für die A-Ketten zweier bakterieller Toxine (Diphtherietoxin und Subtilase Zytotoxin) und des Pflanztoxins Abrin-a kodieren.

Der erste Teil dieser Arbeit widmete sich der *in vitro*-Analyse der Zytotoxizität der drei cmRNAs gegenüber der Leberkrebszelllinie HuH7. Die Hemmung der Proteinsynthese wurde durch Ko-Expression von EGFP nachgewiesen. Weiterhin wurden die dosis- und zeitabhängige Reduzierung der Zellviabilität sowie der Eintritt des Zelltods aufgezeigt. Durch Bestimmung der Caspase-3/7 Aktivität, der Externalisierung von Phosphatidylserin und der Fragmentierung der DNA wurden die apoptotischen Eigenschaften des herbeigeführten Zelltods untersucht. Vielversprechende Folgestudien beinhalten den Schutz gesunder Leber- und hämopoetischer Zellen vor der Expression des Toxins mithilfe der Divergenz des microRNA Expressionsmuster gesunder Zellen gegenüber Tumorzellen sowie des Einbaus entsprechender microRNA Bindestellen in die mRNA Konstrukte. In dieser Hinsicht zeigten qPCR Experimente ein geeignetes Expressionsprofil dreier microRNAs in HuH7 Zellen sowie in drei weiteren Zelllinien.

Ziel des zweiten Teils dieser Arbeit war die Untersuchung der Zytotoxizität der mRNA-kodierten Toxine gegenüber der Gebärmutterhalskrebszelllinie KB *in vitro* und *in vivo*. Zunächst wurden die drei cmRNAs bezüglich ihres Vermögens Zytotoxizität hervorzurufen verglichen und im Anschluss das vielversprechenste Konstrukt, die cmRNA-kodierte A-Kette von Abrin-a, im Detail untersucht. Die erfolgreiche Expression des Proteins Abrin-a nach der Transfektion von KB Zellen mit Abrin-a cmRNA wurde mithilfe eines Western Blots nachgewiesen. Experimente mit „firefly luciferase“ in Retikulozytenlysate sowie Ko-Transfektionsexperimente mit EGFP zeigten das Potential der cmRNA Abrin-a die Proteinsynthese zu hemmen. Ihr zytotoxischer Effekt wurde mittels Viabilitätsassays und Propidiumiodid-Färbungen quantifiziert. Durch Analyse der Caspase-3/7 Aktivität, der Externalisierung von Phosphatidylserin und der Kondensierung des Chromatins mithilfe von Hoechst33258-Färbungen wurde der apoptotische

## Zusammenfassung

Charakter des verursachten Zelltods bestätigt. Wiederholte intratumorale Injektionen komplexierter Abrin-a cmRNA in Mäusen hatten eine signifikante Verminderung (89 %) der KB-Tumorgröße im Vergleich zu einer untranslatierbaren Kontroll-cmRNA zur Folge.

Um nachzuweisen, dass die beobachtete Toxizität ein vom Toxin erzeugter und Transfektions-unabhängiger Effekt ist, wurden zwei Kontroll-cmRNAs für jedes der Toxine verwendet. Eine der Kontroll-cmRNAs war nicht translatierbar während die andere keine oder nur geringfügige Toxizität aufwies.

Diese Studie zeigt erstmals die Effektivität von „Killer-RNAs“ als neuer Anti-Tumorwirkstoff. Weiterführende Studien mit zusätzlichen Tumormodellen sind von hoher Bedeutung um das ganze Potenzial mRNA-basierter Therapeutika zu erkunden.

## 1 Introduction

# 1 Introduction

## 1.1 mRNA in gene expression systems

### 1.1.1 mRNA structure

Messenger RNA (mRNA) is the link between DNA as storage of genetic information and proteins as executing component of countless biochemical functions. DNA sequences are transcribed into mRNA sequences in the nucleus which are further translated into proteins in the cytoplasm. Both procedures are tightly regulated. An mRNA molecule is composed of the 5' cap followed by the 5' UTR (untranslated region), the coding region, the 3' UTR and terminates in the poly(A) tail (fig. 1).



**Figure 1: Structure of a mature eukaryotic mRNA.** GCCACC represents the Kozak element [1]. AUG represents the start codon. UTR: untranslated region.

In order to engineer *in vitro* transcribed (IVT) mRNA sequences with maximum translation efficiency, each of the mRNA components has to be considered carefully. The 5' cap in eukaryotic mRNA is a 7-methylguanosine ( $m^7G$ ) that is linked via a 5'-5'-triphosphate bond to the subsequent nucleotide. A functional 5' cap is essential for translation of the mRNA as it mediates the binding of the eukaryotic translation initiation factors (eIFs) [2]. As decapping can be the first step of mRNA degradation [3], the 5' cap is also of importance in regard to mRNA stability. The *vaccinia* virus capping enzyme is one possibility to equip IVT mRNA with an eukaryotic cap structure [4]. The 5' UTR contributes to the translation efficiency via its length, secondary structures and, as does the 3' UTR, by presenting binding sites for regulatory elements [5]. By altering the untranslated regions of mRNA, enhanced production of IVT mRNA was achieved [6]. In most cases the coding region is preceded by the Kozak element [1], starts with the start codon AUG (fig. 1) and ends with one of the stop codons UAG, UAA or UGA. From start codon to stop codon, each codon represents one amino acid of the protein chain, whereby each amino acid is encoded by several codons. As the number of codons per amino acid varies between different organisms, nucleotide sequences coding for heterologous proteins have to be adjusted to the codon usage of the host for optimal protein production [7]. The poly(A) tail is a stretch of 100-250 A residues [8] that enhances mRNA stability and was also found to increase translation efficiency [9]. The optimal length was found to be between 120 and 150

## 1 Introduction

bases [8]. For initiation of eukaryotic translation, the mRNA molecule is circularized by association of a complex of eIFs which binds to the 5' cap and the poly(A)-binding protein (PABP) (fig. 2).

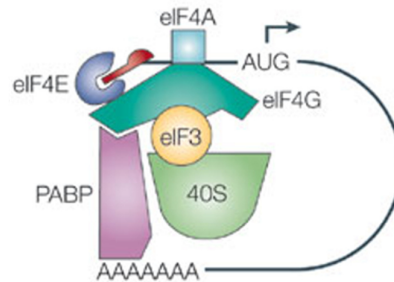


**Figure 2: Circularization of mRNA during translation.** It takes place by association of a complex of eIFs (eukaryotic translation initiation factors) which binds to the 5' cap and the poly(A) binding protein (PABP). AUG: mRNA start codon. 40 S: small ribosomal subunit. Figure was taken from [10].

The small ribosomal subunit (40 S) is attached to this complex and scans the mRNA molecule in 3' direction until it recognizes the start codon (AUG). At this point, the large ribosomal subunit (60 S) is recruited and translation commences [2]. The Kozak element enhances recognition of the start codon by the small ribosomal subunit [1]. An important role during translation elongation plays the eukaryotic elongation factor 2 (eEF-2). As a member of the G-protein super family it is a GTPase that undergoes conformational changes following GTP hydrolysis, resulting in translocation of the tRNA (transfer RNA) molecules [11]. tRNAs are responsible for elongating the polypeptide chain by conveying amino acids to the corresponding mRNA codon. While the amino acid chain is released at the stop codon, circularity of the mRNA molecule (see fig. 2) enables the ribosomal complex to start anew at the cap [12].

### 1.1.2 Immunogenicity and stability of *in vitro* transcribed mRNA

The presumably low stability and high immunogenicity of mRNA prevented its broad application in therapy until the last decade. Since Wolff *et al.* showed the first successful mRNA transfection *in vivo* in 1990 [13], research has identified ways to evade these problems. The immune system recognizes foreign RNA molecules through, among others, Toll-like receptors (TLRs) [14], the protein kinase PKR [15] and by the retinoic acid-inducible gene I (RIG-I) [16]. It was observed in preclinical studies that frequently upregulated cytokines in response to IVT mRNA were interferon- $\alpha$ , IL-6, tumor necrosis factor- $\alpha$  and IP-10 [9]. In contrast to bacterial mRNA, *in vivo* transcribed eukaryotic RNAs contain modified nucleotides, e. g. as 5-methylcytosine or as N6-methyladenosine nucleosides [17]. In consequence, incorporation of modified nucleotides

## 1 Introduction

like pseudouridine (5-ribosyluracil) into IVT mRNA sequences results in a relevant decrease in immunogenicity, as was discovered in 2005 [18] and could be shown by different groups [19-21]. Though pseudouridine was studied extensively, other modified nucleotides like 5-methylcytosine and 2-thiouridine were also applied successfully [20, 22]. Stability of the transfected mRNA molecules is decisive for the period of time in which the encoded protein is produced [9]. Likewise important to the stability and translation efficiency of mRNA molecules are the 5'-cap [23] and the poly(A) tail at the 3' end [24] (refer to section 1.1.1).

### 1.1.3 mRNA transfection

For the transfection of mammalian cells with mRNA similar strategies are applied as for pDNA. Depending on cell type and application procedure, the employment of naked mRNA has shown some, though limited, success regarding cell transfections [25]. Three different approaches can be discerned to facilitate the entry of nucleic acids into cells: biological, physical and chemical. Biological transfection employs viruses to transport the desired nucleic acid into the cell (transduction) and is therefore mainly applicable for DNA and was only rarely used for mRNA transfections [26].

Physical methods, most importantly electroporation and gene gun delivery, work by disrupting the cell membrane to enable cellular entry of the nucleic acids. Electroporation is widely used to transform bacteria with foreign DNA sequences. Penetrability of the cell membrane is achieved by inducing electrical conductivity which causes the formation of pores in cell membranes. *In vivo* electroporation of pDNA into several tissues was performed successfully as were clinical trials applying electroporation for treatment of dendritic cells with mRNA [27]. Gene gun delivery employs heavy metal particles coated with nucleic acids that are accelerated to high velocity in order to break through the cell membrane. This technique proved to serve its function on various tissues and cell types *in vivo* and *in vitro*. Both introduced procedures, however, are laborious and difficult to employ for tissues that are hard to access [27]. Hence, the most frequently used method for mRNA delivery nowadays is chemical transfection utilizing either cationic polymers or, most often, cationic lipids. They display, among others, the advantages of relatively low cytotoxicity, easy systemic administration, simple handling and protection of the nucleic acids from degradation by extracellular RNases. The positively charged chemicals bind to the negatively charged nucleic acids, resulting in a positively charged complex that binds to negatively charged cell membranes and enables cellular entry by endocytosis [27,

## 1 Introduction

28]. A somewhat distinctive strategy called magnetofection implies the formulation of nucleic acids in magnetic nanoparticles, lipid or polymeric, combined with the employment of a magnetic field. In consequence, transfection efficiency could be increased, delivery kinetics improved and transfection confined to the area under the magnetic field [29].

Apart from the magnetofection experiments, cationic lipids, commercially available for *in vitro* and proprietary for *in vivo* experiments, were used for all cell transfections in this thesis.

### 1.1.4 Applications of mRNA in medicine

In the last decade a broad spectrum of possibilities to utilize mRNA in medicine was investigated. Sahin *et al.* compiled a list of potential applications for *in vitro* transcribed mRNA, including: 1) cancer immune therapy, 2) vaccination of infectious diseases, 3) allergy tolerization, 4) protein replacement and supplementation therapies, 5) genome engineering and 6) genetic reprogramming [9]. For instance, systemic anti-tumor immunity was achieved by administering a mixture of three mRNAs which activated tumor-infiltrating dendritic cells [30]. Reprogramming of human cells to pluripotency as well as subsequent differentiation could also be accomplished employing chemically modified mRNA [22].

## 1.2 Cancer treatment

### 1.2.1 Conventional anti-cancer therapy and immunotoxins

Conventional anti-cancer therapy includes chemotherapy, radiation and surgery. All three treatments exhibit special benefits and are often combined to obtain the most effective therapy. However, they are often limited by chemoresistance [31], radiation resistance [32] and severe side effects like cardiotoxicity [33] or neurocognitive deficits [34]. Mechanisms of resistance include, among others, alterations in the degree of drug target expression, enhanced drug efflux, increase in pro-survival signals, mutations in the drug target, augmented DNA repair mechanisms and inhibition of cell death [35]. Therefore, the need for complementary or alternative cancer therapeutic options is immense. One further established approach is the employment of monoclonal antibodies directed against antigens specifically present on tumor cells. Suitable, for instance, are antigens involved in growth and differentiation signaling, like ERBB2, or involved in haematopoietic differentiation, like CD20 which is therapeutically targeted in several lymphomas [36]. Antibodies are also implemented in immunotoxins, anti-

## 1 Introduction

cancer therapeutics which are being tested in clinical studies [37], with first drugs gaining FDA approval [38]. Immunotoxins, also called tumor-targeted toxins, are cell specific ligands linked either to plant or to bacterial toxins, leading to a selective killing of target cells [39, 40]. As ligands antibodies or growth factors, whose counterparts show overexpression on the target cell, are applied. The advantage of this approach, compared to other tumor treatments, is high specificity to the tumor and hence less damage of healthy tissue. A further benefit is their applicability to both solid and non-solid tumors as well as metastases [41]. Still, despite their cell specific toxicity *in vitro*, in some cases damage to healthy tissue, particularly to the liver, was observed [42, 43]. Another disadvantage of immunotoxins is the comparatively slow protein uptake from blood vessels by tumors due to their abnormal tissue architecture [43].

### 1.2.2 DNA therapy in cancer treatment

An alternative that might avoid the deficiencies but shares many of the benefits of immunotoxins is the employment of nucleic acids coding for toxic proteins as suicide cancer therapy. In contrast to many chemotherapeutic drugs, plant and bacterial toxin-based therapeutics do not target the cell cycle and are therefore applicable to fast as well as slow growing tumors. Hochberg and co-workers demonstrated the potential of this approach by applying a plasmid coding for diphtheria toxin [44, 45]. Expression of diphtheria toxin was under control of the H19 promoter which is highly active in a range of human cancers, ensuring that toxin production is confined to the tumor. Clinical trials (Phase 2b) treating bladder cancer with this plasmid-based approach were conducted successfully [44]. New tumor growth was hindered in two thirds of patients and only mild adverse effects were observed. Other groups started to implement and investigate suicide gene therapy. Qu *et al.* tested the well-characterized herpes simplex virus-thymidine kinase/ganciclovir (TK/GCV) suicide gene therapy system under control of the survivin promoter [46]. Survivin belongs to the family of inhibitors of apoptosis and is expressed solely and to a high degree in tumors [47]. In cells expressing the herpes simplex virus thymidine kinase, the guanosine analog ganciclovir is phosphorylated. Following, it can be incorporated into DNA and thereby blocks DNA polymerization, leading to cell death. Aiming to increase the efficacy of suicide gene therapy, Boulaiz and co-workers combined two suicide genes, namely *gef* and *apoptin* [48]. Employing a retrovirus-mediated gene expression system, co-expression increased the degree of apoptosis and necrosis in colon cancer cells in comparison to single expression.

## 1 Introduction

Gene therapy in general shows several advantages over the employment of protein therapeutics. Those include, but are not limited to, less cost-extensive production, reduced immune response, larger treatment intervals and diminished development of drug resistance in tumor cells [49]. Nevertheless, DNA-based gene therapeutics bear some risks and disadvantages, with potential genomic integration followed by mutation being one of the most important safety concerns [50].

### 1.2.3 Advantages of mRNA over DNA therapy

The employment of mRNA instead of DNA is an attractive approach to circumvent several deficiencies of plasmid-based transfection while preserving its aforementioned benefits. First of all, mRNA bears no risk of insertional mutagenesis as it cannot, contrary to pDNA [51], integrate into the genome [9]. Moreover, translation of mRNA is self-limited due to its short half-life and its inability to replicate [9, 52]. Adversely, this implies that for lasting protein production repeated administrations are required. As another advantage, only the sequence of interest is introduced into the cell in case of mRNA transfections. In contrast, viral proteins or further plasmid-encoded proteins are likewise transferred into the cell [53]. The hitherto named benefits all contribute to the elevated security of mRNA compared to pDNA transfections. Moreover, pDNA needs to enter the nucleus for successful transfections whereas this is no prerequisite for mRNA. Consequently, transfection efficiencies are higher in case of mRNA transfections [54]. This circumstance as well as the evasion of transcription explain the markedly earlier onset of protein expression that was observed after transfection with mRNA in contrast to pDNA [53]. Using the TK/GCV system (see section 1.2.2), Wang *et al.* compared mRNA with pDNA for efficacy as anti-cancer therapeutic agent [55]. In case of mRNA transfections the percentage of transfected cells was many times higher than for pDNA. Cells transfected with pDNA, however, demonstrated a considerably elevated expression compared to mRNA transfected cells. As the reduction in tumor growth was significantly greater for mRNA than for pDNA, the authors concluded that the number of transfected cells is more crucial than the degree of expression. Summarizing, transfections with mRNA are safer, more efficient and result in prompter but less persistent protein synthesis compared to pDNA transfections.

## 1 Introduction

### 1.3 Toxins

Hochberg *et al.* [44, 45] as well as various studies applying immunotoxins focused their investigations on Diphtheria Toxin [41], a toxin belonging to the family of AB-toxins [56]. AB-toxins distinguish themselves by comprising a B-subunit which specifically binds to target cells and enables cellular entry of the catalytic A-subunit [57]. Once inside the cell, the A-subunit mediates the toxic effects, e.g. via impairment of protein synthesis, resulting in cell death [58-60]. Other targets of AB-toxins comprise actin, heterotrimeric G-proteins or small GTP-binding proteins [61]. Figure 3 shows a model of AB-toxin binding to and entry into the cell.

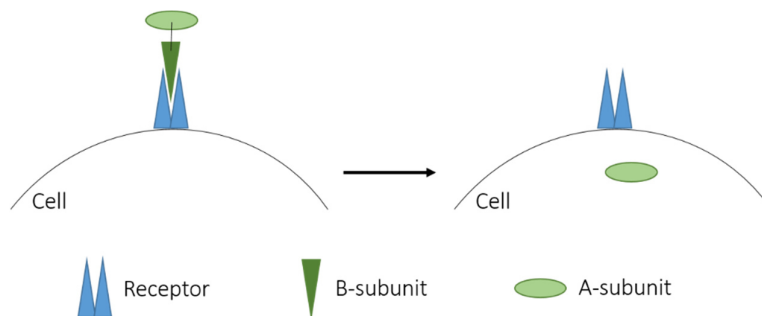


**Figure 3: Model of AB-toxin binding to and entry into the cell.** A- and B-subunit constitute the two parts of the AB-toxin.

This study focused on three AB-toxins that were previously examined as immunotoxins [41, 62-64] and represent different signaling pathways of protein synthesis inhibition [65]. All of them have shown promising anti-tumor effects in pre-clinical or clinical studies [62, 64, 66].

#### 1.3.1 Diphtheria Toxin

One of the investigated toxins is the well-characterized diphtheria toxin which is originally produced by *Corynebacterium diphtheria* [56]. The vast knowledge about diphtheria toxin and its mode of action is a consequence of its early detection in 1888 [67]. As its first toxoid for immunization was already developed around 1921 and was widely used in the early 1930s, the disease is rare in industrialized countries [68]. Moreover, it was for diphtheria toxin that the motif of an AB-toxin was established for the first time [69], when the necessity of protein cleavage for its enzymatic activity was discovered [70, 71]. Because it has been studied intensively, diphtheria toxin is considered a model system for bacterial toxins [72].

The toxin is produced as a single polypeptide chain and cleaved by proteases of the furin family inside the target cell, leaving A- and B-subunit connected via a disulfide bridge [73]. After attachment of the B-subunit (37 kDa) [56] to the cell membrane by binding to the heparin

## 1 Introduction

binding EGF-like growth factor precursor, the whole toxin is engulfed by endocytosis [74]. A change to acidic conditions in the early endosome results in unfolding of the transmembrane domain (a part of the B-subunit) [75], upon which it forms a pore in the vesicle membrane [76, 77]. Translocation of the A-subunit (21 kDa) [56] across the membrane into the cytosol is followed by cleavage of the connecting disulfide bond and refolding of the catalytic subunit into its active form [72, 78]. Subsequently, it transfers an ADP-ribosyl from NAD<sup>+</sup> to the eukaryotic elongation factor 2 (eEF-2), thereby blocking protein synthesis [79, 80] which eventually leads to cell death [58]. The inhibited eEF-2 is an essential part of the eukaryotic protein synthesis machinery as it promotes the translocation of the ribosome. The amino acid of eEF-2 that is ribosylated by diphtheria toxin is a post-translationally modified histidine called diphthamide which has not yet been discovered in another protein and is conserved in eEF-2 in all eukaryotes [81, 82]. Death after infection with *Corynebacterium diphtheria* generally results from heart failure, secondary pneumonia or respiratory failure and ensues in 5-10 % of incidents [68].

### 1.3.2 Subtilase cytotoxin

The second investigated toxin belongs to the sub-family of AB<sub>5</sub>-toxins whose members comprise a pentameric B-part [83]. Subtilase cytotoxin (SubAB) is produced by Shiga toxigenic *Escherichia coli* (STEC) and was first discovered in 1998 during an outbreak of HUS (hemolytic uremic syndrome) [83]. HUS involves hemolytic anemia, thrombocytopenia and renal failure and is preceded by diarrhea [84]. Amaral et al. found that SubAB causes HUS by damaging human glomerular endothelial cells [85]. The A-chain of SubAB, in combination with the epidermal growth factor (EGF), was shown to significantly inhibit tumor growth in mouse studies [62].

In distinction from other AB-toxins, AB<sub>5</sub>-toxins are transported into the endoplasmic reticulum (ER) via the golgi complex after initiating endocytosis [86]. However, SubAB is the only AB<sub>5</sub>-toxin whose substrate is ER-located [87]. The A-subunit of AB<sub>5</sub>-toxins can be cleaved into two parts that are connected via a disulfide bond [88]. One A-fragment poses the catalytic domain while the second mediates contact to the five units of the B-part by hydrophobic interactions [88]. The catalytic subunit of SubAB contains the catalytic triad (Asp, His, Ser) characteristic for members of the family of subtilase proteases [83]. By specifically cleaving its single substrate GRP78 (glucose-regulated protein 78), the A-chain of SubAB initiates the unfolded protein response (UPR), leading to reduced overall protein expression rates and apoptosis [59]. GRP78,

## 1 Introduction

also called BiP, is a member of the hsp70 chaperone family [89]. Cleavage of GRP78 causes its dissociation from three important UPR signaling proteins (IRE1 $\alpha$ , PERK and ATF6), thereby activating their respective signaling pathways [90]. The UPR uses three means to reduce ER stress and enable cell survival: Upregulation of ER chaperones, ER-associated degradation (ERAD) of proteins and decrease in translation in order to reduce the number of proteins requiring folding [90-93]. In case of sustained ER stress signaling, these pro-survival signals are attenuated and cell death is initiated. Cell death ensues, for example, by upregulation of the expression of transcription factor CHOP (C/EBP homologous protein) leading to apoptosis [90, 94]. The principle of UPR induction by the A-chain of SubAB is depicted in figure 4.

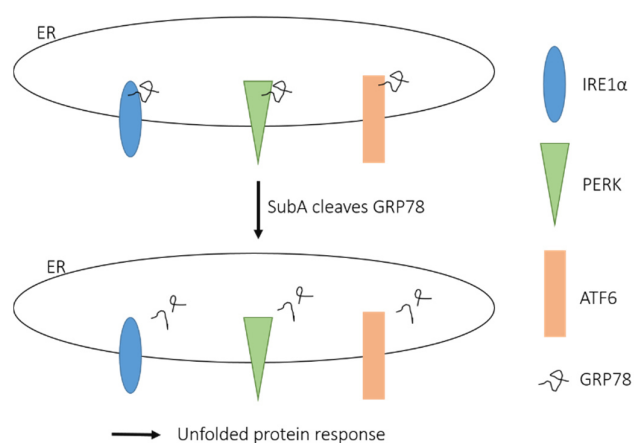


**Figure 4: Induction of the unfolded protein response by the A-chain of subtilase cytotoxin (SubA).**

The induction of the UPR caused by subtilase cytotoxin increases its importance for anti-cancer therapy. For one, Backer *et al.* demonstrated that it can be applied in combination with ER stress inducing drugs to augment their respective toxicities [62]. Moreover, its target GRP78 was found to be upregulated in many tumors as a way to counterbalance ER stress caused by their increased growth rate. In this context, inhibition of GRP78 by subtilase cytotoxin presents an attractive approach for tumor treatment [95]. In addition, SubAB might also be suitable as anti-inflammatory agent as it was observed to prevent LPS-induced inflammation in mice under sub-toxic conditions due to the induction of the UPR [96].

### 1.3.3 Abrin-a

Moreover, the plant toxin abrin-a, a highly potent member of the family of type II ribosome inactivating proteins (RIPs II) [60, 97], was examined. It can be isolated from *Abrus precatorius* which originates from Southeast Asia but is now present throughout various subtropical regions

## 1 Introduction

[98]. Being characterized already in 1887, abrin was the first example of a toxic protein [98]. It has also played a central role in the investigation of immunity by Paul Ehrlich at the end of the 19<sup>th</sup> century [99]. Despite its early importance, the investigation of abrin and other plant toxins, e. g. its close relative ricin [60], was abandoned for a long time as bacterial toxins presented a more pressing field of investigation due to their pathogenicity [98]. Ricin, however, has elicited some interest as a chemical weapon [98]. Though concentration of the toxin is especially high in the seeds of the plant, they are in general not lethal to humans on oral absorption due to their hard shell. In cases where the seeds were brittle, chewed, crushed or pierced for jewelry, however, severe toxicity has been observed [100]. Death ensues as a result of toxin-induced damage to endothelial cells which leads to vascular leak syndrome [101]. The first report regarding the potential of abrin in cancer treatment was made in 1969 when sarcoma growth could be inhibited by protein extracts from *Abrus precatorius* [102].

Type II RIPs are RNA-*N*-glycosidases that inactivate the ribosome by cleaving an adenine residue from the 28 S rRNA, thereby preventing an essential stem-loop configuration and thus blocking binding of the eEF-2 (eukaryotic elongation factor-2) to the ribosome [103, 104]. Complete inhibition of protein synthesis ensues, as binding of the eEF-2 to the ribosome is necessary for the translocation step during translation [104]. While RIP type I molecules possess only the catalytic subunit, type II RIPs are AB-toxins with the A-chain displaying RNA-*N*-glycosidase activity [98]. As the B-chain is a lectin targeting all terminal galactoses, binding of abrin to cell surfaces occurs rather nonspecifically [105]. As cleavage of the polypeptide takes place already inside the plant, the two subunits of the 63 kDa glycoprotein are connected only via a disulfide bridge [78, 97]. Cell-bound abrin is endocytosed and, while the main part is either transported back to the cell surface or to lysosomes for degradation, about 5 % reaches the cytosol after trafficking via the retrograde pathway [98]. Translocation from the endoplasmic reticulum to the cytosol involves the Sec61 complex [106]. In case of abrin exposure, apoptosis does mainly occur as consequence of reduced protein synthesis [107] but is also induced directly. For example, damage to the mitochondrial membrane resulting in decreased membrane potential and production of reactive oxygen species was reported [104, 108]. As for diphtheria toxin and SubAB, its A-chain was already implemented successfully as immunotoxin [63, 64]. Abrin has been isolated in different isoforms whereby the most toxic variant, abrin-a, was chosen for this study [105].

## 1 Introduction

### 1.4 Apoptosis

Apoptosis, the best-investigated form of programmed cell death, plays an essential role throughout life and is especially important for tissue homeostasis. Exemplarily, defects in apoptosis regulation may result in cancer formation and the manner of induced cell death can be crucial for the outcome of anti-cancer therapy. Though apoptosis is a very complex and diverse process, the most important features have been ascertained.

#### 1.4.1 Initiation of apoptosis – Extrinsic and intrinsic pathway

There are two main pathways that initiate apoptosis: the extrinsic and the intrinsic pathway. In case of the extrinsic pathway, the signal for cell death comes from outside of the cell and is transferred to the inside by the binding of a ligand to so-called death receptors, e. g. the TNFR1 or Fas/CD95 [109]. They belong to the family of TNF receptors and contain a death domain on the cytoplasmic side. Following the binding of the ligand and thus activation of the receptor, the adaptor molecule FADD (Fas-associating death domain-containing protein) is recruited, binds to and activates the initiator caspases-8 and -10 [109]. Proteases of the family of caspases possess a cysteine at their active site and cleave their targets after aspartic residues. Next to initiator caspases, effector, also called executioner, caspases are also involved in the apoptotic cascade and are responsible for most apoptotic features [110].

Opposite to the extrinsic pathway, apoptosis in case of the intrinsic pathway is initiated in response to intracellular signals, e. g. DNA damage, ER stress, radiation, hypoxia or cytotoxic drugs [110, 111]. Here, the mitochondrion plays a central role as the aforementioned inducers all lead to a change in the inner mitochondrial membrane potential [111]. As a result, cytochrome c is released into the cytosol where its presence is required for the activation of the apoptosis protease activating factor 1 (APAF-1). Multimerization of APAF-1 with the help of cytochrome c and ATP/dATP leads to the recruitment and activation of the initiator caspase-9 in the multiprotein complex called apoptosome [110]. Loss of the inner mitochondrial membrane potential furthermore leads to the release of Smac/DIABLO (indirect activator of caspases), stop of ATP synthesis and ROS generation as a consequence of lacking cytochrome c [110]. The Bcl-2 family of proteins has an important role in the regulation of mitochondrial properties during apoptosis. At least 25 genes belonging to this family have been discovered with either pro- or anti-apoptotic features [111]. The pro-apoptotic proteins Bid and Bax for one block function of the anti-apoptotic proteins Bcl-2 and Bcl-XL. Furthermore, Bax promotes

## 1 Introduction

apoptosis itself by forming pores in the mitochondrial membrane. If unblocked, Bcl-2 and Bcl-XL stop apoptosis by preventing the release of cytochrome c from mitochondria [111, 112].

### 1.4.2 Execution of apoptosis

Both pathways of apoptosis initiation converge in the activation of the effector caspases-3, -6 and -7 by the respective initiator caspases. They are responsible for the most common properties of the apoptotic process whereby caspase-3 was demonstrated to be the central executioner [113]. Cleavage of the actin-binding protein gelsolin by caspase-3 in turn causes actin cleavage leading to cytoskeletal reorganization, rounding and detachment of the cell and formation of apoptotic bodies. Also, signal transduction and cell division are obstructed [114]. The endonuclease CAD (caspase activated DNase), another substrate of caspase-3, causes chromatin condensation and DNA fragmentation [111]. An essential feature of apoptotic cell death is the phagocytic uptake of dying cells as it prevents inflammation. The caspase-initiated externalization of phosphatidylserine (PS) from the inside of the cell membrane is a prerequisite for phagocytosis [111, 115].

### 1.4.3 Caspase-independent apoptosis

Though it has long been believed that caspases are essential in programmed cell death, multiple cases of caspase-independent programmed cell death have been reported. Most importantly, the pro-apoptotic factors AIF (apoptosis inducing factor) and endonuclease G are released from mitochondria upon mitochondrial membrane permeabilization and subsequently contribute to DNA fragmentation and chromatin condensation [116, 117].

## 1.5 The potential of microRNAs in therapy

### 1.5.1 Approaches for tumor specificity

The major challenge of cancer therapy is to ensure the integrity of healthy tissue, being especially important in case of systemic administration. In chemotherapy, this is commonly achieved by applying agents which primarily target fast-dividing cells. Consequently, slow-growing tumors are spared while other tissues with rapid turn-over are also affected. Immunotoxins are specifically designed to be absorbed only by target cells by means of linking the toxin to a cell-specific moiety [39, 40]. Convenient for this approach are antibodies

## 1 Introduction

corresponding to antigens that are specific to the surface of the target cell as well as ligands binding to receptors present on the surface of tumor cells. A well-studied example is the employment of the epidermal growth factor (EGF) as cell-specific ligand as its receptor is frequently overexpressed on cancer cells [62]. The most obvious solution for gene therapy, whether for DNA plasmids or viral vectors, is to employ promoters that lead to specific expression in target cells. For the expression of diphtheria toxin in tumor cells, the H19 promoter was utilized as it is active in several human tumors [44]. In case of pDNA or mRNA therapies, the transfection reagent can be used to limit transfection to target cells by coupling it to cell-specific ligands. Most commonly, folate or transferrin are employed as their receptors are widely expressed on tumor cells [118]. In the ensuing chapter the emerging possibility of employing microRNAs for cell-specific translation in DNA and mRNA therapy is introduced.

### 1.5.2 Concept of microRNAs

Protein expression is a diverse process and has to be regulated on various levels to ensure that the accurate amount of protein is produced in the correct cell at the right moment. A group of small non-coding RNAs, microRNAs (miRNA) and small interfering RNAs (siRNA), were discovered to control expression on the posttranscriptional level. This process is called RNA interference (RNAi) [119] and exerts its function by initiating mRNA degradation or by obstructing translation. Both events are prompted by the binding of a small non-coding RNA to a complementary sequence in the 3' UTR of the mRNA [120-122]. The significance of the 22 nt long RNAs as well in endogenous processes as for research, diagnostic or therapeutic purposes started to gain attention when it was discovered that the two miRNAs lin-4 and let-7 control development in nematodes [123, 124]. miRNAs, which show high conservation between species [125], were found to regulate expression of 30 % of human genes [126]. Those genes are, among others, involved in differentiation, proliferation, tumorigenesis [127-129] or in counteracting stress conditions [130, 131].

In miRNA production, the transcribed RNA sequences are processed to form a hairpin structure (pre-miRNA) which is subsequently transported to the cytoplasm and cleaved by the endoribonuclease Dicer to form the mature miRNA [120]. Following, the mature miRNA is incorporated in the RNA induced silencing complex (RISC) [120]. After assembling of the complex, it binds to the 3' UTR region of the target mRNA by imperfect base pairing and thereby blocks translation of the mRNA sequence [120], presumably by impairing initiation of

## 1 Introduction

translation [132]. siRNAs, in contrast, display perfect sequence complementarity and cause degradation of the mRNA sequence [121]. The described process is depicted in figure 5.

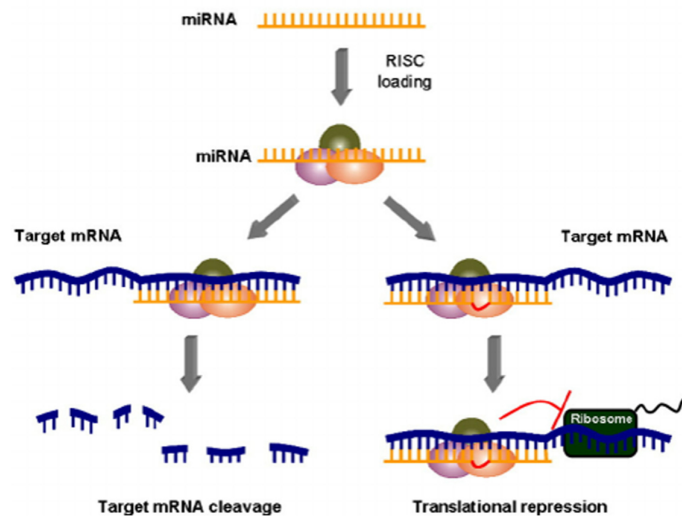


**Figure 5: Translational silencing.** On the left side, cleavage of mRNA is achieved by base pairing with perfect complementarity. On the right side, incomplete base pairing results in translational repression. Figure was taken from [133].

In consequence, influence of miRNAs on translation is comparatively small. Incomplete base pairing enables several miRNAs to target the same mRNA and facilitates that one miRNA can affect different mRNAs. Accordingly, dysregulation of miRNA function can have far-reaching consequences [134].

### 1.5.3 Applications of miRNAs and siRNAs in research and medicine

Due to their great potential in gene silencing, siRNAs have been utilized for gene knockout experiments. Knowledge about the 3' UTR sequence of the mRNA of interest permits the design of according siRNAs. The main challenge of this approach is the toxicity observed by double-stranded RNAs in mammalian cells. Accordingly, different delivery techniques, e. g. siRNA-coated gold nanoparticles, were investigated to circumvent this problem [135-137]. Apart from research intentions, gene silencing presents also a promising strategy for the treatment of various diseases caused by or progressed through pathologically increased expression of distinctive proteins. For instance, a siRNA directed against TNF- $\alpha$  mRNA was able to reduce neuronal apoptosis in consequence to neuroinflammation [138]. Also, tumor growth of orthotopic xenograft models of breast cancer could be inhibited by siRNA mediated silencing of the oncogene Bcl-2 [139]. Another investigation aimed at the inhibition of overexpressed endogenous miRNAs [140]. This was achieved by strong expression of multiple repeats of

## 1 Introduction

binding sites to the targeted miRNA, so-called miRNA sponges, which bind to the miRNA and thereby block its action.

A very auspicious strategy to confine expression of the therapeutic gene to the target cells is the employment of binding sites for endogenous, tissue-specific miRNAs. For instance, myocytes could be protected from the activity of an oncolytic virus by incorporating the binding sites for the muscle-specific miR-133a and miR-206 [141]. Brown *et al.* [142] combined the binding sites for two miRNAs in order to protect hematopoietic cells (miR-142-3p) and hepatocytes (miR-122-5p) from expression of the transgene.

## 1 Introduction

### 1.6 Objectives

The overall aim of this study was to explore chemically modified mRNAs (cmRNA) coding for toxins as potential alternative in cancer therapy. The need for new therapies arises from the obstacles still present in conventional anti-cancer treatment and the consequently high mortality rates. The employment of bacterial or plant toxins for cancer therapy has proven worthwhile for immunotoxins (fusion molecules of toxic proteins and a cell-specific moiety) and gene therapy (plasmid encoded toxins under the control of a tumor-specific promoter). In this thesis, cmRNAs encoding the two bacterial toxins diphtheria toxin and subtilase cytotoxin or the plant toxin abrin-a were investigated for their ability to reduce cancer cell growth both *in vitro* and *in vivo*. For this purpose, two different cell culture systems were applied. The liver carcinoma cell line HuH7 served as a platform which enables follow-up studies employing miRNAs for cell-specific toxicity. The cervix carcinoma cell line KB was chosen due to its suitability for *in vivo* experiments.

The present thesis comprises the following objectives:

- 1) Design, cloning and production of the various chemically modified mRNA sequences.
- 2) *In vitro* examination of the toxicity of the three toxins on HuH7 cells (comprising protein synthesis, cell viability, cell proliferation, cell death, apoptotic features of cell death and the occurrence of a bystander effect).
- 3) Devising a scheme for the investigation of the potential of miRNA binding sites to limit translation to target cells.
- 4) Determination of the expression of abrin-a protein in KB cells by Western blot analysis [65].
- 5) *In vitro* examination of the toxicity of the three toxins on KB cells (comprising protein synthesis, cell viability, cell death and apoptotic features of cell death) [65].
- 6) *In vivo* proof of concept in KB tumors that toxin-encoding chemically modified mRNAs are suitable to induce a reduction in tumor growth in mice [65].

## 2 Material and Methods

## 2 Material and Methods

### 2.1 Material

#### 2.1.1 Chemicals and Substances

**Table 1:** List of chemicals and substances and their providers.

Chemical/Substance	Provider
0.05 % Trypsin-EDTA	Gibco® Life Technologies (Darmstadt, Germany)
1 kb DNA Ladder	Plasmid Factory (Bielefeld, Germany)
100 bp DNA Ladder	Plasmid Factory (Bielefeld, Germany)
100 bp DNA Ladder plus	Plasmid Factory (Bielefeld, Germany)
2'-Thio-rUTP	Jena Bioscience (Jena, Germany)
2x RNA Loading Dye	Thermo Scientific (Waltham, MA, USA)
2x RNA loading dye	Thermo Scientific (Waltham, MA, USA)
32 % hydrochloric acid	Roth (Karlsruhe, Germany)
4 % – 12 % polyacrylamide gels	Thermo Scientific (Waltham, MA, USA)
5'-Methyl-rCTP	Jena Bioscience (Jena, Germany)
6x loading dye	Thermo Scientific (Waltham, MA, USA)
Acetic acid, 100 %	Roth (Karlsruhe, Germany)
AgarAgar, Kobe I	Roth (Karlsruhe, Germany)
Agarose Standard	Roth (Karlsruhe, Germany)
Alkaline phosphatase	Thermo Scientific (Waltham, MA, USA)
Alkaline phosphatase buffer	Thermo Scientific (Waltham, MA, USA))
Ammonium acetate solution	AppliChem (Darmstadt, Germany)
Annexin V Alexa Fluor® 488 conjugate	Thermo Scientific (Waltham, MA, USA)
Anti-abrin-a antibody	Tetracore (Rockville, MD, USA)
Anti-vinculin antibody	Abcam (Cambridge, UK)
<i>Aqua ad injectabilia</i>	Braun (Melsungen, Germany)
<i>Aqua bi-dest</i>	Kerndl (Weißenfeld, Germany)
BCA assay	Thermo Scientific (Waltham, MA, USA)
Bolt® LDS Sample Buffer (4X)	Thermo Scientific (Waltham, MA, USA)
Bolt® MES SDS Running Buffer	Thermo Scientific (Waltham, MA, USA)
Bolt® Sample Reducing Agent (10X)	Thermo Scientific (Waltham, MA, USA)
BSA, Protein standard	Sigma-Aldrich (Steinheim, Germany)
Capping buffer (10x)	New England Biolabs (Frankfurt, Germany)

## 2 Material and Methods

Chemical/Substance	Provider
Caspase-Glo® 3/7 Assay	Promega (Madison, USA)
cDNA synthesis kit	Exiqon (Vedbaek, Denmark)
CellTiter-Glo® Luminescent Cell Viability Assay	Promega (Madison, USA)
Chloroform	Roth (Karlsruhe, Germany)
cOmplete protease inhibitor	Sigma Aldrich (Steinheim, Germany)
D-Luciferin	Roche (Unterhaching, Germany)
DMEM (1x) + GlutaMax™	Gibco® Life Technologies (Darmstadt, Germany)
DNA 1 kb ladder	Plasmid Factory (Bielefeld, Germany)
DNA 100 bp ladder	Plasmid Factory (Bielefeld, Germany)
DNA 100 bp plus ladder	Plasmid Factory (Bielefeld, Germany)
DNA primer	EuroFins (Ebersberg, Germany)
DNase I	Thermo Scientific (Waltham, MA, USA)
DNase I (RNase-free)	Thermo Scientific (Waltham, MA, USA)
DreamFect™ Gold Transfection Reagent	OZ Biosciences (Marseille, France)
Dulbecco's PBS (1x)	Gibco® Life Technologies (Darmstadt, Germany)
EDTA x 2 Na x 5 H <sub>2</sub> O	Roth (Karlsruhe, Germany)
EGFP cmRNA (pVAXA120-EGFP-NotI)	Ethris GmbH (Planegg, Germany)
ElectroMAX™ DH10B™ cells	Invitrogen™ Life Technologies (Darmstadt, Germany)
Eosin Y solution, aqueous	Sigma Aldrich (Steinheim, Germany)
Ethanol, 99.5 % Ph. Eur. reinst.	Roth (Karlsruhe, Germany)
Ethanol, 99.8 %, denatured	Roth (Karlsruhe, Germany)
ExiLENT SYBR® Green master mix	Exiqon (Vedbaek, Denmark)
FastDigest enzymes	Thermo Scientific (Waltham, MA, USA)
FastDigest Green Buffer (10X)	Thermo Scientific (Waltham, MA, USA)
FastDigest green buffer, 10x	Thermo Scientific (Waltham, MA, USA)
FBS	Gibco® Life Technologies (Darmstadt, Germany)
FBS, heat inactivated	Gibco® Life Technologies (Darmstadt, Germany)
Firefly luciferase cmRNA (pVAXA120-luc-NotI)	Ethris GmbH (Planegg, Germany)

## 2 Material and Methods

Chemical/Substance	Provider
GeneArt® Seamless Cloning & Assembly	Invitrogen™ Life Technologies (Darmstadt, Germany)
Glycerol for molecular biology ≥99% pure	Sigma Aldrich (Steinheim, Germany)
GTP	New England Biolabs (Frankfurt, Germany)
HEK293 cells	DSMZ (Braunschweig, Germany)
Hematoxylin Solution, Mayer's	Sigma Aldrich (Steinheim, Germany)
HEPES	Sigma Aldrich (Steinheim, Germany)
HepG2 cells	DSMZ (Braunschweig, Germany)
Hoechst33258	Thermo Scientific (Waltham, MA, USA)
HRP-conjugated anti-rabbit antibody	Santa Cruz Biotechnology (Dallas, TX, USA)
HuH7 cells	Creative Bioarray (Shirley, NY, USA)
Hydrochloric acid (HCl)	Roth (Karlsruhe, Germany)
Inorganic Pyrophosphatase	Thermo Scientific (Waltham, MA, USA)
Isoflurane	CP-Pharma
Kanamycinsulfat	Roth (Karlsruhe, Germany)
KB cells	DSMZ (Braunschweig, Germany)
LB-Medium (Luria/Miller)	Roth (Karlsruhe, Germany)
LF132	Ethris GmbH (Planegg, Germany)
LighCycler® 480 Multiwell Plate 96, white	Roche (Mannheim, Germany)
Lipofectamine® 2000 Transfection Reagent	Invitrogen™ Life Technologies (Darmstadt, Germany)
Luminata Western HRP substrate	Merck Chemicals (Darmstadt, Germany)
MEM (1x) + GlutaMax™	Gibco® Life Technologies (Darmstadt, Germany)
miRNeasy Mini Kit	Qiagen (Hilden, Germany)
mRNA Cap 2' o Methyltransferase	New England Biolabs (Frankfurt, Germany)
NaCl	Roth (Karlsruhe, Germany)
NucleoBond® Xtra Maxi	Macherey-Nagel (Düren, Germany)
NucleoSpin® Gel and PCR clean-up	Machery & Nagel (Düren, Germany)
NucleoSpin® Plasmid	Machery & Nagel (Düren, Germany)
One Shot® TOP10 Chemically Competent <i>E. coli</i>	Invitrogen™ Life Technologies (Darmstadt, Germany)
Paraplast®	Leica Biosystems (Wetzlar, Germany)
Penicillin/Streptomycin	Gibco® Life Technologies (Darmstadt, Germany)

## 2 Material and Methods

Chemical/Substance	Provider
peqGREEN	VWR Life Science (Erlangen, Germany)
Primer 5 S rRNA	Exiqon (Vedbaek, Denmark)
Primer hsa-miR-122-5p	Exiqon (Vedbaek, Denmark)
Primer hsa-miR-125b-5p	Exiqon (Vedbaek, Denmark)
Primer hsa-miR-142-3p	Exiqon (Vedbaek, Denmark)
Propidiumiodide	Sigma Aldrich (Steinheim, Germany)
Protease inhibitor, complete, EDTA-free	Roche (Unterhaching, Germany)
Protein Assay Dye Reagent Concentrate	Bio-Rad (Munich, Germany)
PVDF membranes	Bio-Rad (Munich, Germany)
Rabbit Reticulocyte Lysate System	Promega (Madison, USA)
rATP	Jena Bioscience (Jena, Germany)
rCTP	Jena Bioscience (Jena, Germany)
RealTime-Glo™ MT Cell Viability Assay	Promega (Madison, USA)
rGTP	Jena Bioscience (Jena, Germany)
RiboLock™ RNase Inhibitor	Thermo Scientific (Waltham, MA, USA)
RiboRuler™ High Range RNA Ladder	Thermo Scientific (Waltham, MA, USA)
RNaseA	Invitrogen™ Life Technologies (Darmstadt, Germany)
Roti®-Histofix 4 %	Roth (Karlsruhe, Germany)
Roti®-Histokit II	Roth (Karlsruhe, Germany)
Rotiphorese® 50 x TAE Puffer	Roth (Karlsruhe, Germany)
RPMI1640 (1x) + GlutaMax™	Gibco® Life Technologies (Darmstadt, Germany)
rUTP	Jena Bioscience (Jena, Germany)
S-Methyladenosine	New England Biolabs (Frankfurt, Germany)
Sodium acetate ≥ 99% p.a.	Roth (Karlsruhe, Germany)
SO-Mag5	Kindly provided by O. Mykhaylyk
Sucrose	Sigma Aldrich (Steinheim, Germany)
T4 ligase	Thermo Scientific (Waltham, MA, USA)
T4 ligation buffer	Thermo Scientific (Waltham, MA, USA)
T7 Polymerase	Thermo Scientific (Waltham, MA, USA)
Transcription buffer 1 (10x)	Ethris GmbH (Planegg, Germany)
Tris	Roth (Karlsruhe, Germany)
Triton® X-100	Roth (Karlsruhe, Germany)
Trypanblue solution (0.4%)	Sigma Aldrich (Steinheim, Germany)

## 2 Material and Methods

Chemical/Substance	Provider
TrypLE Express Enzyme (1X), no phenol red	Thermo Scientific (Waltham, MA, USA)
U937 cells	DSMZ (Braunschweig, Germany)
Vaccinia Virus Capping Enzyme	New England Biolabs (Frankfurt, Germany)
Western Breeze blocking solution	Thermo Scientific (Waltham, MA, USA)
Xylene (Isomere)	Roth (Karlsruhe, Germany)

### 2.1.2 Consumables

**Table 2:** List of consumables and their providers.

Consumables	Provider
Cell culture flasks, Tissue Culture Treated	Corning Incorporated, (NY, USA)
Cell culture plates, Tissue Culture Treated	Corning Incorporated (NY, USA)
Cell scraper	Omnilab (Bremen, Germany)
Centrifuge tubes (15 ml; 50 ml)	Corning Incorporated (NY, USA)
Combitips advanced®	Eppendorf Biopur (Hamburg, Germany)
Costar Stripette (5 ml, 10 ml, 25 ml, 50 ml)	Corning Incorporate, (NY, USA)
Countess cell counting chamber slides	Life Technologies (Darmstadt, Germany)
CoverGlass 23.8 x 50 mm	Medite (Burgdorf, Germany)
Diamond® Tipack™	Gilson (Middleton, WI, USA)
Diamond® Tower Pack™	Gilson (Middleton, WI, USA)
Electronic microtiter plates (E-Plates®)	ACEA Biosciences (San Diego, CA, USA)
Eppendorf tubes	Corning Incorporated (NY, USA)
Menzel-Gläser Superfrost® Plus	Thermo Scientific (Waltham, MA, USA)
Micro-Fine™ (29G Insulinspritzen)	BD Pharmaceuticals (Franklin Lakes, New Jersey, USA)
NORM-JECT®	Henke Sass Wolf
Sterican® (27G Kanülen)	Braun (Melsungen, Germany)
Suspension Culture Dish, non-treated, polystyrene	Corning Incorporated (NY, USA)

## 2 Material and Methods

### 2.1.3 Equipment

**Table 3:** List of equipment and their providers.

Equipment	Provider
Attune™ NxT	Thermo Fisher (Waltham, MA, USA)
Centrifuge 5180 R	Eppendorf (Hamburg, Germany)
Centrifuge 5415 D	Eppendorf (Hamburg, Germany)
ChemiDoc™ XRS	Bio-Rad (Munich, Germany)
Consort E834	PeqLab (Erlangen, Munich)
Countess	Life Technologies
IVIS <i>In Vivo</i> Imaging System	PerkinElmer (Waltham, MA, USA)
Leica DM 2000 LED	Leica (Wetzlar, Germany)
Leica DMI8	Leica (Wetzlar, Germany)
Leica EG 1150H	Leica (Wetzlar, Germany)
Leica RM 2235	Leica (Wetzlar, Germany)
LightCycler® 96 thermal cycler	Roche (Mannheim, Germany)
Mikro22R	Hettich (Tuttlingen, Germany)
Multifuge 3L	Heraeus (Hanau, Germany)
Nanodrop 2000c Spectrophotometer	Thermo Fisher (Waltham, MA, USA)
PowerPac™ 300	Bio-Rad (Munich, Germany)
Tecan Infinite® 200 PRO	Tecan (Männedorf, Swiss)
Thermomixer compact	Eppendorf (Hamburg, Germany)
Trans-Blot® Turbo™ Transfer System	Bio-Rad (Munich, Germany)
Varifuge 3.OR	Heraeus (Hanau, Germany)
Wallac Victor <sup>2</sup> 1420 Multilabel Counter	PerkinElmer (Waltham, Massachusetts, USA)
xCELLigence RTCA MP	ACEA Biosciences (San Diego, CA, USA)

## 2 Material and Methods

### 2.1.4 Buffers and solutions

**Table 4:** List of utilized buffers and solutions.

	Substance	Final concentration
DNA dye solution	Dulbecco's PBS (1x)	
	FBS	2 %
	Propidiumiodide	50 µg/ml
	RNaseA	0.5 mg/ml
Annexin V binding buffer (5x), pH 7.4	HEPES	50 mM
	NaCl	700 mM
	CaCl <sub>2</sub>	12.5 mM
DNA staining solution	Dulbecco's PBS (1x)	
	Propidiumiodide	20 µg/ml
	RNaseA	0.2 mg/ml
Lysis buffer (10x), pH 7.8	Tris-HCl	250 mM
	Triton X-100	1 %
HCl – Ethanol (2x)	Ethanol (100 %)	70 %
	<i>Aqua bi-dest</i>	
	HCl (32 %)	0.25 %

## 2.2 Methods

### 2.2.1 Preparation of the buffers and solutions

The composition of the employed buffers and solutions can be found in section 2.1.4.

#### 2.2.1.1 Annexin V binding buffer

A five-time stock solution was prepared by mixing all substances and adjustment to the appropriate volume with *aqua ad injectabilia*. The pH was set to 7.4 using HCl.

#### 2.2.1.2 DNA dye solution

All substances were mixed in Dulbecco's PBS (1x). The dye was utilizable for two subsequent days if stored at 4 °C.

#### 2.2.1.3 DNA staining solution

All substances were mixed in Dulbecco's PBS (1x).

## 2 Material and Methods

### 2.2.1.4 Eosin Y solution, acidified

Shortly before use, the aqueous Eosin Y solution was acidified by adding 6 drops of acetic acid (100 %) to 180 ml solution.

### 2.2.1.5 Lysis buffer

A ten-time stock solution was prepared by mixing the substances and adjustment to the appropriate volume with *aqua ad injectabilia*. The pH was set to 7.8 using HCl.

### 2.2.1.6 HCl – Ethanol

The two times stock solution was prepared by mixing all substances. Shortly before use, the solution was mixed with an equal volume 70 % ethanol.

## 2.2.2 Design of mRNA constructs

Several aspects had to be considered during the design of the mRNA constructs and are briefly described here:

- Since cytotoxicity of each of the three investigated toxins is evoked by the catalytic A-subunit [83, 143, 144], mRNAs coding only for that part were designed [65]. The cell binding and transporting B-chain was substituted by suitable transfection reagents for *in vitro* and proprietary lipid formulations for *in vivo* studies. Also, in case of immunotoxins and for RNA/DNA transfections, typically only the A-subunit is employed [41, 44, 45, 62-64].
- To address the adverse immunogenic effects of non-modified mRNA [9, 14-16, 19], chemically modified mRNA (cmRNA) comprising 5'-methylcytosine and 2'-thiouridine were used [65]. These modifications were previously shown to result in stabilized non-immunogenic mRNA [20].
- Two control cmRNAs for each of the toxins were employed in this study. The nonfunctional control cmRNA served as reference for toxicity conveyed by the presence of exogenous protein. For this purpose, point mutations regarding the protein sequence were inserted that had been demonstrated to result in proteins without or with considerably reduced cytotoxicity [145-148]. To be able to estimate the cytotoxicity that ensues from the transfection process itself, an untranslatable control cmRNA was applied. It displays the same sequence as the corresponding toxin cmRNA, but has a scrambled Kozak [1] element and the start as well as all in frame downstream ATGs were mutated to TAGs in order to prevent translation [65].

## 2 Material and Methods

- To achieve optimal protein production, the nucleotide sequences were optimized for expression in *homo sapiens*.
- In contrast to abrin-a and diphtheria toxin, the target of subtilase cytotoxin (GRP78) resides in the endoplasmic reticulum. Hence, after translation of the transfected mRNAs, SubA protein needs to be retained in the ER to perform its function. In order to enhance ER retention, the KDEL motif (Lys-Asp-Glu-Leu) was included at the carboxy-terminal of the protein sequence. The KDEL motif was shown to be present in most ER-resident proteins, including GRP78, and to be essential for their ER retention [149]. It was demonstrated before that by addition of the KDEL sequence, retention of a plasmid expressed protein in the ER can be achieved [150, 151].

### 2.2.3 Cloning procedures and cmRNA production

For all digestions performed in this thesis, FastDigest (FD) Enzymes were employed. The maximal incubation times given by the manufacturer were respected. All digestions were performed at 37 °C. FastDigestion (FD) green buffer was employed to enable direct loading onto agarose gels. For the preparation of gels, agarose was solved in 1 x TAE buffer which was also employed as running buffer. peqGREEN was utilized to visualize the nucleic acids. 1 x TAE buffer was prepared with *aqua* bi-dist for DNA or *aqua ad injectabilia* for RNA gel electrophoresis.

#### 2.2.3.1 Cloning procedures and plasmid preparation

The different constructs were cloned into the backbone pVAX1-A120 [20] (for the sequence see table S2 in the appendix) at the *KpnI* site as described elsewhere [65]. The three toxin constructs (ST, DT, AT) and their corresponding nonfunctional (SN, DN, AN) and untranslatable (SU, DU, AU) controls were produced by GeneArt® as DNA strings in two parts. The sequences, codon-optimized for expression in *Homo sapiens*, can be found in table S1 (appendix). To enable subsequent cloning by homologous recombination, an overlap of at least 15 bp between the two insert parts and the vector were designed. 10 µg of vector backbone were linearized with 1 µl *KpnI* in 100 µl total volume overnight and completeness of the digest was tested on 1 % agarose gel. Following, purification of the DNA was performed using the NucleoSpin® Gel and PCR Clean-up following the manufacturer's instructions. The concentration of DNA after elution was determined using a Nanodrop device. The DNA strings were solubilized in *aqua ad injectabilia* to a concentration of 100 ng/µl. Subsequent sub-cloning into the linearized pVAX1-

## 2 Material and Methods

A120 was performed using the GeneArt® Seamless Cloning and Assembly Enzyme Mix and One Shot® TOP10 Chemically Competent *E. coli*. Seamless Cloning was performed according to the manufacturer's instruction and 100 ng DNA of each insert and 50 ng of vector DNA were applied. Transformation in Chemically Competent *E. coli* was performed following the instructions, except for the subsequent alterations: 25 µl instead of 50 µl of bacteria were employed for 3 µl of seamless cloning reaction and a Thermomixer compact at 42 °C was utilized in place of a 42 °C water bath. Culture of transformed bacteria was plated on 1.5 % agar plates (1.5 g AgarAgar in 100 ml LB-Medium) containing 50 µg/µl kanamycinsulfate and incubated over night at 37 °C. Of each construct, five clones were picked and inoculated in 6 ml LB-Medium containing 50 µg/µl kanamycinsulfate. After overnight incubation at 37 °C and 200 rpm, glycerol stocks were done by carefully mixing 200 µl glycerol with 800 µl bacteria suspension and freezing them at -20 °C respectively at -80 °C for long term storage.

In order to screen for correct clones, DNA was purified from the remaining bacteria culture employing the NucleoSpin® Plasmid kit according to the manufacturer's instructions. Elution was performed by incubating the membrane twice with 15 µl elution buffer for 3 min at 70 °C followed by 1 min of centrifugation at 800 rcf and 1 min of centrifugation at 11,000 rcf. DNA concentration was measured using a Nanodrop device. Constructs were sequenced by Eurofins using primers targeting the T7 promoter (TAATACGACTCACTATAG) and additionally, in case of the three SubA constructs, targeting a region further downstream (GCTTATCACCTGTGTCCAG). Moreover, the completeness of the A120 tail was confirmed by digesting 6 µg of DNA with 1 µl of *Pst*I and 1 µl of *Not*I in a total volume of 25 µl overnight and examination on a 2 % agarose gel.

For the production of larger quantities of DNA, bacteria were incubated in 500 ml LB-Medium (50 µg/ml kanamycinsulfate) overnight at 37 °C and DNA was purified using the NucleoBond® Xtra Maxi kit according to the manufacturer's instructions. The dried DNA pellet was re-suspended in *aqua ad injectabilia* by gentle mixing and 30 min incubation at room temperature. DNA was stored at -20 °C.

### 2.2.3.2 cmRNA production/In vitro transcription

cmRNA production was performed as described elsewhere [65]. DNA plasmids were linearized downstream of the poly(A) tail with the restriction enzyme *Not*I by incubating 10 µg of DNA with 1 µl of enzyme at 37 °C overnight. Completeness of digestion was controlled by agarose gel electrophoresis. Purification of the DNA from the reaction mixture was performed by

## 2 Material and Methods

chloroform extraction and ethanol precipitation. For this purpose, chloroform was added in an amount at least equal to the volume of the reaction mixture and, after mixing thoroughly and centrifuging with a benchtop centrifuge, the top phase was transferred into a new eppendorf tube. Next, twice the volume of -20 °C cold pure ethanol was added as well as sodium acetate to a final concentration of 0.3 M. The DNA was allowed to precipitate for 30 min at -20 °C and afterwards centrifuged at 14,000 rcf for 30 min at 4 °C. The supernatant was discarded and the remaining pellet washed with 70 % ethanol by centrifuging again at 14,000 rcf for 10 min at 4 °C. The supernatant was discarded again and, after letting the pellet dry, it was solubilized in *aqua ad injectabilia*.

The linearized plasmids were used as template for *in vitro* transcription (IVT). IVT-mix: 0.1 µg/µl plasmid, transcription buffer 1, 1 U/µl RiboLock™ RNase Inhibitor, 0.015 U/µl Inorganic Pyrophosphatase 1, 2 U/µl T7 Polymerase, 7.5mM rATP, 7.5 mM rGTP, 5.6 mM rCTP, 5.6 mM rUTP, 1.9 mM 5'-Methyl-rCTP and 1.9 mM 2'-Thio-rUTP. The complete IVT-mix was incubated at 37 °C for 4.5 h, following which 1 U/µl DNase I was added to remove the plasmid template and the reaction was incubated an additional 25 min at 37 °C. cmRNA (chemically modified mRNA) was precipitated with ammonium acetate at a final concentration of 2.5 mM by incubation at 4 °C for 45 min and centrifugation at 4 °C and 19,000 rcf for 15 min. The pellet was washed twice with 70 % ethanol by centrifuging at 4 °C and 19,000 rcf for 5 min before it was re-suspended in *aqua ad injectabilia*. The precipitation and washing step was repeated once and, following, cmRNA concentration was determined on a Nanodrop device. The correct size and purity of the cmRNA constructs were determined with a 1 % agarose gel (150 V) and RiboRuler™ High Range RNA Ladder. The agarose gel was imaged using a ChemiDoc™ XRS. cmRNA was stored at -80 °C.

### 2.2.3.3 cmRNA capping

Subsequently, the *in vitro* produced cmRNA was capped at a final concentration of 1 mg/ml as described elsewhere [65] and denatured in advance at 65 °C for 15 min. The capping reaction mix contained: 1 x capping buffer, 0.5 mM GTP, 0.2 mM S-Methyladenosine, 0.5 U/µl Vaccinia Virus Capping Enzyme, 2.5 U/µl mRNA Cap 2'-o-Methyltransferase and 1 U/µl RiboLock™ RNase Inhibitor. The reaction mix was incubated at 37 °C for 60 min before the RNA was precipitated with ammonium acetate at a final concentration of 2.5 mM by incubation at 4 °C for 45 min and centrifugation at 4 °C and 19,000 rcf for 15 min. The pellet was washed twice with 70 % ethanol by centrifuging at 4 °C and 19,000 rcf for 5 min before it was re-suspended

## 2 Material and Methods

in *aqua ad injectabilia*. The precipitation and washing step was repeated once and cmRNA concentration was determined on a Nanodrop device. cmRNA was stored at -80 °C.

### 2.2.4 Reticulocyte assay

In order to determine protein synthesis of luciferase firefly from luc cmRNA in a cell free system, the Rabbit Reticulocyte Lysate System was applied according to the manufacturer's instructions. Per reaction of 35 µl lysate, 1 µg luc cmRNA and either 0.1 µg AT or 0.1 µg AU cmRNA were employed simultaneously. After an incubation of 45 minutes at 30 °C, luminescence was measured using the Tecan Infinite® 200 PRO Reader with white 96 well cell culture plates.

### 2.2.5 Cell culture handling

#### 2.2.5.1 Thawing and passaging of cells

Cells were stored in liquid nitrogen. For thawing of cells they were warmed in a 37 °C water bath before adding complemented cell culture medium, mixing and centrifuging for 5 min at 1,100 rpm. Subsequently, the supernatant was removed and the cells re-suspended in fresh supplemented cell culture medium. Cells were passaged every three to four days when reaching a confluence of 60-80 %. Cells were cultured either in 25 cm<sup>2</sup>, 75 cm<sup>2</sup> or in 175 cm<sup>2</sup> flaks at 37 °C and 5 % CO<sub>2</sub> in a humidified incubator. For passaging, cells were washed with Dulbecco's PBS (1x) and detached with 0.05 % Trypsin-EDTA by incubating for 3-5 min at 37 °C. Afterwards, three times the volume fresh cell culture medium with additives was added to the cells before 1/3 to 1/20 was transferred into a new flask with fresh supplemented cell culture medium. In case of the suspension cell line U937, cells were cultures at a maximal density of 1 x 10<sup>6</sup> cells/ml medium. KB cells were cultured in RPMI1640 (1x) + GlutaMax™ with 10 % FBS and 1 % Penicillin/Streptomycin. HuH7 cells were cultured in DMEM (1x) + GlutaMax™ low glucose supplemented with 10 % FBS and 1 % Penicillin/Streptomycin. HepG2 and U937 cells were cultured in RPMI1640 (1x) + GlutaMax™ with 10 % heat inactivated FBS and 1 % Penicillin/Streptomycin. HEK293 cells were cultured in MEM (1x) + GlutaMax™ with 10 % FBS and 1 % Penicillin/Streptomycin.

## 2 Material and Methods

### 2.2.5.2 Seeding of cells

In order to seed the cells prior to transfection, cells were harvested as described in 2.2.5.1. After washing cells with Dulbecco's PBS (1x), detachment with trypsin-EDTA and addition of fresh complemented cell culture medium, cells were centrifuged at 1,100 rpm in a Heraeus Multifuge (3 l) for 5 min. Subsequently, the supernatant was removed and the cells resuspended in fresh supplemented cell culture medium before counting them using a Countess. The number of seeded cells as well as the applied cell culture plates are specified in table 5 and 6.

### 2.2.5.3 Transfection of cells in culture

After incubating seeded cells (see 2.2.5.2) for about 20 h at 37 °C, transfection of cells was performed. Transfections were done according to the following description: First the respective amount of cmRNA was resuspended in medium without additives and Lipofectamine® 2000, 2 µl for each µg of cmRNA, was diluted in an equal volume of medium without additives. Five min after the preparation of the lipid, the cmRNA solution was added to the Lipofectamine® 2000 solution. After an incubation of 5 min at room temperature, the transfection mixture was divided onto a varying number of replicate wells where the medium had been changed to medium without additives beforehand. The total volume per well of a 96 well plate was 100 µl. For the untransfected control the medium was also replaced by fresh medium without additives. Following transfection, the cells were incubated at 37 °C and 5 % CO<sub>2</sub> until further application or measurement. For the applied cmRNAs refer to sections 2.2.3.1-2.2.3.3. 4 h post transfection, the medium was discarded and replaced by supplemented cell culture medium. The employed cmRNA doses are specified in table 5 and 6 and the applied volumes per well in table 7. In order to examine the effectiveness of LF132-complexed AT and AU cmRNA (formulation performed by Ethris GmbH) *in vitro*, cells were transfected with 10, 50 or 100 ng/100 µl. 2 % sucrose (diluted accordingly) was applied as vehicle control. Also, 4 h after transfection, medium was discarded and supplemented cell culture medium added. For transfections with magnetic nanoparticles, refer to section 2.2.6.6.

### 2.2.6 Cell culture assays

General transfection protocol can be found in section 2.2.5.3. Images were taken with a Leica DMi8 fluorescence microscope. Flow cytometry analysis was performed with an Attune™ NxT instrument. All luminescence measurements were done in the Tecan Infinite® 200 PRO Reader

## 2 Material and Methods

with white 96 well cell culture plates. In case of the RealTime-Glo™ MT Cell Viability Assay, white 96 well cell culture plates with  $\mu$ clear bottom were used. Table 5 and 6 show the applied cell numbers, the utilized cell culture plates, employed toxin or control cmRNA doses and the time point at which the assay was performed. In table 7, the volumes employed per well are depicted.

**Table 5: HuH7 cell culture assays.** Compilation of the applied cell numbers, the cell culture treated plates, the toxin and control cmRNA doses and time points of assay.

	Number of cells seeded/100 $\mu$ l	Cell culture plate	cmRNA dose [ng/100 $\mu$ l]	Time of assay after transfection [h]
EGFP co-transfection	8,000	96 well with black walls and $\mu$ clear bottom	1:2 dilution starting at 10, ending at 0.005	24
CellTiter-Glo™	3,000	Clear 96 well	1:2 dilution starting at 100, ending at 3.125	48
RealTime-Glo™	1,000	96 well with white walls and $\mu$ clear bottom	50	5-69
Cell impedance	3,000/6,000	E-Plate® 96 well	50	5-96
Scratch assay	Confluent layer	Clear 96 well	50	0, 96, 192
Cell cycle analysis	5,000	Clear 48 well	50	24, 48
Caspase-Glo® 3/7 Assay	3,000	Clear 96 well	30	72
AnnexinV-AF488 PI Assay	7,500	Clear 24 well	50	72
Nicoletti Assay	7,500	Clear 24 well	50	48, 72
Bystander effect				
- Transfection	17,000	Clear 6 well	50	24
- Transfer	2,000	Clear 96 well	-	72
Magnetofection	8,000; Equates 80,000/well	Clear 12 well	6.25; equates 25 ng/well	48

## 2 Material and Methods

**Table 6: KB cell culture assays.** Compilation of the applied cell numbers, the cell culture treated plates, the toxin and control cmRNA doses and time points of assay.

	Number of cells/100 $\mu$ l	Cell culture plate	cmRNA dose [ng/100 $\mu$ l]	Time of assay after transfection [h]
Western blot	20,000	Clear 6 well	40, 80	24
EGFP co-transfection	10,000	96 well with black walls and $\mu$ clear bottom	0.0005, 0.05, 5	24
CellTiter-Glo™	10,000	Clear 96 well	10, 50, 100	48, 96
Dead cells/PI flow cytometry	10,000	Clear 96 well	10, 50, 100	48
Caspase-Glo® 3/7 Assay	10,000	Clear 96 well	10, 50, 100	24
AnnexinV-AF488 PI Assay	10,000	Clear 24 well	10, 50, 100	24
Hoechst33258	10,000	96 well with black walls and $\mu$ clear bottom	10, 50, 100	48

**Table 7: Sum up of applied volumes per well.**

Cell culture plate	96 well	48 well	24 well	12 well	6 well (HuH7)	6 well (KB)
Volume per well [ $\mu$ l]	100	200	400	1000 for seeding, 400 for transfection	1,500	3,000

### 2.2.6.1 EGFP co-transfection/Protein synthesis inhibition

Co-transfections were performed by mixing 50 ng EGFP cmRNA with the toxin or control cmRNAs before addition to the Lipofectamine® 2000 dilution. To determine EGFP expression, cell culture medium was put aside, cells washed with Dulbecco's PBS (1x), trypsinized with TrypLE™ Express Enzyme at 37 °C, re-suspended in the cell culture medium and stored on ice until analyses by flow cytometry. Cells were gated on singlets. EGFP fluorescence was determined in BL1.

### 2.2.6.2 Cell viability/Cell proliferation/Toxicity assays

To determine cell viability, the CellTiter-Glo® Luminescent Cell Viability Assay was performed according to the manufacturer's instruction. In case of KB cells, the plate was centrifuged for

## 2 Material and Methods

5 min at 1100 rpm, the medium discarded and fresh supplemented cell culture medium was added before addition of the substrate and measurement of luminescence (1 s). In this assay, the ATP content of cells is measured as a degree for cell viability. On basis of the cell viability measurements, toxicity of the cmRNAs was also assessed by calculating the inhibition of cell growth (GI) in comparison to untransfected cells. For luminescence values that were higher at 48 h than at 0 h post transfection, the percentage of cell growth was calculated as follows:  $((Ti-Tz)/(C-Tz)) \times 100$  with Tz: luminescence at 0 h, Ti: luminescence of sample at 48 h and C: luminescence of UT cells at 48 h post transfection. In the case of  $Ti < Tz$ , the percentage of growth was calculated by:  $((Ti Tz)/Tz) \times 100$ . A value of 100 % means that cells grew in the same degree as UT cells, 0 % signifies no change in cell viability since the time of transfection and -100 % implies complete cell death.

Changes in cell viability over time were examined using the RealTime-Glo™ MT Cell Viability Assay following the assays instructions. This assay also determines the ATP content of cells as a measure for cell viability applying a reagent that is stable in medium over 72 h. The mixed reagents were added 4 h post transfection. Luminescence measurements (1 s) were performed at the indicated time points.

Impedance values were acquired with an xCELLigence instrument applying an E-plate®. The measured impedance values correspond with the degree of cell confluence at the well bottom. For the scratch assay, Huh7 cells were transfected when grown to confluency and 4 h after transfection the cell layer was scratched with a 200 µl pipette tip. Scratching was done prior to medium change in order to dispose of remaining cell debris. The protocol was adjusted from previous publications [152, 153]. The time required for the scratch to close was monitored by light microscopy as it is indirect proportional to the proliferating potential of the cells.

Dead cells can be counted by staining with the membrane impermeable dye PI. For this purpose, cell culture medium was put aside, cells washed with Dulbecco's PBS (1x), trypsinized with TrypLE™ Express Enzyme at 37 °C, re-suspended in the cell culture medium and Dulbecco's PBS (1x), containing 5 µg/ml propidiumiodide (PI), was added at 1:5 (v/v) to the cell suspension and stored on ice until analysis by flow cytometry. Cells were gated on singlets and PI fluorescence was determined in BL3.

### 2.2.6.3 Cell cycle analysis

Stoichiometric DNA dyes as propidiumiodide (PI) are dyes that bind in proportion to the amount of DNA present in the cell and can accordingly be used to analyze cell cycle. Cells in the S phase

## 2 Material and Methods

of the cell cycle will have more DNA than cells in G<sub>0</sub>/G<sub>1</sub> phase. They will take up proportionally more dye and will fluoresce more brightly until they have doubled their DNA content. The cells in G<sub>2</sub>/M phase will be approximately twice as bright as cells in G<sub>0</sub>/G<sub>1</sub> phase. For assay performance, the cell culture medium was discarded, cells washed with Dulbecco's PBS (1x), trypsinized with TrypLE™ Express Enzyme at 37 °C and re-suspended in Dulbecco's PBS (1x) containing 2 % FBS. After transfer into a round bottom plate, cells were centrifuged at 4 °C and 300 rcf for 5 min. The supernatant was discarded and cells re-suspended in Dulbecco's PBS (1x) with 2 % FBS before slowly adding 2.33 times the volume 100 % ethanol by careful pipetting, resulting in 70 % ethanol. At this point, cells were either stored for 1 h at 4 °C or kept at -20 °C for longer time periods before further processing. Afterwards, cells were washed twice by centrifuging at 4 °C and 300 rcf for 5 min, discard of the supernatant and re-suspension of cells in Dulbecco's PBS (1x) containing 2 % FBS. Following another centrifugation step, cells were re-suspended in DNA dye solution and incubated at room temperature in the dark for 20 min before analysis by flow cytometry. A slow flow rate was used, cells gated on singlets and PI fluorescence was determined in BL3.

### 2.2.6.4 Apoptotic assays

All assays designed to determine apoptosis were executed solely for the toxin and the untranslatable control cmRNAs.

An important characteristic of apoptotic cell death is the activity of the effector caspases-3 and -7. Their activity was assessed with the Caspase-Glo® 3/7 Assay according to the manufacturer's instruction. Luminescence measurements (1 s) were performed at the indicated time point.

Cells undergoing apoptosis evert the membrane compound phosphatidylserine (PS) to the outside while still keeping their membrane intact [154]. Accordingly, apoptotic cells can be identified in flow cytometry by performing a double-staining with the PS binding Annexin V conjugated to a fluorophore (Annexin V AF488) [154] and the membrane impermeable DNA dye PI. For this purpose, the cell culture medium was put aside, cells washed with Dulbecco's PBS (1x), trypsinized with TrypLE™ Express Enzyme at 37 °C and re-suspended in the cell culture medium. Following, cells were centrifuged at 4 °C and 300 rcf for 5 min, the supernatant discarded and cells washed in cold Dulbecco's PBS (1x) prior to another centrifugation step. After discard of the supernatant, the cells were re-suspended in 1x Annexin V binding buffer (prepared in *aqua ad injectabilia*). 5 µl Annexin V-AF488 and 10 µl of a 10 µg/ml PI solution in

## 2 Material and Methods

1x Annexin V binding buffer per 100  $\mu$ l final volume were added to the cells (final concentration PI: 1  $\mu$ g/ml). After an incubation period of 15 min at room temperature in the dark, an equal volume of Annexin V binding buffer (1x) was added and cells were analyzed by flow cytometry. Cells were gated on singlets. Annexin V-AF488 fluorescence was determined in BL1 and PI fluorescence in BL3.

The procedure of the Nicoletti Assay was adapted from Riccardi and Nioletti (2006) [155]. By treatment of cells with ethanol they become permeable for PI and DNA fragments, arising from apoptotic chromatin cleavage, diffuse from the cell, resulting in reduced DNA content. As the DNA content is directly proportional to the PI fluorescence intensity, the hypodiploid DNA content of apoptotic cells is mirrored in the SubG<sub>1</sub> peak. For assay performance, the cell culture medium was put aside, cells washed with Dulbecco's PBS (1x), trypsinized with TrypLE™ Express Enzyme at 37 °C and re-suspended in the cell culture medium. Subsequently, cells were washed twice in cold Dulbecco's PBS (1x) followed by centrifugation at 4 °C and 300 rcf for 5 min. The supernatant was discarded and cells re-suspended in Dulbecco's PBS (1x) before slowly adding 2.33 times the volume of pure ethanol by careful pipetting, resulting in 70 % ethanol. At this point, cells were stored at -20 °C until further analysis. Subsequently, cells were washed by centrifuging at 4 °C and 300 rcf for 5 min and discard of the supernatant. Following a repetition of the centrifugation step, cells were re-suspended in DNA staining solution and incubated at room temperature in the dark for 30 min before analysis by flow cytometry. Cells were gated on singlets and PI fluorescence was determined in BL3.

When stained with Hoechst33258, cells undergoing apoptosis show far higher fluorescence than normal cells. Staining with the Hoechst33258 dye was performed according to the manufacturer's instructions. Cell culture medium was discarded and the Hoechst33258 dye employed at 10  $\mu$ g/ml in supplemented cell culture medium. Cells were incubated for 15 min at room temperature in the dark. Before examination of the cells under the fluorescence microscope, Hoechst33258 was discarded and fresh supplemented cell culture medium added.

### **2.2.6.5 Bystander effect – Transfer of supernatant and lysates**

Cells were co-transfected with 33 ng/100  $\mu$ l EGFP cmRNA by mixing it with the toxin or control cmRNAs prior addition to the Lipofectamine® 2000 solution. 24 h after transfection, transfection efficiency was controlled by examining cells microscopically for EGFP fluorescence. Also, phase contrast images were taken. Supernatants of the transfected cells were collected and stored at -80 °C. In order to remove cells, cold Dulbecco's PBS (1x) containing 1x protease

## 2 Material and Methods

inhibitor was added and cells detached with a cell scraper. Subsequently, cells were lysed by four freeze-thaw cycles. For this, cells were frozen at  $-80\text{ }^{\circ}\text{C}$  and thawed again at room temperature followed by vigorous vortexing. Next, supernatants and lysates were centrifuged at  $19,000\text{ g}$  and  $4\text{ }^{\circ}\text{C}$  for 5 min to get rid of any cell debris. The protein content of the lysates was determined by a Bradford assay. For the calibration line, a 1:2 serial dilution of BSA protein standard was performed in *aqua ad injectabilia* starting with a concentration of  $0.7\text{ mg/ml}$ . A duplicate of the calibration line was done.  $200\text{ }\mu\text{l}$  of 20 % Bio-Rad Protein Assay reagent (in *aqua ad injectabilia*) were added to  $5\text{ }\mu\text{l}$  of each lysate sample or each concentration of the calibration line. If necessary, a 1:5 dilution of the samples in *aqua ad injectabilia* was done beforehand to stay in the range of the calibration line. Measurement was performed at  $600\text{ nm}$  with a Wallac Victor<sup>2</sup>.  $100\text{ }\mu\text{l}$  of undiluted supernatant or of diluted lysates were transferred on pre-seeded HuH7 cells. For lysates, 5 or  $50\text{ }\mu\text{g}$  protein/ $100\text{ }\mu\text{l}$  were employed. Cell lysates of the differentially transfected cells were diluted to equal concentrations with Dulbecco's PBS (1x) before further dilution with complemented cell culture medium was done. Cell viability was determined using the CellTiter-Glo<sup>®</sup> Luminescent Cell Viability Assay according to the manufacturer's instruction. Luminescence measurements (1 s) were performed at the indicated time point.

### 2.2.6.6 Bystander effect – Magnetofection experiment

The experiment was performed in 12 well plates. While  $1\text{ ml}$  of medium per well was utilized for seeding and also after media change following transfection,  $400\text{ }\mu\text{l}$  of total volume were employed during transfection in order to enhance the magnetic effect.  $25\text{ ng/well}$  (corresponds to  $6.25\text{ ng}/100\text{ }\mu\text{l}$ ) of either EGFP or DT cmRNA were applied. DreamFect<sup>™</sup> Gold Transfection Reagent (DFG) was diluted in *aqua ad injectabilia* before mixing it with the iron-containing magnetic nanoparticles (SO-Mag5 [156]). The cmRNA was diluted in non-supplemented cell culture medium and subsequently added to the DFG-SO-Mag5 mixture and incubated for 20 min at room temperature. This complex contained  $0.004\text{ }\mu\text{g cmRNA}/\mu\text{l}$ ,  $0.002\text{ }\mu\text{g SO-Mag5}/\mu\text{l}$  and 1:63 (v/v) diluted DFG. Cell culture medium was discarded and replaced by  $394\text{ }\mu\text{l}$  medium without additives. Small magnets the size of a 96 well were placed directly below the bottom of the wells during the transfection procedure.  $6.25\text{ }\mu\text{l}$  of cmRNA-DFG-SO-Mag5 mixture were dripped on the wells above the center of the magnet. After an incubation time of 30 min at  $37\text{ }^{\circ}\text{C}$  and 5 %  $\text{CO}_2$ , medium was changed to supplemented cell culture medium ( $1\text{ ml}$ )

## 2 Material and Methods

and the magnet was removed. For each cmRNA, two identical wells were transfected; one with magnet and one without. 48 h post transfection, images were taken.

### 2.2.6.7 SDS page and Western blot

For Western blot detection, cells were seeded in 6 well plates. The assay was conducted 24 h post transfection. After washing the cells with cold PBS, they were detached from the well using cell scrapers and lysed in 1x lysis buffer with 1x cOMplete protease inhibitor and 150 U/ml DNase I for 30 minutes on ice. Total protein content was determined by the bicinchoninic acid (BCA) assay, following the manufacturer's instructions, and samples were mixed with Bolt LDS Sample Buffer and Bolt Sample Reducing Agent. Cell lysates (45 µg of total protein per sample) were separated on 4 % – 12 % polyacrylamide gels using Bolt® MES SDS Running Buffer in a PowerPac™ 300 and transferred to polyvinylidene fluoride (PVDF) membranes using a Trans-Blot® Turbo™ Transfer System. Membranes were blocked in Western Breeze blocking solution and probed with antibodies against abrin-a (6.7 µg/mL) and vinculin (1:10,000). For protein detection, horseradish peroxidase (HRP)-conjugated anti-rabbit (1:10,000) antibodies were added. For signal detection, Luminata Western HRP substrate was applied according to the manufacturer's protocol. The membrane was imaged using a ChemiDoc™ XRS and the Image Lab™ Software (Bio-Rad, Bremen, Germany).

### 2.2.7 miRNA expression analysis

3x10<sup>6</sup> cells of the cell lines U937, HuH7, HepG2 and HEK293 were pelleted at 1100 rpm for 5 min and frozen at -80 °C until RNA was isolated using the miRNeasy Mini Kit according to the manufacturer's instructions. cDNA was synthesized with the Universal cDNA synthesis kit following the manufacturer's instructions with a final RNA concentration of 25 ng/µl. miRNA expression was determined employing the ExiLENT SYBR® Green master mix and carried out on a LightCycler® 96 thermal cycler with a final cDNA dilution of 1:200 according to the manufacturer's instructions. The sequences of the utilized primers are shown in table 8. Table 9 displays the qPCR steps. For each cell line, the results were normalized to the expression of 5 S RNA by the following equation with RE: relative expression, Ef: efficiency of amplification and Cq: quantification cycle.

$$RE(miRNA) = \frac{Ef(miRNA)^{-Cq(miRNA)}}{Ef(5 S RNA)^{-Cq(5 S RNA)}}$$

## 2 Material and Methods

**Table 8: Primers utilized for miRNA expression analysis.**

Primer name	Product number (Exiqon)	Target sequence 5'-3'
hsa-miR-122-5p	205664	UGGAGUGUGACAAUGGUGUUUG
hsa-miR-125b-5p	205713	UCCCUGAGACCCUAACUUGUGA
hsa-miR-142-3p	204291	UGUAGUGUUCCUACUUUAUGGA

**Table 9: Process steps of the qPCR analysis.**

Process step	Time	Temperature	Step
Polymerase Activation/Denaturation	10 min	95°C	Hold
Amplification	10 sec	95°C	40 cycles
	1 min	60°C	

### 2.2.8 Animal experiments

#### 2.2.8.1 Expression of luciferase cmRNA in a KB tumor model and inhibition of KB tumor growth

The animal experiments were performed at the chair of Pharmaceutical Biotechnology at Ludwig-Maximilians-Universität München (Prof. Dr. Ernst Wagner) and executed by Eva Kessel.  $5 \times 10^6$  KB cells were injected into the flank of female, 6 weeks old NMRI-nu mice (RjOrl:NMRI-Foxn1<sup>nu</sup>/Foxn1<sup>nu</sup>, Janvier Labs). For the pre-experiment testing expression characteristics of the complexed cmRNA, 10 µg of lipid nanoparticle formulated cmRNA coding for firefly luciferase (luc) in 50 µl 2 % sucrose were injected into the formed tumors on days 9, 11 and 13 after injection of tumor cells in anesthetized mice (isoflurane). 24 h after the third application, 100 µl luciferin (60 mg/ml in PBS) were injected intraperitoneal 15 min prior to imaging. Luminescence was measured using an IVIS *in Vivo* Imaging System with Living Image software 3.2 (Caliper Life Sciences, California, USA). For the reduction of tumor growth, the cmRNAs (AT and AU) were formulated in a proprietary lipid formulation (LF132) by Ethris GmbH (Germany) in 2 % sucrose. The cationic lipid formulation LF132 was based on Jarzebinska *et al.* [157]. Treatment was started as soon as tumors had reached the size of about 100 mm<sup>3</sup> (day 9). 50 µl of solution containing either 10 µg of AT-LF132, 10 µg of AU-LF132 or 2 % sucrose were injected intratumorally in anesthetized mice (isoflurane) on days 9, 11, 13 and 18 post injection of tumor cells. Throughout the experiment, the tumor volume was determined with a caliper using the formula  $a \times b^2/2$ , with  $a$  indicating the length of the tumor and  $b$  the width. On day 21 after injection of tumor cells, mice were euthanized by cervical dislocation and the tumors explanted and stored in Roti®-Histofix 4 % for 24 h before measurement of the tumor size was repeated

## 2 Material and Methods

using the formula  $a \times b \times c/2$ . The tumors underwent automatic dehydration and were embedded in paraffin (Paraplast®). Any paraffin block included one transverse section on the level of highest tumor dimension as well as two longitudinal segments from both endings. Tissue blocks were cut into 4 µm thin sections and applied to a glass slide. For histopathological analysis, hematoxylin-eosin staining was performed according to the protocol in the following section. The protocols for animal experiments were approved by the animal ethics committee and the government of Oberbayern (May 26, 2014; Permit Number: Az. 55.2-1-54-2531-53-09) and experiments were executed in accordance with the German Animal Welfare Law.

### 2.2.8.2 Hematoxylin-eosin staining of tumor sections

Sections were heated at 85 °C for 1 h. Following, paraffin was removed by incubation in xylene and the sections hydrated by a succession of descending ethanol concentrations ending in distilled water (*aqua bi-dest*). The sections were incubated in Mayer's Hematoxylin solution for 2.5 min before rinsing them with tap water for 10 min. Subsequently, they were differentiated by dipping them five times into HCl – ethanol followed by immediate rinsing in tap water for 10 min. After incubating the sections for 6 min in acidified Eosin Y solution, they were rinsed again in tap water for 10 min. Dehydration was conducted using a succession of ascending ethanol concentrations and ending in xylene. A coverslip was applied and sealed with Roti®-Histokit II. Quality check was performed before histomorphologic evaluation applying light microscopy (Leica DM 2000 LED microscope) was done. Furthermore, 11 random pictures in vital areas of neoplastic tissue were taken of each tumor with 40x magnification (214 µm x 286 µm) and the number of degenerating cells and cells in mitosis was counted in each picture. Morphologically, the following findings were interpreted to be associated to cell death: 1) shrinkage and dark staining of nucleus, 2) karyorrhexis (fragmentation of nucleus), 3) swelling or shrinkage of the cell with hypereosinophilia of cytoplasm or 4) cellular fragmentation in general. Cells undergoing mitosis were identified by mitotic figures with chromatin condensations and arrangement in physiologic and pathologic manner. In addition, the percentage of necrotic area in relation to the whole tumor tissue on one slide was estimated.

## 2 Material and Methods

### 2.3 Data analysis

Flow cytometry data was analyzed by FlowJo v.10.0.8. GraphPad Prism 6 was utilized for statistical analysis. For analysis of qPCR data and determination of C<sub>q</sub> values, LightCycler® 96 (Roche Diagnostics, Mannheim, Germany) was utilized.

## 3 Results

### 3 Results

The overall aim of the thesis was to test the feasibility of chemically modified mRNAs (cmRNAs) coding for toxic proteins of bacterial or plant origin for employment in anti-cancer therapy. For this purpose two cell culture systems were used with different objectives. A) The hepatocarcinoma cell line HuH7 was employed as it is suitable for follow-up studies exploiting miRNA expression characteristics for cell specific translation. B) Tumors derived from the cervix carcinoma cell line KB are well-suited for first *in vivo* experiments testing the toxin-encoding cmRNAs. Following transfection with toxin-encoding cmRNA both cell lines were examined *in vitro* and, in case of KB cells, in an *in vivo* tumor model.

#### 3.1 Cloning of toxin constructs and cmRNA production

At the beginning, the design, cloning and cmRNA production of the A-chains of three different AB-toxin constructs and their controls was performed. The utilized toxins were subtilase cytotoxin (SubA), diphtheria toxin (DTA) and abrin-a (AA). Two control cmRNAs were employed for each toxin; one showing mutations of one or two amino acids in the protein sequence, allegedly rendering the protein non-functional (SN, DN, AN). The other one displayed a scrambled Kozak sequence [1] and the start codon as well as all downstream ATGs were changed to TAGs, resulting in a non-translatable cmRNA (SU, DU, AU). The corresponding DNA sequences were cloned into a pVAX1-A120 plasmid [20] and cmRNA containing the modified nucleotides 5'-methylcytosine and 2'-thiouridine was produced in an *in vitro* transcription (IVT) reaction and was followed by post-capping. The single bands of the agarose gel in figure 6 show that the produced cmRNAs displayed the correct size (SubA: 1.3 kb, DTA: 0.8 kb, AA: 1.0 kb) and high purity.

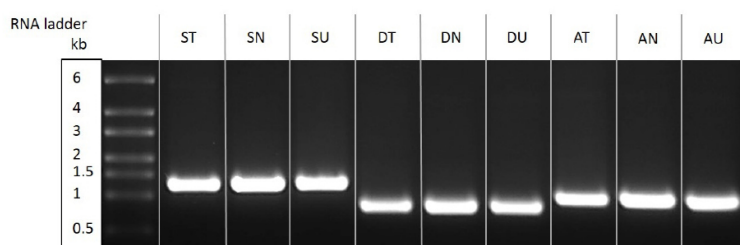


**Figure 6: Agarose gel electrophoresis of SubA, DTA and AA toxin and control cmRNAs.** 2  $\mu$ g cmRNA of each construct were loaded on 1 % agarose gel. RiboRuler High Range RNA ladder (Thermo Fisher) was used to determine the correct length (SubA: 1.3 kb, DTA: 0.8 kb, AA: 1.0 kb) of the transcripts. As expected, only a single band was present for each construct.

## 3 Results

### 3.2 HuH7 cells – A cell culture system for investigation of cell specific mRNA translation

In the first part of the thesis, HuH7 cells were examined *in vitro* for the effects of transfection with toxin-encoding cmRNA by examining protein expression, cell viability and cell death, apoptosis and the occurrence of a bystander effect. Also, designs for cell-specific translation of the cmRNAs were performed.

#### 3.2.1 Transfection of HuH7 cells with toxin-encoding cmRNAs *in vitro*

##### 3.2.1.1 Inhibition of EGFP fluorescence by toxin-encoding cmRNAs in HuH7 cells

To confirm the activity of the transfected cmRNAs, the degree of protein synthesis inhibition was assessed. For this purpose, 50 ng EGFP cmRNA were co-transfected with varying amounts of either one of the toxin cmRNAs or their controls. 24 h post transfection, EGFP fluorescence was evaluated by fluorescence microscopy (fig. 7a) and flow cytometry analysis (fig. 7b-c). Inhibition of translation was indirectly proportional to the measured EGFP fluorescence. The flow cytometry results were normalized to cells transfected only with EGFP cmRNA (EGFP ctrl, 100 %).

The fluorescence images (10 ng toxin or control cmRNA) in fig. 7a displayed no fluorescence after transfection with the toxin cmRNAs while cells transfected with the untranslatable control cmRNAs showed high fluorescence. In contrast to SN and DN, AN transfection also lead to reduced fluorescence intensity. Measurements of the Mean Fluorescence Intensity (MFI) of EGFP (fig. 7b) confirmed the previous results. In comparison to EGFP ctrl cells, a reduction of 20 % (ST), 62 % (DT) and 51 % (AT) for 0.04 ng and of 90 % (ST), 96 % (DT) and 97 % (AT) for 5 ng cmRNA was detected. Similarly, the percentage of EGFP positive cells decreased with rising amounts of toxin cmRNA (fig. 7c). At 5 ng, only 12 % of cells transfected with DT or AT cmRNA displayed EGFP fluorescence when compared to EGFP ctrl. For ST, the percentage of EGFP positive cells remained above 50 % at 5 ng cmRNA. At the lower dose, 87 % of cells were still EGFP positive for DT or AT cmRNA while no reduction in the fraction of EGFP expressing cells could be detected for ST cmRNA. Transfection with AN cmRNA showed an inhibiting influence on protein expression at the higher dose, albeit to a smaller extent than AT cmRNA. For the nonfunctional controls SN and DN cmRNA, no changes in EGFP production compared to EGFP ctrl cells were noticed. The mentioned alterations in MFI of EGFP and in the percentage of EGFP

### 3 Results

positive cells were statistically significant compared to the respective untranslatable control cmRNAs.

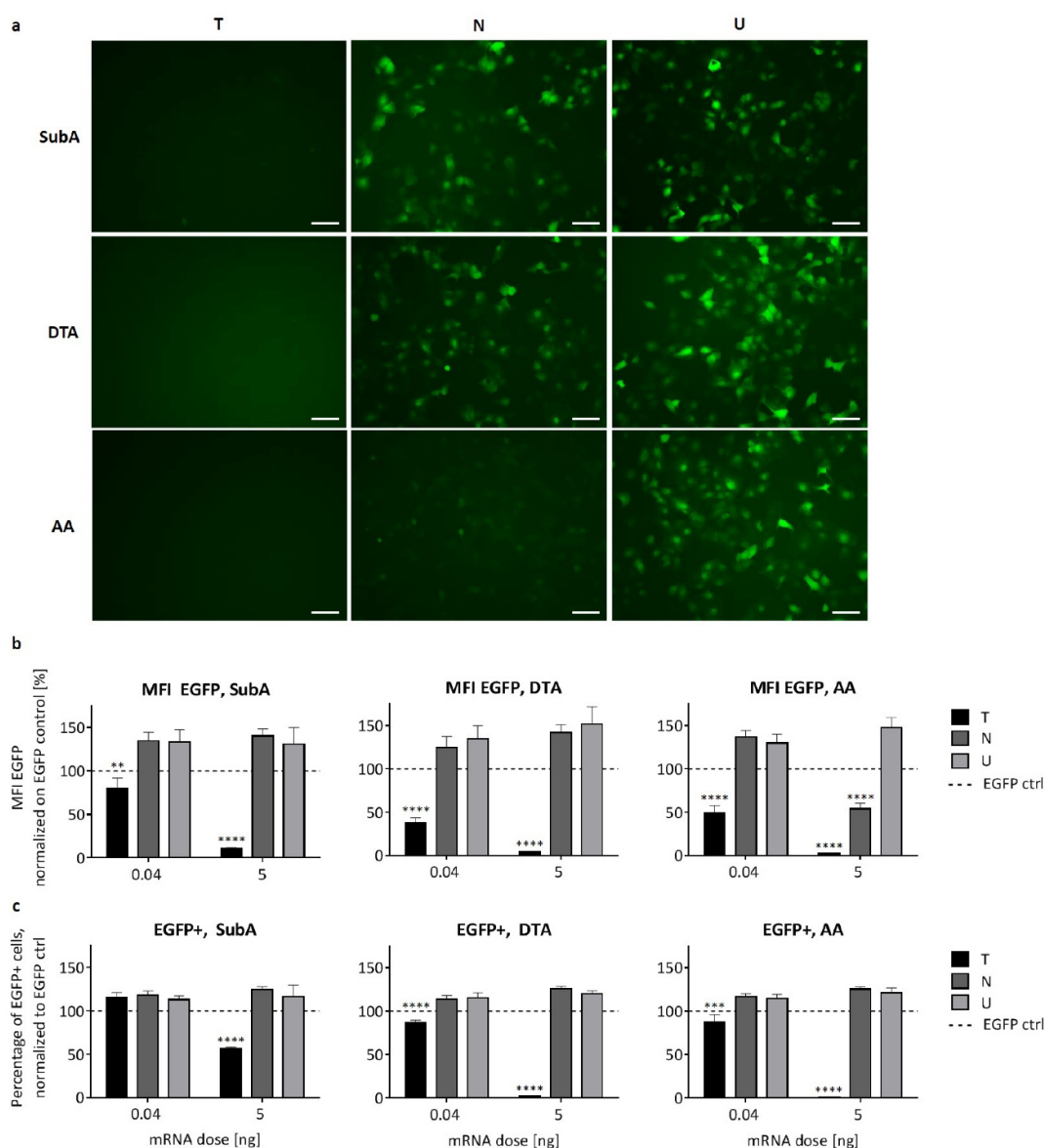


**Figure 7: Inhibition of EGFP fluorescence in HuH7 cells by toxin-encoding cmRNAs.** HuH7 cells (96 well plate, 8,000 cells/100 μl, 100 μl medium per well) were co-transfected using the lipofectamine® 2000 transfection reagent (Thermo Fisher) with 50 ng/100 μl EGFP cmRNA and toxin (T), nonfunctional control (N) or untranslatable control (U) cmRNA coding for SubA, DTA or AA. cmRNA doses are given in ng/100 μl. 24 h post transfection, inhibition of protein synthesis was assessed by fluorescence microscopy (a) and flow cytometry (b, c). Representative images of cells transfected with 10 ng/100 μl toxin or control cmRNA are shown (a). The scale bars represent 100 μm. Mean Fluorescence Intensity (MFI) (b) and percentage of EGFP positive cells (c) are depicted. Data are represented as mean in % ± SEM of control cells transfected only with EGFP cmRNA (EGFP ctrl, dotted line). Cells were gated on singlet cells. Statistical significance versus the respective untranslatable control was assessed by 2-way ANOVA adjusted for multiple comparisons, with \*\*: p<0.01 and \*\*\*\*: p<0.0001. The experiment was repeated three (SubA) or four (DTA and AA) times with n=2 each.

### 3 Results

Figure 8 displays a comparison of the protein synthesis inhibitory capacity of the three toxin cmRNAs. Remarkably, though EGFP fluorescence in cells treated with ST cmRNA could be inhibited almost completely (fig. 8a), a high percentage of cells remained EGFP positive (fig. 8b). This observation is further illustrated by the flow cytometry histograms shown in figure 8c. While EGFP fluorescence was not altered for all three untranslatable controls, it was substantially reduced at 0.16 ng and completely inhibited at 10 ng for DT and AT cmRNA. At 10 ng ST cmRNA, though EGFP fluorescence was clearly reduced, a considerable number of cells remained EGFP positive. From the half-logarithmic plots, the IC50 values – the values where the MFI of EGFP (fig. 8a) or the percentage of EGFP positive cells (fig. 8b) were reduced by 50 % - were calculated (fig. 8d). These IC50 values illustrate that higher cmRNA doses (28-, 9- or 10-fold respectively for ST, DT or AT) were necessary to reduce the percentage of EGFP positive cells by 50 % than to halve the MFI of EGFP, each in comparison to EGFP ctrl cells. Also, AT and DT cmRNA proved to be more potent in the reduction of EGFP expression than ST cmRNA.

### 3 Results

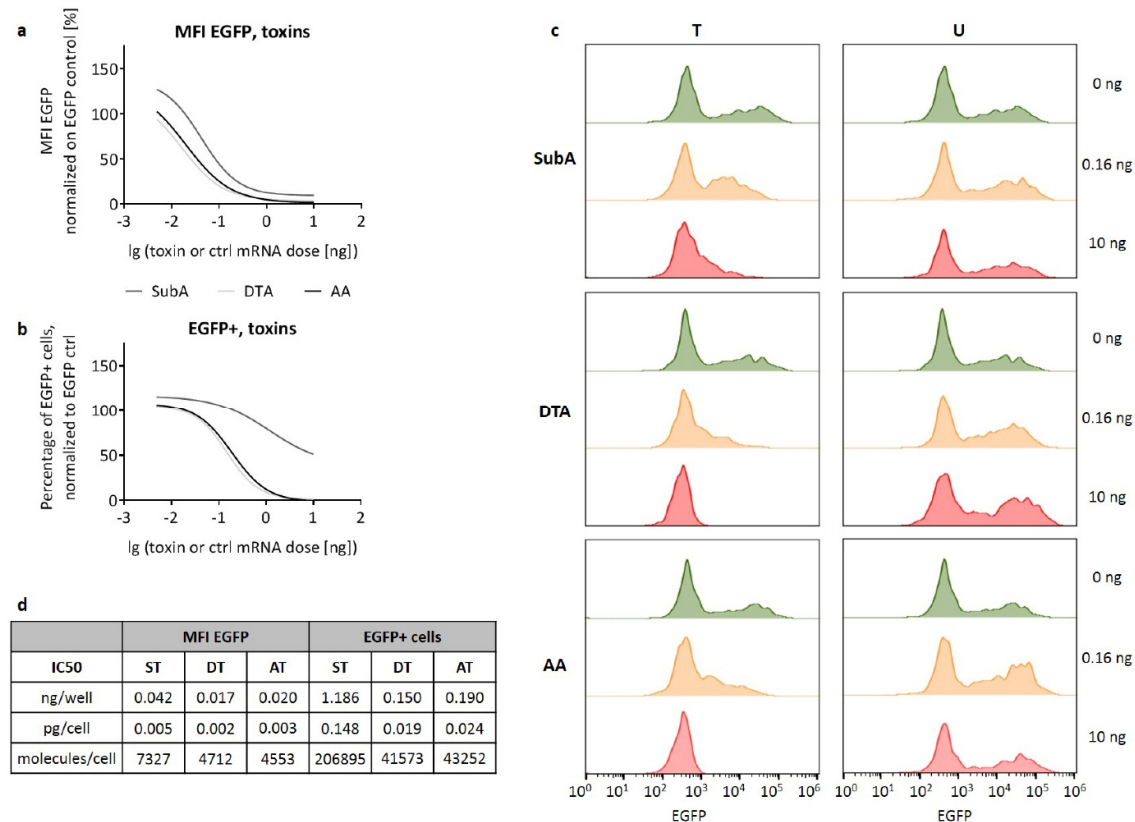


**Figure 8: Inhibition of EGFP fluorescence in HuH7 cells – comparison of effectivity.** HuH7 cells (96 well plate, 8,000 cells/100  $\mu$ l, 100  $\mu$ l medium per well) were co-transfected using the lipofectamine<sup>®</sup> 2000 transfection reagent (Thermo Fisher) with 50 ng/100  $\mu$ l EGFP cmRNA and toxin (T) or untranslatable control (U) cmRNA coding for SubA, DTA or AA. cmRNA doses are given in ng/100  $\mu$ l. 24 h post transfection, inhibition of protein synthesis was assessed by flow cytometry. Cells were gated on singlet cells. Half-logarithmic plots showing the dose-dependency of the Mean Fluorescence Intensity (MFI) (a) and of the percentage of EGFP positive cells (b) after transfection with the toxin cmRNAs are depicted. Data are represented as mean in %  $\pm$  SEM of control cells transfected only with EGFP cmRNA (EGFP ctrl, dotted line). Representative flow cytometry histograms compare cells transfected with different doses of the toxin or the untranslatable control cmRNAs (c). The IC50 values are given in ng/well, pg/cell and molecules/cell (d) for the three toxin cmRNAs. The experiment was repeated three (SubA) or four (DTA and AA) times with n=2 each.

These experiments could demonstrate that the three toxin-encoding cmRNAs are translated into active proteins upon transfection and inhibit protein synthesis considerable in a dose-dependent manner.

#### 3.2.1.2 Toxicity of toxin-encoding cmRNAs on HuH7 cells

As next step the cytotoxicity after transfection was investigated by assessing influence on cell viability and on cell growth. In a first assay, HuH7 cells were transfected with the three toxin cmRNAs or their controls and 48 h post transfection cells were examined microscopically (fig. 9a) and cell viability was determined by measuring the ATP content (fig. 9b).

The images in figure 9a clearly show reduced cell numbers and a change in morphology of cells transfected with 50 ng ST, DT or AT cmRNA in comparison to untransfected control cells (UT)

### 3 Results

or cells transfected with the untranslatable control cmRNAs (U). In a small number of cells, morphological alterations were visible for the nonfunctional control cmRNAs DN and AN. The results of the cell viability measurements were normalized to the values of UT cells (100 %) (fig. 9b). At 3.125 and 6.25 ng doses, no significant changes in cell viability were observed for any of the applied cmRNAs. For all three toxin cmRNAs, cell viability was reduced by about 80 % at the highest dose and by approximately 60 % at 50 ng in comparison to UT cells [65]. At 12.5 ng cmRNA, decrease in cell viability was highest for DT cmRNA with 31 % and lowest for ST cmRNA with 21 % compared to UT cells. Remarkably, transfection with DN or AN cmRNA also lead to a considerable decrease in cell viability. Although less toxic than the respective toxin cmRNAs, luminescence was reduced up to 70 % at 100 ng dose compared to UT cells. At this dosage, SN cmRNA also reduced cell viability significantly in comparison to UT cells and the untranslatable control cmRNAs likewise demonstrated minor toxicity. The reduction in cell viability was, in case of the toxin cmRNAs for dosages starting at 12.5 ng and for DN and AN at 25, 50 and 100 ng doses, statistically significant when compared to the respective untranslatable control cmRNAs.

### 3 Results

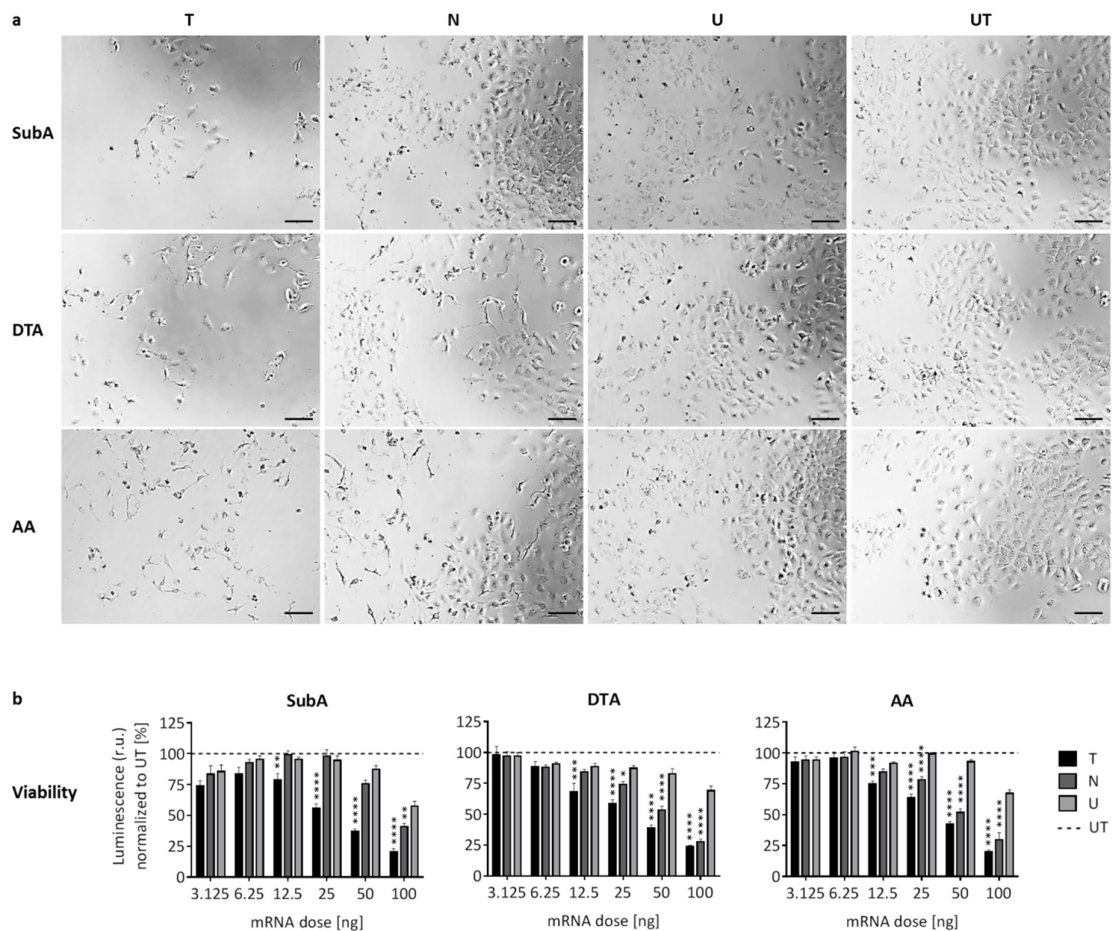


**Figure 9: Toxicity of toxin-encoding cmRNAs on HuH7 cells – dose-dependency.** 48 h post transfection of HuH7 cells (96 well plate, 3,000 cells/100  $\mu$ l, 100  $\mu$ l medium per well) using the lipofectamine<sup>®</sup> 2000 transfection reagent (Thermo Fisher) with toxin (T), nonfunctional control (N) or untranslatable control (U) cmRNA coding for SubA, DTA or AA. a) Representative pictures were taken of cells transfected with 50 ng/100  $\mu$ l cmRNA. The scale bars represent 100  $\mu$ m. b) Cell viability was determined by measuring ATP content with the CellTiter Glo<sup>®</sup> Luminescence Viability Assay (Promega). Cell viability was proportional to the measured luminescence. Data is represented as mean in %  $\pm$  SEM of untransfected control cells (UT, dotted line). cmRNA doses are given in ng/100  $\mu$ l. Statistical significance versus the respective untranslatable control was assessed by 2-way ANOVA and adjusted for multiple comparisons, with \*:  $p < 0.05$ , \*\*:  $p < 0.01$ , \*\*\*:  $p < 0.001$  and \*\*\*\*:  $p < 0.0001$ . The experiment was repeated three times with  $n=3$  each.

In the ensuing experiments time-dependency was examined (fig. 10). For this, cell growth was surveyed by assessment of cell viability and by measuring impedance in the well bottom as an indication for the degree of cell density. Cell viability (fig. 10a) was determined by quantifying the ATP content over 69 h. Figure 10b and 10c show the impedance measurements performed over 96 h at two different starting cell densities. For all three experiments, 50 ng of cmRNA were applied and results were set to 100 % (viability) or to 1 (impedance) at 5 h after transfection.

All three experiments clearly showed a slowdown or stop of cell growth after transfection with the toxin-encoding cmRNAs. In the first 24 h after transfection, cell viability continued to rise,

### 3 Results

though markedly slower than in case of UT cells (fig. 10a). From 24 h post transfection onwards cell viability decreased in case of all three toxins, though to a higher degree for ST than for DT or AT cmRNA. Transfection with the untranslatable control cmRNAs (U) or SN cmRNA showed only marginal influence on cell viability. For transfections with the nonfunctional control cmRNAs DN and AN, however, considerable toxicity was observed and cell viability remained constant after 24 h post transfection. 96 h after transfection, luminescence of UT cells was increased 5.7 times compared to 5 h after transfection.

Two different cell numbers were plated for the impedance measurements. At 3,000 plated cells (fig. 10b), all three toxin cmRNAs lead to a decrease in cell density directly after transfection, with the highest decline seen for DT followed by ST. No recurrence of cell growth could be observed at the lower cell number. At 6,000 plated cells (fig. 10c), following a first recession, cell density increased again around 40 h post transfection with DT or AT cmRNA. Though no decline in impedance was seen for transfections with ST cmRNA with 6000 plated cells, cell density remained constant. For all impedance experiments, no divergence from untransfected control cells (UT) was observed for cells transfected with one of the untranslatable control cmRNAs (U). As also noticed in the preceding assays, cells transfected with DN or AN cmRNA displayed considerable toxicity while cells transfected with SN cmRNA showed none. The cell density of untransfected cells at 96 h was 6-fold higher than at 5 h for 3,000 plate cells while it increased only 2.4 times for 6,000 plated cells.

### 3 Results

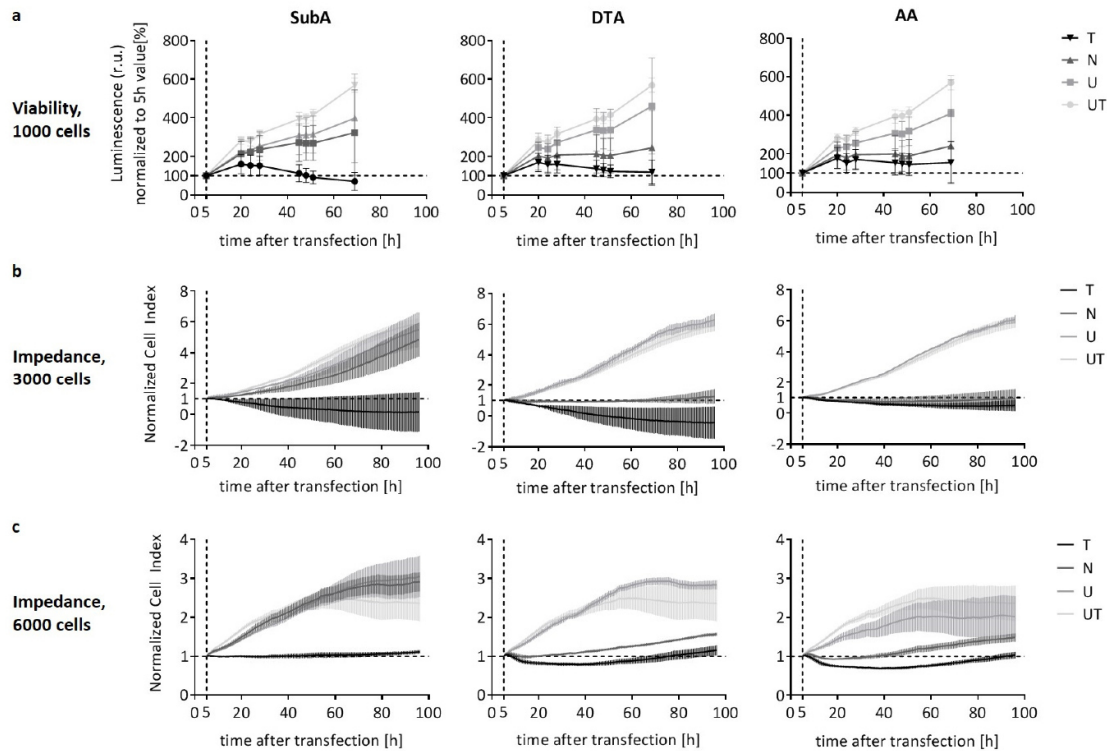


**Figure 10: Toxicity of toxin-encoding cmRNAs on HuH7 cells – time-dependency.** HuH7 cells (96 well plate, 100  $\mu$ l medium per well) were transfected using the lipofectamine<sup>®</sup> 2000 transfection reagent (Thermo Fisher) with 50 ng/100  $\mu$ l of toxin (T), nonfunctional control (N) or untranslatable control (U) cmRNA coding for SubA, DTA or AA. a) 1,000 cells per well. Cell viability was determined by measuring ATP content with the RealTime-Glo<sup>™</sup> MT Cell Viability Assay (Promega). Cell viability was proportional to the measured luminescence. Data is represented as mean  $\pm$  SEM of the value 5 h post transfection (dotted line). The experiment was repeated three times with  $n=1$  each. b), c) Impedance measurements were performed on an xCELLigence instrument. Data is represented as mean  $\pm$  SEM of the multiple of values at 5 h post transfection (dotted line). The experiment was repeated twice with  $n=1$  (b) and  $n=2$  (c) each. (b) 3,000 cells/100  $\mu$ l medium. (c) 6,000 cells/100  $\mu$ l medium.

In order to investigate the inhibition of cell growth in a third manner, a so-called scratch experiment was performed. The time required for the scratch to close is indirect proportional to the proliferating potential of the cells. Confluent HuH7 cells were transfected with 50 ng cmRNA and the cell layer was scratched at 4 h post transfection. Cell growth was monitored microscopically over 192 h (figure 11). In case of the two examples of untransfected cells (UT), the scratch was closed by half after 96 h and was no longer visible at 192 h post transfection. For all three toxin-encoding cmRNAs, ingrowth of cells was slower than for UT cells. At 192 h post transfection, a broad scratch was still apparent, larger for DT and AT than for ST cmRNA. In case of the untranslatable control cmRNAs SU and AU the scratch was closed 192 h after transfection while a small gap was still visible for DU cmRNA transfected cells. For all groups, gap width was reduced at 96 h compared to 0 h.

### 3 Results

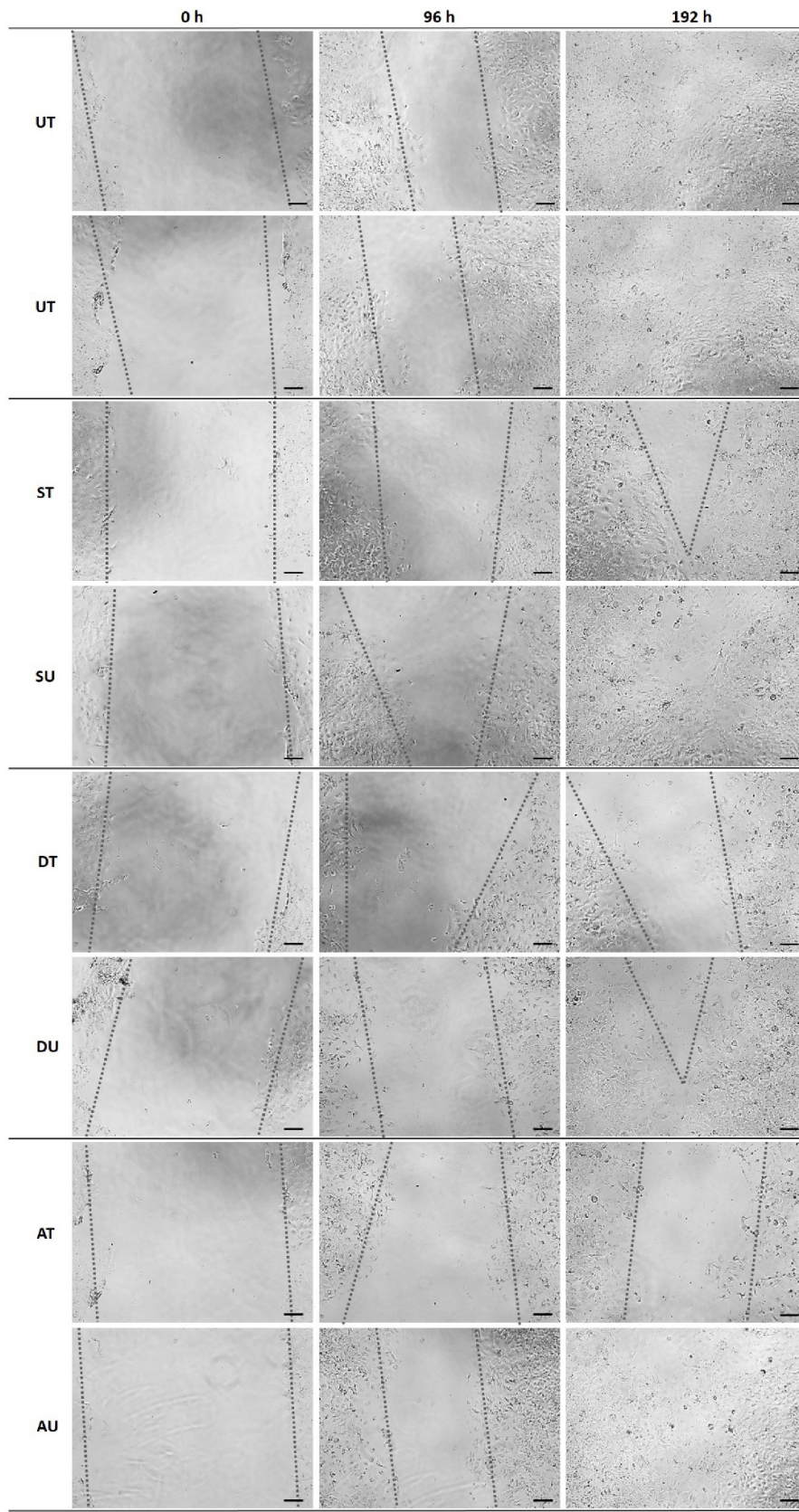


**Figure 11: Inhibition of cell growth by toxin-encoding cmRNAs in HuH7 cells: Scratch Assay.** A confluent layer of HuH7 cells (96 well plate, 100  $\mu$ l medium per well) was transfected using the lipofectamine<sup>®</sup> 2000 transfection reagent (Thermo Fisher)

### 3 Results

with 50 ng/100  $\mu$ l of toxin (T) or untranslatable control (U) cmRNA coding for SubA, DTA or AA. 4 h after transfection, the cell layer was scratched. The ingrowth of cells into the scratch was monitored over time. The scale bars represent 100  $\mu$ m.

The foregoing experiments showed that transfection with the three toxin-encoding cmRNAs reduced cell viability and cell growth in a dose- and time-dependent manner.

#### 3.2.1.3 Influence on cell cycle in HuH7 cells by toxin-encoding cmRNAs

Variations in cell cycle progression of HuH7 cells transfected with 50 ng cmRNA were examined (fig. 12) next. Figure 12a depicts a representative flow cytometry histogram of untransfected cells at 24 h post transfection. The graphs in figure 12b show the distribution of cells between the three phases of the cell cycle determined by flow cytometry. 24 h post transfection, the fraction of cells in the  $G_0/G_1$  phase was increased while fewer cells were found in the S phase for all three SubA cmRNAs (T, N, U) when compared to untransfected control cells (UT). No change was noticeable for the  $G_2/M$  phase. At 48 h, however, fewer cells were present in the  $G_2/M$  phase but more in the  $G_0/G_1$  phase in comparison to UT cells. Compared to UT cells, the percentage of cells that were in S phase was decreased for ST cmRNA. In case of DTA, the fraction of cells in the S and in the  $G_2/M$  phase was reduced but enhanced in the  $G_0/G_1$  phase for the toxin (T) and the nonfunctional control (N) cmRNA at 24 h post transfection compared to UT cells. It remained unchanged in all three phases for cells transfected with DU cmRNA. At 48 h time point, DT cmRNA induced a reduction of cells in all three phases, DN cmRNA lowered the percentage of cells in S and  $G_2/M$  phase and transfection with DU cmRNA resulted in a decreased number of cells in the  $G_2/M$  phase compared to UT cells. 24 h post transfection, the three AA cmRNAs each displayed a behavior similar to, but less extensive, than DTA. 48 h post transfection, more cells in the case of AU but fewer cells for AT and AN cmRNA were detected in the S phase in comparison to UT cells. The percentage of cells in the  $G_2/M$  phase was similar to UT cells for AT and AN but was diminished in case of AU cmRNA.

### 3 Results

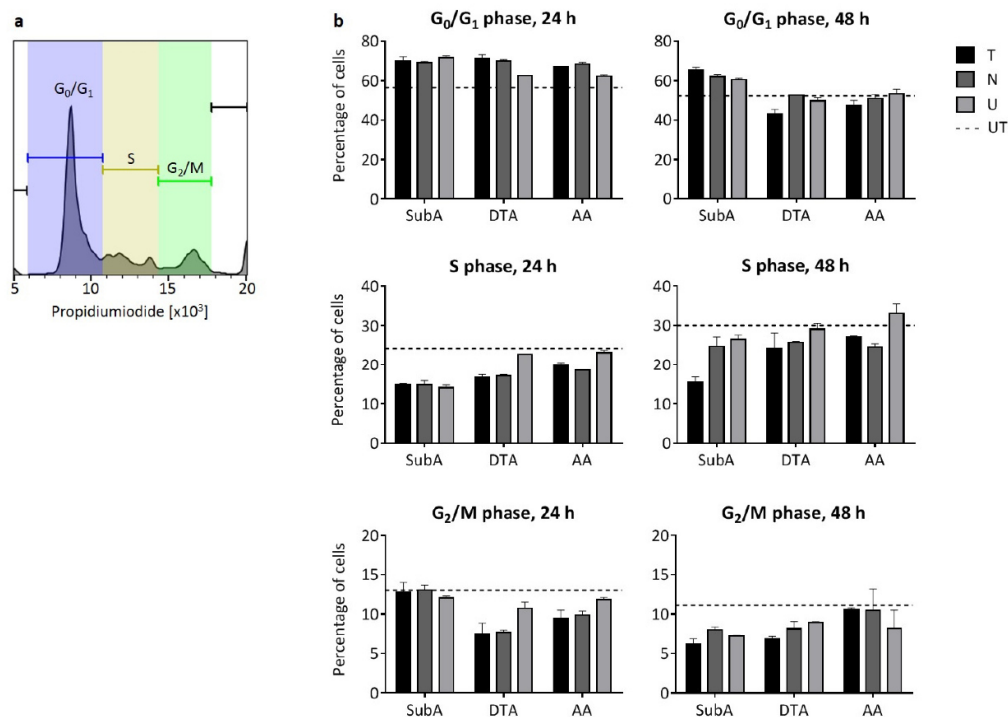


**Figure 12: Cell cycle analysis of HuH7 cells after transfection with toxin-encoding cmRNAs.** HuH7 cells (96 well plate, 8,000 cells/100  $\mu$ l and 100  $\mu$ l medium per well at 24 h; 48 well plate, 5000 cells/100  $\mu$ l, 200  $\mu$ l medium per well at 48 h) were transfected using the lipofectamine<sup>®</sup> 2000 transfection reagent (Thermo Fisher) with 50 ng/100  $\mu$ l of toxin (T), nonfunctional control (N) or untranslatable control (U) cmRNA coding for SubA, DTA or AA. At the indicated time points, cells were fixed and permeabilized with ethanol and subsequently stained with a solution containing the DNA dye propidium iodide (PI) and RNase A before analysis by flow cytometry. Cells were gated on singlet cells. a) Representative flow cytometry histogram. The degree of PI fluorescence is directly proportional to the DNA content of the cell and thus signifies the cell cycle phases G<sub>0</sub>/G<sub>1</sub>, S and G<sub>2</sub>/M. b) Results of the flow cytometry assay are given in percentages of cells in the respective phases of cell cycle. Data is represented as mean in %  $\pm$  SEM and compared to the level of untransfected control cells (UT, dotted line). The experiment was performed once with n=2.

These results demonstrate that only small changes in cell cycle progression were elicited by transfection with toxin-encoding cmRNAs and that those were mainly due to transfection itself. Considerable divergence from the values for cells transfected with the untranslatable control cmRNAs was observed only for ST cmRNA at 48 h and for DT cmRNA at 24 h post transfection.

#### 3.2.1.4 Apoptotic characteristics of cell death in HuH7 cells after transfection with toxin-encoding cmRNAs

Having confirmed that the three toxin cmRNAs induce cell death (refer to section 3.2.1.2), the manner of cell death was investigated by examining the toxin cmRNAs and their untranslatable controls (fig. 13).

First, the activity of caspases-3 and -7 was assessed (fig. 13a) and the results were normalized to the value of untransfected control cells (UT, 100 %). 72 h post transfection, caspase-3 and -7

### 3 Results

activity was induced by ST cmRNA and reached values twice as high as for UT cells. In comparison to UT cells, transfection with DT or AT cmRNA resulted in reduction of luminescence by 30 or 40 %, respectively. Those changes showed statistical significance versus the respective untranslatable control cmRNAs. The three untranslatable cmRNAs (U) showed little effect, with a decrease in luminescence by 10-15 %.

Apoptotic cells can be identified in flow cytometry by performing a double-staining with Annexin V-AF488 and propidiumiodide (PI). Figure 13b and 13c present the results of this experiment 72 h after transfection, with figure 13b showing a representative dot plot. The Annexin V positive but PI negative population corresponds to cells in apoptosis, the double positive to dead cells and the double negative cells are viable. 7 % apoptotic cells were present in UT cells and a slight increase in the percentage of apoptotic cells to 18 % of all cells could be observed after transfection with one of the three toxin cmRNAs. The change was significant for ST and DT cmRNA versus the respective untranslatable controls. As for the caspase-3 and -7 assay, no alterations were induced by the control cmRNAs.

In a third experiment, DNA fragmentation following transfection was investigated employing the so-called Nicoletti Assay [155, 158]. Representative flow cytometry histograms at 72 h after transfection are depicted in figure 13d. The formation and heightening of the SubG<sub>1</sub> peak, representing apoptotic cells, was clearly visible for toxin cmRNA (T) transfected cells in contrast to cells transfected with the untranslatable control cmRNAs (U). 48 h post transfection, the percentage of apoptotic cells rose to 29 % for ST and to 35 % for AT cmRNA in contrast to UT cells (16 %) (fig. 13e). However, a slight increase to 23 % was detected for the respective control cmRNAs (SU, AU). Transfection with DT cmRNA resulted in 34 % apoptotic cells and the alteration was significant compared to the control cmRNA (DU). The fraction of apoptotic cells at 72 h post transfection rose to 42 (ST), 33 (DT) or 55 % (AT), while it was 15 % for UT cells. At the later time point, transfections with the control cmRNAs (U) had no influence on the number of cells in apoptosis and alterations caused by the toxin cmRNAs were statistically significant.

### 3 Results

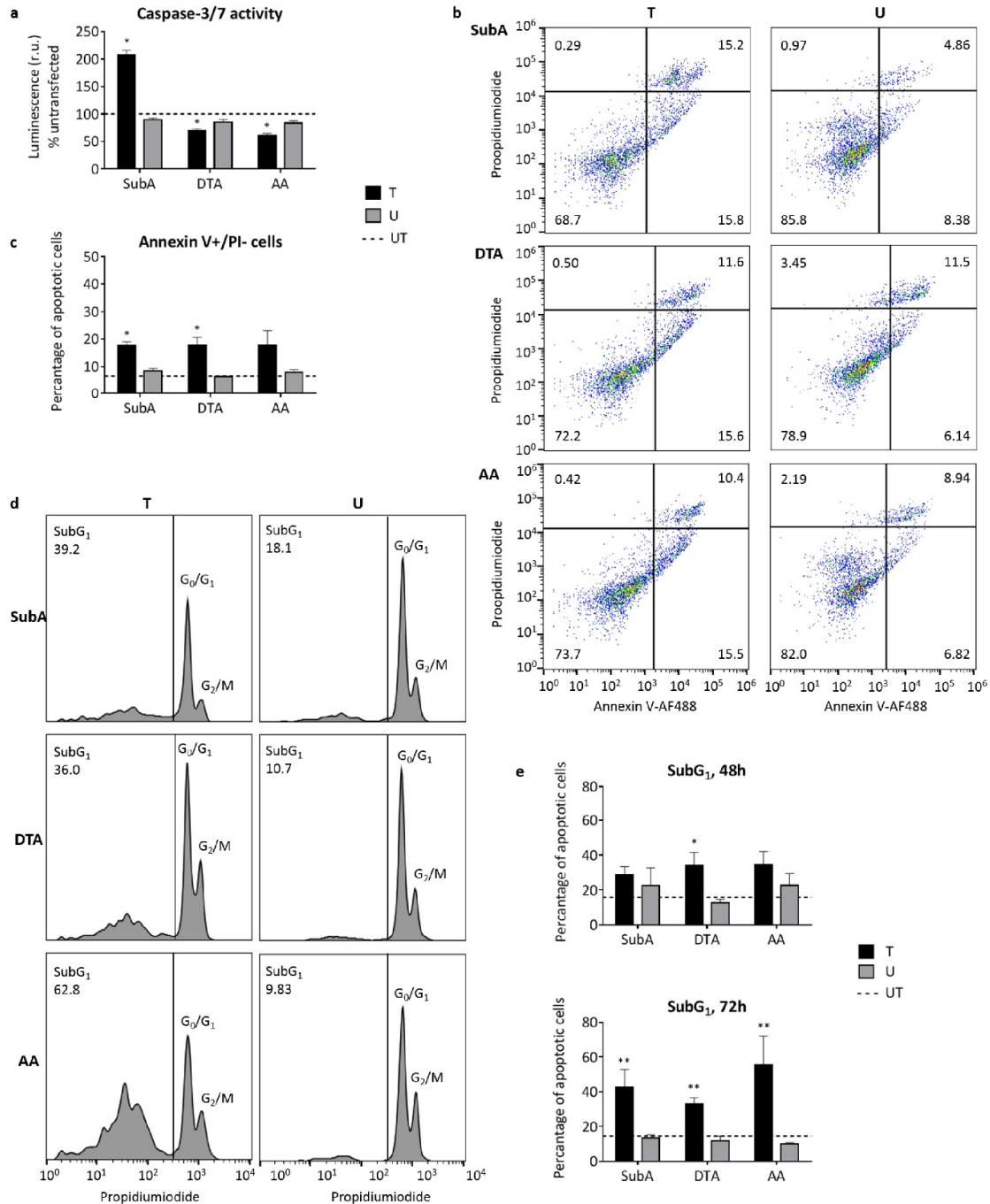


**Figure 13: Apoptotic characteristics of cell death induced by toxin-encoding cmRNAs on HuH7 cells.** HuH7 cells were transfected using the lipofectamine® 2000 transfection reagent (Thermo Fisher) with the toxin (T) or untranslatable control (U) cmRNAs coding for SubA, DTA or AA. a) Caspase-3 and -7 activity was determined using the Caspase-Glo® 3/7 Assay (Promega) 72 h after transfection with 30 ng cmRNA/100 µl medium. 96 well plates with 3,000 cells/100 µl and 100 µl medium per well were employed. Data is represented as mean in % ± SEM of untransfected control cells (UT, dotted line). The experiment was repeated twice with n=2 each. Statistical significance versus the respective untranslatable control was assessed by Mann-Whitney test with \*: p<0.05. b), c) Apoptotic cells (identified as Annexin V positive and propidium iodide (PI) negative) were analyzed by flow cytometry of cells stained with the fluorophore Annexin V-AF488 (Thermo Fisher) and PI (Sigma). The experiment was done 72 h post transfection with 50 ng cmRNA/100 µl medium. Cells were gated on singlets. 24 well plates with 7,500 cells/100 µl medium and 400 µl medium per well were employed. b) Representative flow cytometry dot plots. Percentages of cells in a certain population are given in the respective corners. c) Flow cytometry results. Data is represented

### 3 Results

as mean in %  $\pm$  SEM and compared to untransfected control cells (UT, dotted line). Statistical significance versus the respective untranslatable control was assessed by Mann-Whitney test with \*:  $p < 0.05$ . The experiment was repeated three times with  $n=1$  or  $n=2$  each. d), e) Apoptotic cells (identified as hypodiploid/SubG<sub>1</sub> peak) were analyzed by flow cytometry after permeabilization with ethanol and staining with PI (Sigma). The experiment was done at 48 h and 72 h post transfection with 50 ng cmRNA/100  $\mu$ l medium. Cells were gated on singlets. 24 well plates with 7,500 cells/100  $\mu$ l medium and 400  $\mu$ l medium per well were employed. d) Representative flow cytometry histograms. The peaks of diploid (G<sub>0</sub>/G<sub>1</sub>), tetraploid (G<sub>2</sub>/M) and hypodiploid (SubG<sub>1</sub>) cells are indicated and the percentage of hypodiploid cells is given. (e) Flow cytometry results. Data is represented as mean in %  $\pm$  SEM and compared to untransfected control cells (UT, dotted line). Statistical significance versus the respective untranslatable control was assessed by Mann-Whitney test with \*:  $p < 0.05$  and \*\*:  $p < 0.01$ . The experiment was repeated twice with  $n=2$  each for 48 h and performed two to four times with  $n=1$  or  $n=2$  each for 72 h.

Summarizing, these results demonstrated that, at least in part of the cells, transfection with the toxin-encoding cmRNAs resulted in apoptosis.

#### 3.2.1.5 Bystander effect after transfection of HuH7 cells with toxin-encoding cmRNAs

Two assays were designed to detect the existence of a possible bystander effect after transfection of HuH7 cells.

In the first experiment (fig. 14), supernatants and lysates (5 or 50  $\mu$ g of total protein) of transfected cells were added to HuH7 cells 24 h post transfection. 72 h afterwards, cell viability was quantified. Figure 14a displays HuH7 cells 24 h post transfection as well as cells 72 h after the transfer of lysates (50  $\mu$ g protein). In cells transfected with the toxin cmRNAs morphological alterations were observed and, in case of AT, a reduced number of cells was seen when compared to untransfected cells (UT). Cells treated with the lysates of DT or AT cmRNA transfected cells showed no observable difference to cells treated with the lysate of UT cells. In contrast, only few cells were visible after treatment with the lysate of ST cmRNA transfected cells. These observations were confirmed by cell viability measurements (fig. 14b). The quantified luminescence, directly proportional to cell viability, was normalized to cells treated with the supernatant or with the lysates of untransfected control cells (UT, 100 %). Apart from ST cmRNA, the supernatants and lysates of transfected cells showed no increased toxicity compared to those of UT cells. Cells treated with the supernatant or lysates of cells transfected with ST cmRNA, however, displayed statistically significant reduction in luminescence. Decrease in cell viability for ST cmRNA, compared to the UT control, lay at 28 % (supernatant), 45 % (5  $\mu$ g lysate) or 53 % (50  $\mu$ g lysate).

### 3 Results

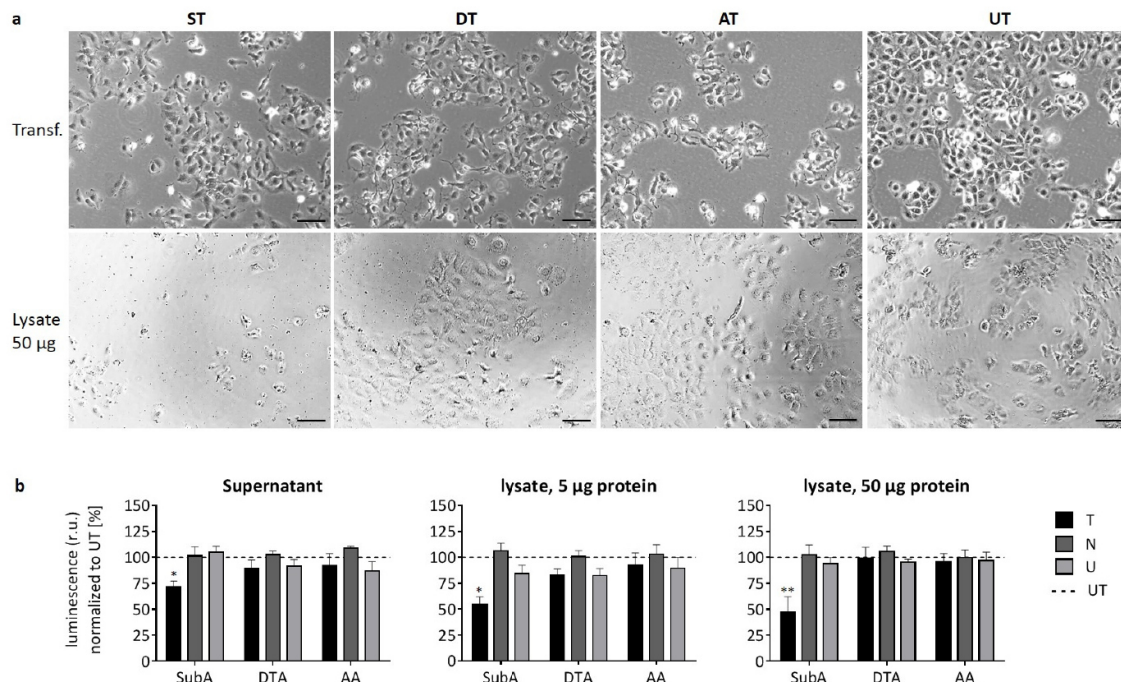


**Figure 14: Bystander effect – Transfer of supernatants and lysates of HuH7 cells transfected with toxin-encoding cmRNAs.** HuH7 cells (6 well plate, 17,000 cells/100 µl and 1.5 ml medium per well) were transfected using the lipofectamine® 2000 transfection reagent (Thermo Fisher) with 50 ng/100 µl of toxin (T), nonfunctional control (N) or untranslatable control (U) cmRNA coding for SubA, DTA or AA and 33 ng/100 µl EGFP cmRNA as transfection control. Untransfected control cells (UT) were applied as control. 24 h after transfection, the supernatant was collected and the cells lysed. The supernatants and two dilutions of the lysates (5 µg or 50 µg protein/100 µl) were added on HuH7 cells (96 well plate, 2000 cells/100 µl, 100 µl medium per well). (a) Representative images of cells 24 h post transfection and of cells 72 h post transfer of supernatant or lysate are depicted. The scale bar represents 100 µm. (b) Cell viability was measured 72 after transfer of supernatant or lysate employing the CellTiter Glo® Luminescence Viability Assay (Promega). Cell viability was proportional to the measured luminescence. Data is represented as mean in % ± SEM of UT cells (dotted line). Statistical significance versus the respective untranslatable control was assessed by Kruskal-Wallis test adjusted for multiple comparisons for supernatants and by 2-way ANOVA, adjusted for multiple comparisons, for the lysates. \*: p<0.05 and \*\*: p<0.01. The experiment was repeated three times with n=2-4 each.

The second assay designed to examine the influence of transfected cells on their surrounding was a magnetofection experiment and was performed exemplarily for DT cmRNA. Transfection was carried out utilizing a transfection reagent comprising magnetic nanoparticles and a magnetic field, leading to locally defined transfection of cells. This was verified by employment of EGFP cmRNA. Fluorescence images taken 48 h after transfection clearly show that EGFP fluorescence was chiefly confined to a circle-shaped area (fig. 15, upper panel). When no magnet was employed, fluorescent cells were distributed more equally around the well. By performing the same experiment with DT-encoding cmRNA, analogous results were obtained (fig. 15, lower panel). In the area corresponding to the magnet, very few viable cells were found while exterior none or only small toxicity to the cells was visible. A confluent cell layer and no signs of toxicity were observed for DT transfections without the magnet.

### 3 Results

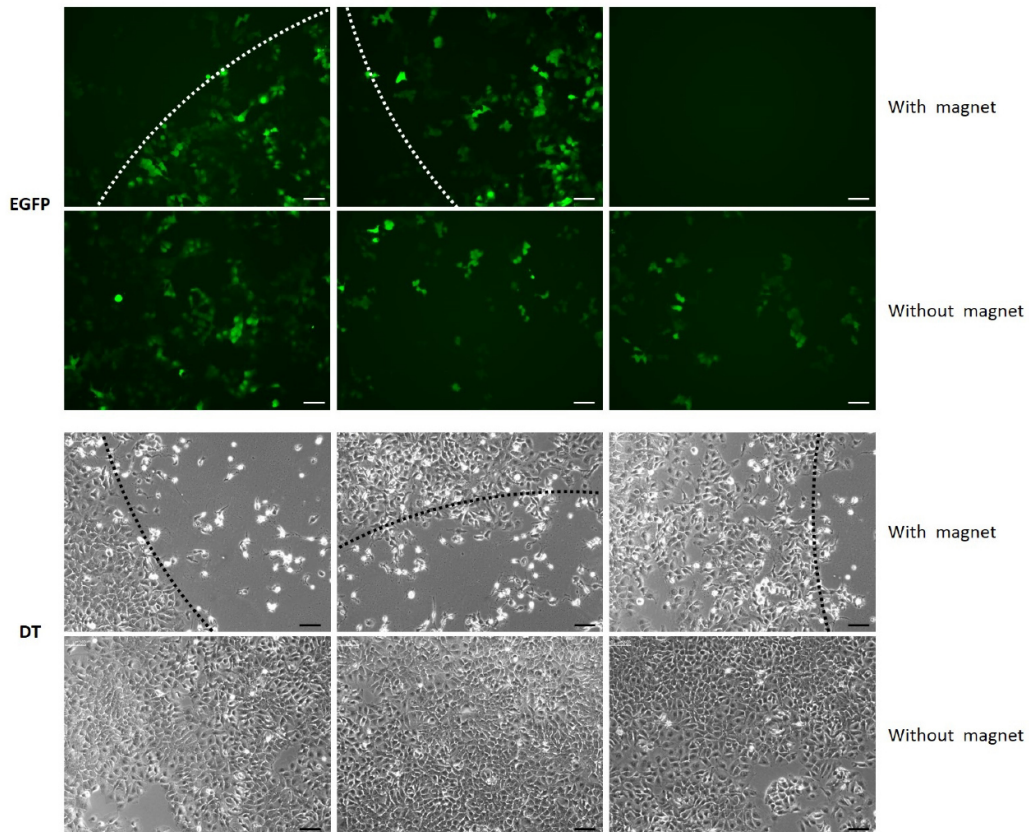


**Figure 15: Bystander effect – Magnetofection of HuH7 cells with DT-encoding cmRNA.** HuH7 cells (12 well plate, 8,000 cells/100  $\mu$ l and 1 ml medium per well) were transfected using DreamFect™ Gold Transfection Reagent (OZ Biosciences) containing magnetic nanoparticles and 25 ng cmRNA/well coding for EGFP or DT (DTA Toxin). 10  $\mu$ l of transfection reagent were added to 390  $\mu$ l medium. In one set of experiments (“with magnet”), a magnet the size of a 96 well plate well was positioned directly below the well for 30 minutes during transfection and the media was changed directly afterwards. Representative pictures were taken 48 h after transfection.

The so far performed experiments could give indications that a bystander effect can be expected after transfection with ST, but not with DT or AT cmRNA.

## 3 Results

### 3.2.2 HuH7 cells – Gaining cell specificity by exploiting miRNA expression profiles

The following part of the study dealt with the objective of rendering cmRNA translation cell specific by incorporation of miRNA binding sites in untranslated regions of cmRNA (cf. fig. 16a). Designs how this could be achieved and a preliminary screening of three miRNA expression profiles in four cell lines were performed. The following cell lines were utilized: HuH7 cells (human liver cancer), HepG2 cells (human liver cancer), U937 cells (human monocytes) and HEK293 cells (human kidney). Figure 16b depicts the expression profiles of the three chosen miRNAs normalized to the expression of 5S RNA in the different cell lines.

The three miRNAs show varieties in their expression level between the different cell lines. miR-122-5p was expressed almost 500 times more in HuH7 cells than in HepG2 cells and 10,000 times more than in U937 cells. In HEK293 cells, no expression was detected. miR-125b-5p was expressed to a similar in degree in HEK293 cells as in HuH7 cells and also to a comparable degree in U937 cells. In HepG2 cells, however, expression was 27-fold lower than in HuH7 cells. miR-142-3p showed high expression in U937 cells. In comparison, this miRNA was expressed 600 times less in HepG2 cells, 8,000 times less in U937 cells and almost no expression was detectable in HuH7 cells. In HuH7 cells, expression of miR-122-5p was around ten times as great as expression of miR-125b-5p. The expression of all three miRNAs was very low in HepG2 cells. In HEK293 cells only miR-125b-5p was expressed to a considerable degree. In U937 cells, miR-122-5p was expressed to a very low extent, miR-125b-5p to a medium degree and miR-142-3p highly. Figure 16c presents a summary table of the expression profiles of the three miRNAs in the four employed cell lines. On the basis of these results, different 3' UTR constructs were designed with the aim of inhibiting translation of the mRNA in one cell line while keeping it active in another. A compilation of the different constructs is depicted in figure 16d. Next to combining different miRNA binding sites, varying numbers of repeats were included. According to the obtained qPCR results, binding sites for miR-122-5p or miR-125b-5p would be suitable to reduce or block translation of the transfected mRNA in HuH7 cells. Binding sites for miR-142-3p in case of U937 cells and for miR-125b-5p regarding U937 and HEK293 cells would be appropriate to hinder mRNA translation.

### 3 Results

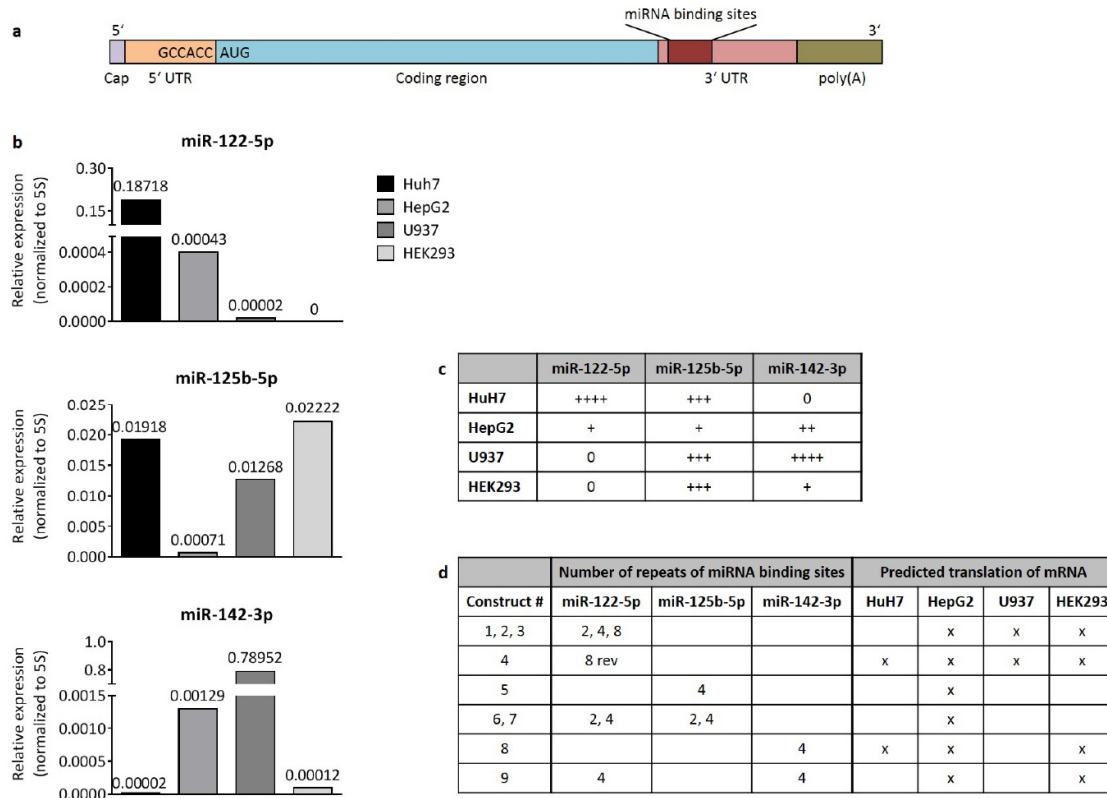


**Figure 16: Exploiting miRNAs for cell-specific translation.** a) Structure of a mature eukaryotic mRNA with incorporated miRNA binding sites in the 3' UTR (3' untranslated region). GCCACC represents the Kozak element [1]. AUG represents the start codon. b) Expression profile of three miRNAs in four cell lines. RNA was isolated from  $3 \times 10^6$  cells using the miRNeasy Mini Kit (Qiagen) and cDNA synthesized with the Universal cDNA synthesis kit (Exiqon). miRNA expression was determined employing the ExiLent SYBR® Green master mix (Exiqon). Triplicates were done. For each cell line and miRNA, the results were normalized to the expression of 5 S RNA by the following equation with RE: relative expression, Ef: efficiency of amplification and Cq: mean of the quantification cycle.  $RE(miRNA) = \frac{Ef(miRNA)^{-Cq(miRNA)}}{Ef(5\ S\ RNA)^{-Cq(5\ S\ RNA)}}$  c) Summary of the expression profiles determined in b). 0: <0.0001, +: 0.0001-0.001, ++: 0.001-0.01, +++: 0.01-0.1, ++++: 0.1-1. d) Display of the constructs designed for cell specific translation. The miRNA binding sites for the according miRNAs were inserted in the 3' UTR of the mRNA. Rev: reverse sequence of miRNA binding site. The table also shows in which cell lines, according to the expression profile, translation of the corresponding mRNA construct would be expected (x).

## 3 Results

### 3.3 KB cells – Investigating *in vitro* and *in vivo* the effects of transfection with toxin-encoding cmRNAs

In the second part of this thesis, the cervix carcinoma cell line KB was employed as it presents a suitable model for tumor experiments. As for HuH7 cells, cytotoxicity, inhibition of protein synthesis and apoptotic characteristics of cell death after transfection with toxin-encoding cmRNAs were examined *in vitro*. Also, the effectivity of the best-performing toxin-encoding cmRNA was tested on KB tumors in mice.

#### 3.3.1 Transfection of KB cells *in vitro* with toxin-encoding cmRNAs

##### 3.3.1.1 Toxicity of toxin-encoding cmRNAs on KB cells

To begin with, the three toxin cmRNAs SubA, DTA and AA were compared regarding their toxicity on KB cells by examining cell viability following transfection. For this purpose, KB cells were investigated 48 h post transfection with toxin (T), nonfunctional control (N) or untranslatable control cmRNA (U) (fig. 17).

The images in figure 17a (50 ng cmRNA) show that transfection with all three toxin cmRNAs had a toxic influence on the cells [65]. In contrast to DN and AN cmRNA, cells transfected with the untranslatable control cmRNAs or with SN cmRNA displayed no alteration compared to untransfected control cells (UT). Cell viability, directly proportional to the measured luminescence, was normalized to UT cells (100 %) (fig. 17b). At 10 ng, no reduction in cell viability compared to UT cells was observed for any of the tested cmRNAs [65]. In case of ST cmRNA, decrease in luminescence was comparatively small with 24 % at 50 ng cmRNA and 32 % at 100 ng dose [65]. With around 40 % at 50 ng and 60 % at 100 ng, decline in cell viability was similar for DT and AT cmRNA [65]. As already observed in the microscopic images, the nonfunctional controls of DTA and AA also exhibited considerable cytotoxicity. At 50 ng DN or AN cmRNA, cell viability was decreased by almost 30 % compared to UT cells and by more than 40 % at 100 ng dose. In contrast, SN cmRNA showed very little reduction in cell viability of 11 % at 100 ng dose. None of the untranslatable control cmRNAs (U) induced a decrease in cell viability at the applied doses [65]. Differences in cell viability between the toxin and the untranslatable control cmRNAs as well as for the nonfunctional control versus the corresponding untranslatable control cmRNAs displayed statistical significance.

Figure 17c presents the results acquired in figure 17b in a way to directly illustrate cell growth and growth inhibition (GI). Positive values (between 0 and 100 %) indicate reduced cell growth

### 3 Results

while negative values suggest that cell death outweighed cell growth. Values above 100 % imply increased cell growth compared to UT cells. Firstly, no negative values and thus no reduction in cell viability compared to the time of transfection were detectable for ST cmRNA. Cell growth was reduced by 63 % and 81 % compared to UT cells for 50 or 100 ng ST cmRNA, respectively. For 50 ng DT or AT cmRNA, cell growth was decreased by more than 90 % in comparison to UT cells. At 100 ng DT or AT cmRNA, cell viability was diminished by about 30 % compared to the time of transfection. While in case of SN cmRNA cell growth was reduced only by 30 % compared to UT cells at the highest dose, the reportedly nonfunctional controls DN and AN displayed considerable toxicity. In comparison to the time point of transfection, cell viability was reduced by approximately 10 % after transfection with 100 ng DN or AN cmRNA. The three untranslatable control cmRNAs displayed no influence on cell growth at the tested concentrations.

According to the acquired results, AT showed slightly higher toxicity than DT cmRNA. Considering the different size of the two RNAs (DT: 0.8 kb versus AT: 1.0 kb), more DT molecules were required to induce similar effects on cell viability as for AT [65]. This led to the conclusion that AT was the most potent toxin [65] and was therefore employed for subsequent experiments in KB cells.

### 3 Results

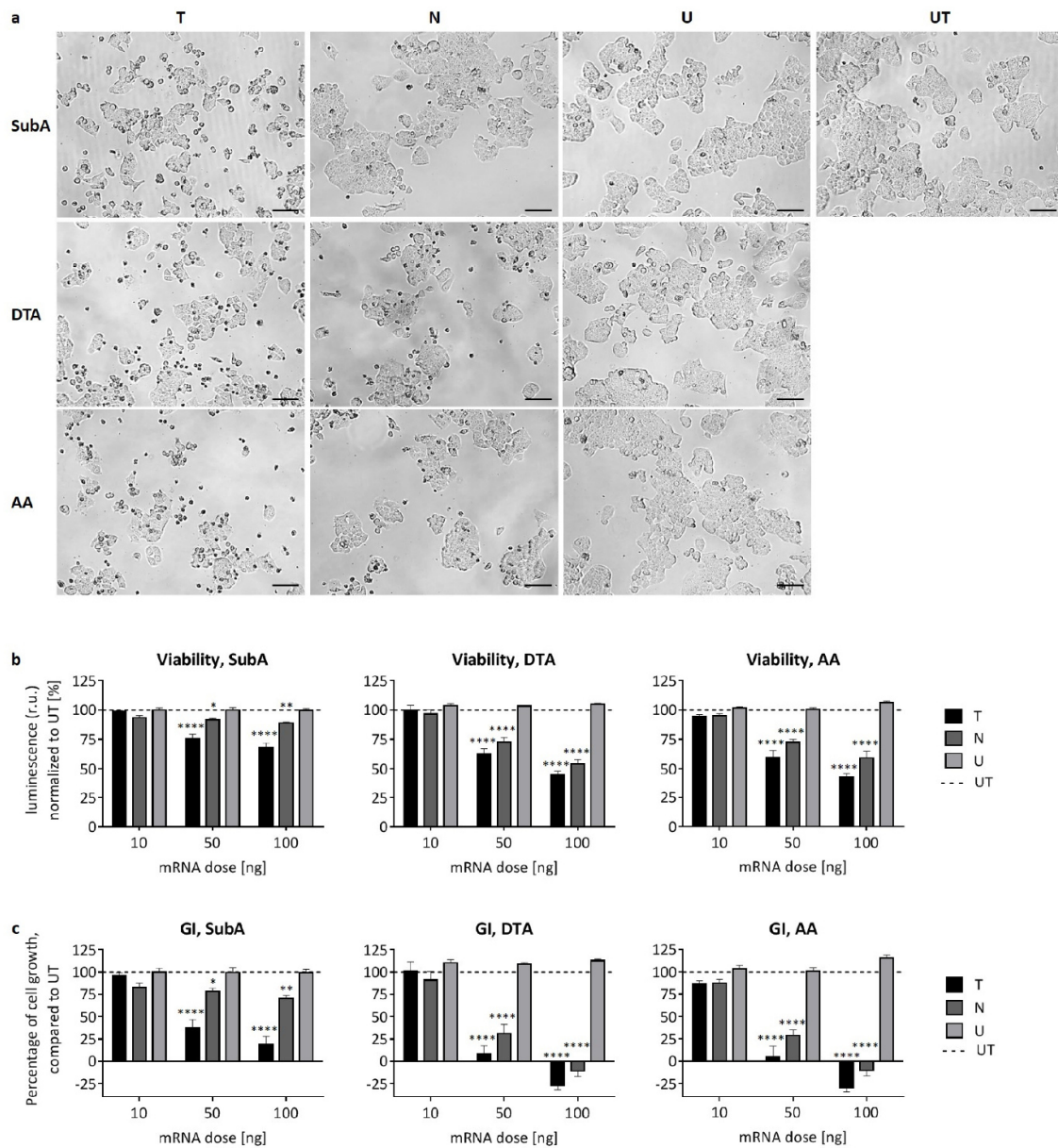


**Figure 17: Toxicity of toxin-encoding cmRNAs on KB cells – a comparison.** 48 h post transfection of KB cells (96 well plate, 10,000 cells/100  $\mu$ l, 100  $\mu$ l medium per well) using the lipofectamine<sup>®</sup> 2000 transfection reagent (Thermo Fisher) with toxin (T), nonfunctional control (N) or untranslatable control (U) cmRNA coding for SubA, DTA or AA. a) Representative pictures were taken of cells transfected with 50 ng/100  $\mu$ l cmRNA. The scale bars represent 100  $\mu$ m. b) Cell viability and growth inhibition (GI) were determined by measuring ATP content with the CellTiter Glo<sup>®</sup> Luminescence Viability Assay (Promega). Cell viability was proportional to the measured luminescence. Data is represented as mean  $\pm$  SEM of untransfected control cells (UT, dotted line). cmRNA doses are given in ng/100  $\mu$ l. Calculation of GI: For  $T_i > T_z$ :  $((T_i - T_z)/(C - T_z)) \times 100$  and for  $T_i < T_z$ :  $((T_i - T_z)/T_z) \times 100$  with  $T_z$ : luminescence at 0 h,  $T_i$ : luminescence of sample at 48 h and C: luminescence of UT cells at 48 h post transfection. Statistical significance versus the respective untranslatable control was assessed by 2-way ANOVA, adjusted for multiple comparisons, with \*:  $p < 0.05$ , \*\*:  $p < 0.01$ , and \*\*\*\*:  $p < 0.0001$ . The experiment was repeated three times with  $n = 3$  each.

The foregoing experiment examined cell viability at 48 h post transfection. In order to investigate the development over time, cell viability was determined at 96 h (fig. 18a). Growth inhibition (GI) and cell viability were normalized to untransfected control cells (UT, 100%). The

### 3 Results

decrease in cell viability at 96 h post transfection with 100 ng AT cmRNA was equal to the time point 48 h. In case of the 50 ng dose, however, cell viability in comparison to UT cells lay at 86 % after 96 h but at 60 % 48 h post transfection. Regarding the control cmRNAs, influence on cell viability at 96 h was detectable only for 100 ng AN cmRNA. Differences between the time points could best be observed in the growth inhibition (GI) analysis. At 48 h post transfection, diminished viability compared to the time of transfection had been identified for 100 ng AT cmRNA (fig. 17c). This was not the case at 96 h, though cell growth was reduced by 65 % compared to UT cells. For 50 ng AT cmRNA and for 100 ng AT or AN cmRNA, the disparity in cell viability or cell growth compared to AU cmRNA was statistically significant.

Another experiment quantified the number of dead cells 48 h after transfection by propidium iodide staining (fig. 18b). In case of UT cells, 9 % of all cells were PI positive [65]. The fraction of dead cells was increased to 18 % at 10 ng AT cmRNA, although no change in cell viability had been observed [65]. At 50 and 100 ng AT cmRNA, half of the cells were PI positive [65]. Transfection with AN cmRNA was also ensued by cell death to a degree comparable to AT cmRNA at 100 ng cmRNA dose. The untranslatable control cmRNA also showed limited toxicity with a maximum of 17 % dead cells at 100 ng cmRNA [65]. The variations in the number of dead cells after transfection with AT or AN cmRNA were statistically significant in comparison to the untranslatable control cmRNA.

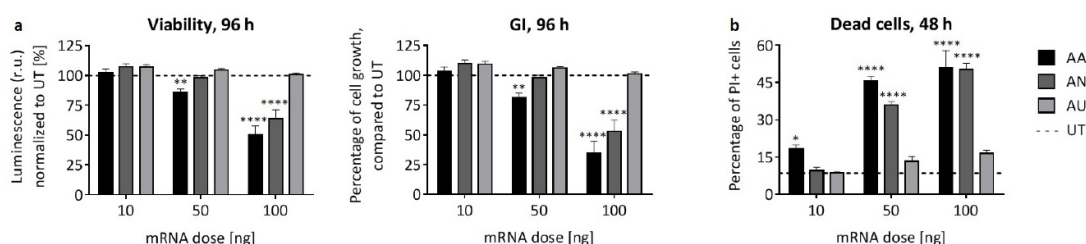


**Figure 18: Toxicity of AT cmRNA on KB cells.** Transfection of KB cells (96 well plate, 10,000 cells/100  $\mu$ l, 100  $\mu$ l medium per well) using the lipofectamine<sup>®</sup> 2000 transfection reagent (Thermo Fisher) with toxin (AT), nonfunctional control (AN) or untranslatable control (AU) cmRNA coding for AA. a) Cell viability and growth inhibition (GI) at 96 h post transfection were determined by measuring ATP content with the CellTiter Glo<sup>®</sup> Luminescence Viability Assay (Promega). Cell viability was proportional to the measured luminescence. Data is represented as mean in %  $\pm$  SEM of untransfected control cells (UT, dotted line). cmRNA doses are given in ng/100  $\mu$ l. Calculation of GI: For  $T_1 > T_2$ :  $((T_1 - T_2) / (C - T_2)) \times 100$  and for  $T_1 < T_2$ :  $((T_1 - T_2) / T_2) \times 100$  with  $T_2$ : luminescence at 0 h,  $T_1$ : luminescence of sample at 48 h and C: luminescence of UT cells at 48 h post transfection. b) Number of dead cells at 48 post transfection was counted using propidium iodide (PI, Sigma) staining and flow cytometry analysis. Percentage of PI positive cells was compared to untransfected control cells (UT, dotted line) and is shown as mean in %  $\pm$  SEM. a-b) Statistical significance versus the respective untranslatable control was assessed by 2-way ANOVA, adjusted for multiple comparisons, with \*\*:  $p < 0.01$ , \*\*\*\*:  $p < 0.0001$ . The experiment was repeated three times with  $n = 3$  each.

The performed experiments clearly demonstrated AT-related cytotoxicity represented by a decrease in cell viability and an induction of cell death.

### 3 Results

#### 3.3.1.2 Detection of AA protein after transfection of KB cells with AT cmRNA cells by Western blot

The expression of AA protein after transfection of KB cells with AT cmRNA was verified by Western blot analysis. For this, KB cells were transfected with 40 ng and 80 ng AT or AU cmRNA, lysed 24 h post transfection and SDS page and Western blot was performed. Figure 19 clearly demonstrates AA protein production in KB cells after transfection with AT cmRNA in a concentration dependent manner [65]. After transfection with AU cmRNA and in case of untransfected control cells (UT), no AA protein was detected [65].



**Figure 19: Detection of AA protein after transfection of KB cells with AT cmRNA by Western blot.** KB cells (6 well plate, 20,000 cells/100  $\mu$ l, 3 ml medium per well) were transfected using the lipofectamine<sup>®</sup> 2000 transfection reagent (Thermo Fisher) with 40 or 80 ng/100  $\mu$ l toxin (AT) or untranslatable control (AU) cmRNA coding for AA. 24 h post transfection, cells were lysed and SDS page and Western blot was performed. 45  $\mu$ g of total protein were loaded for SDS page. Anti-abrin antibody was employed at 6.7  $\mu$ g/ml and anti-vinculin (1:10,000) antibody was used as loading control. The experiment was repeated twice. A representative blot, including untransfected control cells (UT), is shown.

#### 3.3.1.3 Inhibition of protein synthesis by AT cmRNA in reticulocyte lysate and in KB cells

The capability of AT to inhibit protein synthesis was assessed first by co-treatment of rabbit reticulocyte lysate with 1  $\mu$ g cmRNA coding for firefly luciferase (luc) and 0.1  $\mu$ g AT cmRNA. 45 min after treatment, luminescence was reduced to 0.1 % compared to lysate treated with luc cmRNA only (luc ctrl, 100 %, fig. 20a) [65]. Addition of AU cmRNA, however, resulted only in a relatively minor decrease of luc activity to 74 % in comparison to luc ctrl [65]. The difference between AT and AU cmRNA was statistically significant.

Subsequently, the capability of AT to inhibit protein synthesis was assessed in KB cells by co-transfection of 50 ng EGFP cmRNA in addition to AT cmRNA or one of its controls. 24 h after transfection, fluorescence images were taken and the cells were analyzed by flow cytometry (fig. 20b-e).

KB cells transfected with AT cmRNA showed considerable EGFP fluorescence at 0.0005 ng but no EGFP fluorescence was visible at 0.05 or 5 ng (fig. 20b) [65]. While EGFP fluorescence in cells transfected with AU cmRNA was not affected at any of the tested concentrations, no EGFP fluorescent cells could be observed at 5 ng AN cmRNA [65]. These microscopic observations were further confirmed by flow cytometry analysis, showing both the mean fluorescence intensity (MFI) of EGFP (fig. 20c) and the percentage of EGFP positive cells (fig. 20d). The

### 3 Results

obtained results were normalized to cells transfected only with EGFP cmRNA (EGFP ctrl, 100 %). At 0.0005 ng AT cmRNA, the MFI of EGFP was unchanged whereas at 0.05 and 5 ng it was decreased to 3.4 % and 1.7 %, respectively, in comparison to EGFP ctrl cells [65]. Similar to the results acquired with MFI, the number of EGFP positive cells was unchanged at 0.0005 ng AT cmRNA and reduced by 77 % at 0.05 ng or by 100 % at 5 ng compared to EGFP ctrl cells [65]. Transfections with AN cmRNA also lead to a decrease in the MFI of EGFP; slightly at 0.05 ng but considerably at 5 ng dosage with a reduction of 90 % compared to EGFP ctrl [65]. Interestingly, only very small changes in the percentages of EGFP positive cells could be detected for AN cmRNA Paper. At 5 ng, only 10 % less cells were EGFP positive than in case of the EGFP ctrl cells [65]. Apart from changes in the fraction of EGFP positive cells at 0.05 ng AN cmRNA, the differences between AT and AU as well as between AN and AU cmRNA were statistically significant for 0.05 and 5 ng. Figure 20e shows three representative flow cytometry histograms. It can be clearly seen that though EGFP fluorescence was diminished substantially by 5 ng AN cmRNA, a high number of cells was still EGFP positive. While no changes in EGFP fluorescence could be detected for transfections with AU cmRNA, already 0.05 ng AT cmRNA lead to an almost complete abolishment of fluorescence.

### 3 Results

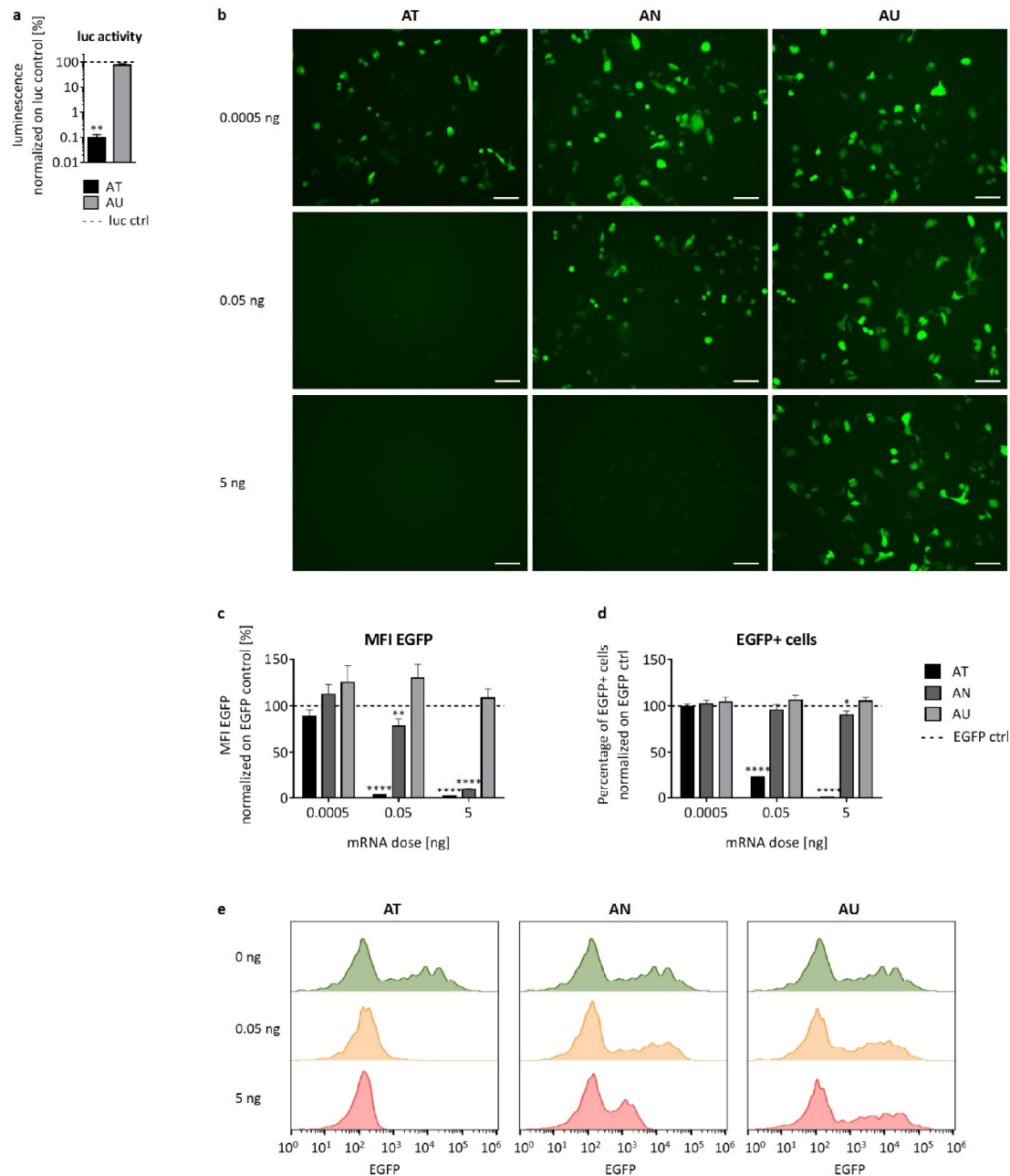


**Figure 20: Inhibition of protein synthesis by AT cmRNA.** (a) Inhibition of translation of firefly luciferase (luc) cmRNA in a rabbit reticulocyte lysate system by AT cmRNA. Rabbit reticulocyte lysate was treated with 1  $\mu$ g luc cmRNA and 0.1  $\mu$ g toxin (AT) or untranslatable control (AU) cmRNA coding for AA in 35  $\mu$ l lysate. Luminescence as a measure of luc activity was determined 45 min after start of the reaction. Data are presented as mean in %  $\pm$  SEM of lysate treated only with luc cmRNA (luc ctrl, dotted line). Statistical significance versus AU cmRNA was assessed by Mann Whitney U test, with \*\*:  $p < 0.01$  and  $N = 3$ . (b-e) KB cells (96 well plate, 10,000 cells/100  $\mu$ l, 100  $\mu$ l medium per well) were co-transfected using the lipofectamine<sup>®</sup> 2000 transfection reagent (Thermo Fisher) with 50 ng/100  $\mu$ l EGFP cmRNA and toxin (AT), nonfunctional control (AN) or untranslatable control (AU) cmRNA coding for AA. cmRNA doses are given in ng/100  $\mu$ l. 24 h post transfection, inhibition of protein synthesis was assessed by fluorescence microscopy (b) and flow cytometry (c-e). Representative images are shown (b). The scale bars represent 100  $\mu$ m. Mean Fluorescence Intensity (MFI) (c) and percentage of EGFP positive cells (d) are depicted. Data are represented as mean in %  $\pm$  SEM of control cells transfected only with EGFP cmRNA (EGFP ctrl, dotted line). Cells were gated on singlet cells. Statistical significance versus the respective untranslatable control was assessed by 2-way ANOVA adjusted for multiple comparisons, with \*\*:  $p < 0.01$  and \*\*\*\*:  $p < 0.0001$ . The experiment was repeated three times with  $n = 3$  each. Representative flow cytometry histograms are depicted (e).

## 3 Results

The experiment clearly demonstrated the high inhibitory capacity of AT cmRNA on protein synthesis in reticulocyte lysate and in KB cells [65].

### 3.3.1.4 Apoptotic characteristics of cell death in KB cells after transfection with AT cmRNA

Having demonstrated in section 3.3.1.1 that transfection with AT cmRNA induced cell death in KB cells, its apoptotic characteristics were examined next (fig. 21). The untranslatable cmRNA was utilized in the upcoming experiments as control.

Morphologically, apoptotic cells distinguish themselves by 'membrane blebbing' and nuclear fragmentation. Both could be perceived 48 h after transfection with AT cmRNA after staining with the DNA dye Hoechst33258 (fig. 21a) [65]. No morphological aberrations, however, were displayed after transfection of cells with AU cmRNA [65]. When stained with Hoechst33258, cells undergoing apoptosis show far higher fluorescence than normal cells. In figure 21b, Hoechst33258 positive cells are shown 48 h post transfection with AT or AU cmRNA. The number of Hoechst33258 positive cells is displayed as multiple of untransfected control cells (UT) in figure 21c. In case of 50 or 100 ng AT cmRNA transfected cells, a 3.6-fold higher number of apoptotic cells was observed [65]. Only small variations in the fraction of apoptotic cells were detected for cells transfected with AU cmRNA [65]. The increase in apoptotic cells for AT compared to AU cmRNA transfected cells was statistically significant.

As another important characteristic of apoptotic cell death, the activity of the caspases-3 and -7 was determined (fig. 21d). The measured luminescence was directly proportional to the activity and was normalized to UT cells (100 %). 24 h after transfection, an increase in activity was already observable at 10 ng/100  $\mu$ l [65]. In case of 50 ng and 100 ng/100  $\mu$ l, the activity of caspases-3 and -7 was five times higher for AT than for AU cmRNA transfected cells [65]. For all three tested doses, the increase in luminescence was statistically significant for AT compared to transfections with AU cmRNA.

Apoptotic cells can furthermore be identified in flow cytometry by performing a double-staining with Annexin V-AF488 and propidiumiodide (PI). Figure 21e and 21f present the results of this experiment 24 h after transfection, with figure 21e showing two representative dot plots. The Annexin V positive but PI negative population corresponds to cells in apoptosis, the double positive to dead cells and the double negative cells were viable. Clearly, cells transfected with AT cmRNA showed a substantial shift from viable to apoptotic as well as dead cells in comparison to AU cmRNA transfected cells [65]. While 4.2 % of UT cells were Annexin V positive and PI negative, the percentage of apoptotic cells increased to 8.4 % at 10 ng AT cmRNA and

### 3 Results

to 27.3 % or 40.7 % at 50 ng or 100 ng dose, respectively [65]. For AU cmRNA, the amount of apoptotic cells at the highest dosage was 5.5 % [65]. The differences in percentage of apoptotic cells between cells transfected with AT or AU cmRNA were statistically significant for 50 and for 100 ng of cmRNA.

### 3 Results

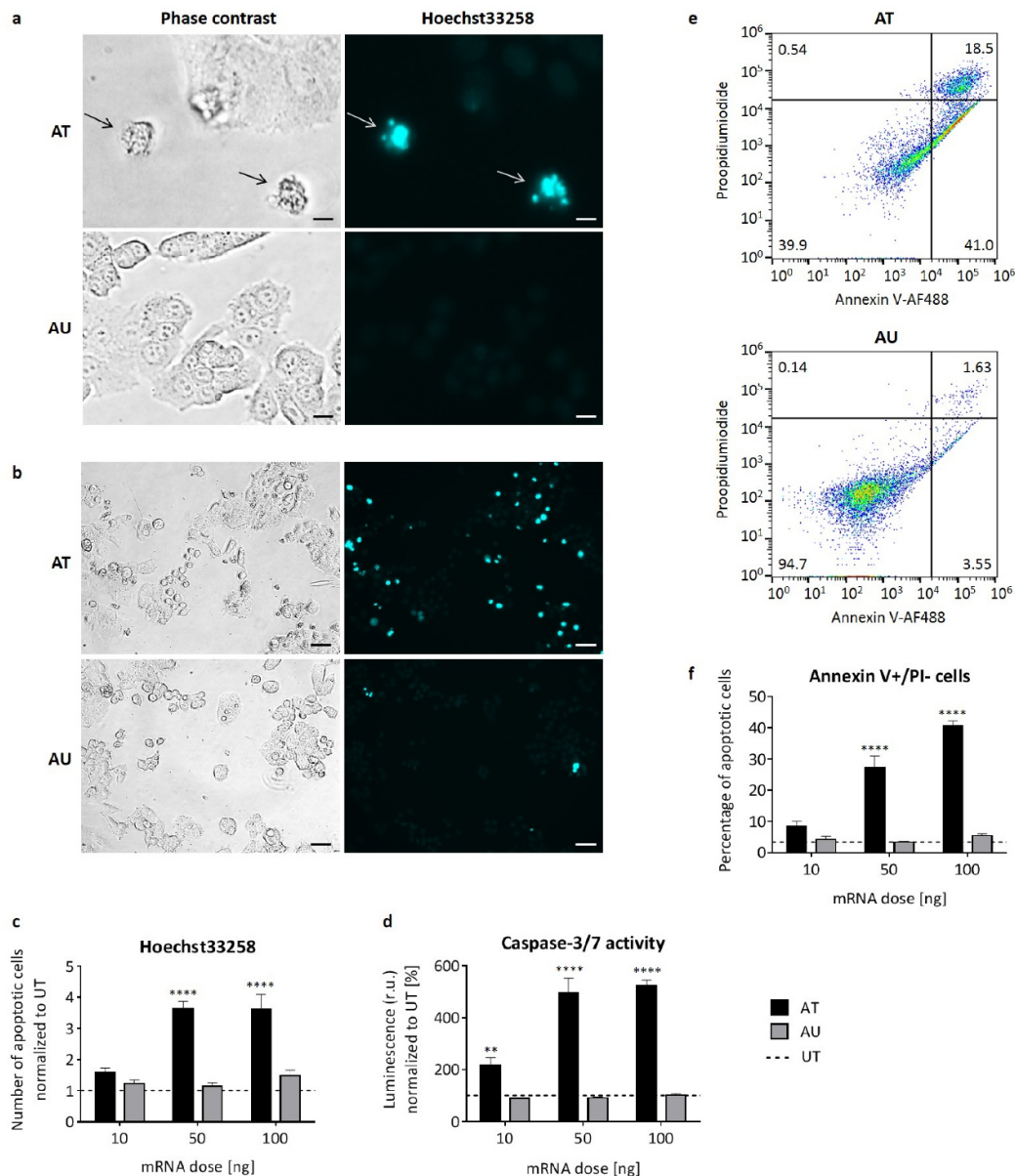


**Figure 21: Apoptotic characteristics of cell death induced by AT cmRNA on KB cells.** KB cells were transfected using the lipofectamine® 2000 transfection reagent (Thermo Fisher) with toxin (AT) or untranslatable control (AU) cmRNA coding for AA. cmRNA doses are given in ng/100 µl. a-d) 96 well plate, 10,000 cells/100 µl, 100 µl medium per well were employed. a-b) Representative phase contrast pictures and fluorescence images of cells transfected with 100 ng cmRNA and stained with Hoechst33258 are displayed at 48 h post transfection. a) Arrows depict cells showing ‘membrane blebbing’ or nuclear fragmentation. The scale bars represent 10 µm. b) The scale bars represent 50 µm. (c) Number of Hoechst33258 positive cells 48 h post transfection with 100 ng cmRNA. Data (mean ± SEM) is presented as multiple of untransfected control cells (UT, dotted line). d) Caspase-3 and -7 activity was determined 24 h after transfection using the Caspase-Glo® 3/7 Assay (Promega). Activity was proportional to the measured luminescence. Data is represented as mean in % ± SEM of untransfected control cells (UT, dotted line). (e, f) Apoptotic cells (identified as Annexin V positive and propidium iodide (PI) negative) were analyzed by flow cytometry of cells stained with the fluorophore Annexin V-AF488 (Thermo Fisher) and PI (Sigma). Experiment was done 24 h post transfection. Cells were gated on singlets. 24 well plates with 40,000 cells/100 µl medium and 400 µl medium per well were employed. (e) Representative flow cytometry dot plots of cell transfected with 100 ng cmRNA/100 µl medium. Percentages of cells in a certain population are given in the respective corners. (f) Flow cytometry results. Data is represented as mean in % ± SEM and compared to untransfected control cells (UT, dotted line). Statistical significance versus AU cmRNA was assessed by 2-way ANOVA adjusted for multiple comparisons, with \*\*: p<0.01, \*\*\*\*: p<0.0001. The experiment was repeated three times with n=3 each.

### 3 Results

Taken together, it could be demonstrated that KB cells die in an apoptotic manner after transfection with AT cmRNA.

#### 3.3.2 Inhibition of KB tumor growth *in vivo* after transfection with AT cmRNA

The toxic efficacy of AT cmRNA could be demonstrated vastly in the foregoing experiments in cell culture. As last step of this thesis, its applicability was examined *in vivo* using the in-house produced transfection reagent LF132 in mice (fig. 22). Prior, LF132 was tested *in vitro* on KB cells for its effectiveness. 48 h after *in vitro* transfection, very high toxicity of AT-LF132 but no toxic effect of AU-LF132 or 2 % sucrose (vehicle control) on KB cells was observed microscopically (fig. 22a) [65]. This was further confirmed by assessing cell viability (fig. 22b). The measured luminescence, directly proportional to cell viability, was normalized to untransfected control cells (UT, 100 %). Compared to UT cells, cell viability was reduced by 56 %, 99 % or 100 % for 10, 50 or 100 ng of AT-LF132, respectively. Accordingly, AT-LF132 showed far higher toxicity than AT-Lipofectamine® 2000 (fig. 17b), where cell viability was decreased by 57 % at 100 ng AT cmRNA compared to UT cells [65]. With a cell viability of 65 % in relation to UT cells, AU-LF132 also showed some toxicity at higher concentrations, though far less compared to AT-LF132 [65].

To test the anti-tumor activity of AT-LF132 *in vivo*,  $5 \times 10^6$  KB cells were injected into the flank of immunosuppressed NMRI-nu mice. In a small pre-experiment, the expression characteristics of intratumorally injected RNA were investigated. Therefore, 10  $\mu$ g of lipid nanoparticle formulated cmRNA coding for firefly luciferase was injected three times. 24 h after the third application, considerable and locally defined luciferase activity was observed (fig. 22c) [65]. In the main experiment, the complexed cmRNAs or 2 % sucrose were injected intratumorally as soon as the tumors reached a size of about 100 mm<sup>3</sup>. The treatment was repeated three times in two to five day intervals. Treatment intervals were the same for all mice and were chosen with regard to the degree of inflammation at the site of injection. Three out of ten mice treated with AT-LF132 had to be euthanized after the 2<sup>nd</sup> or the 3<sup>rd</sup> application due to bad health condition. Surveillance of general condition and body weight during treatment as well as examination of blood parameters (white blood cells, red blood cells, hemoglobin, hematocrit and platelets) on day 21 after injection of tumor cells showed no disparities between the three groups (data not shown) [65]. However, while the formation of cutaneous lesions up to ulcers

### 3 Results

was not observed in AU-LF132 or 2 % sucrose treated mice, it was present in all animals of the AT-LF132 group but one [65].

Measurement of the tumor volume throughout the treatment demonstrated a marked difference in growth rate between the different groups (fig. 22d) [65]. Twelve days after the first injection, tumor volume was determined *ex vivo* (fig. 22e). It could be shown that treatment resulted in a significantly lower tumor size for AT-LF132 than for AU-LF132 or for 2 % sucrose [65]. With a mean volume of 50 mm<sup>3</sup>, AT-LF132 treated tumors were 89 % smaller than tumors injected with AU-LF132 [65]. The difference in tumor size concerning AU-LF132 and 2 % sucrose was statistically not significant [65].

### 3 Results

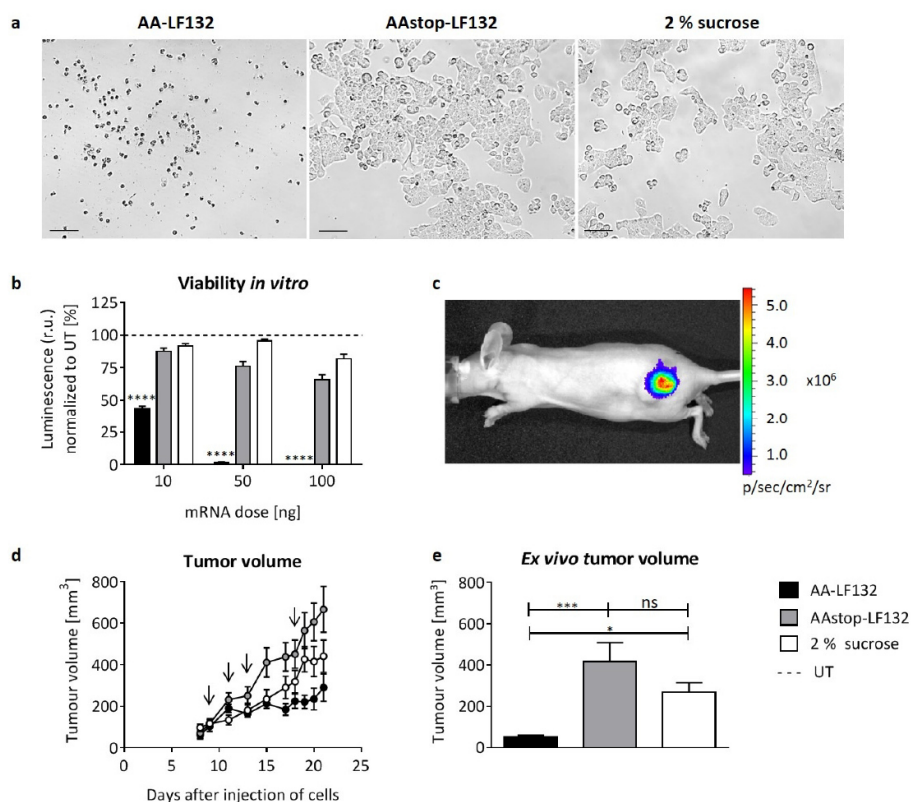


**Figure 22: Decrease in cell viability by AT-LF132 *in vitro* and its influence on tumor growth *in vivo*.** (a, b) *In vitro* assessment of toxicity on KB cells (96 well plate, 10,000 cells/100  $\mu$ l, 100  $\mu$ l medium per well) at 48 h post transfection with AT-LF132, AU-LF132 or treatment with 2 % sucrose (vehicle control). (a) Representative pictures of KB cells transfected with 100 ng cmRNA 48 h after transfection are depicted. The scale bars represent 100  $\mu$ m. (b) Cell viability at 48 h post transfection was determined by measuring ATP content with the CellTiter Glo<sup>®</sup> Luminescence Viability Assay (Promega). ATP content was directly proportional to the measured luminescence. Data is presented as mean in %  $\pm$  SEM of untransfected control cells (UT, dotted line). Statistical significance versus AU-LF132 was assessed by 2-way ANOVA adjusted for multiple comparisons, with \*\*\*\*:  $p < 0.0001$ . The experiment was repeated three times with  $n = 3$  each. (c) Luciferase activity was determined. Representative picture out of two mice is shown.  $5 \times 10^6$  KB cells were injected into the flank of NMRI-nu mice (Janvier Labs). 10  $\mu$ g of lipid nanoparticle formulated cmRNA coding for firefly luciferase was injected intratumorally on days 9, 11 and 13 after injection of tumor cells. On day 14, bioluminescence was determined using an IVIS *In Vivo* Imaging System. (d, e) *In vivo* anti-tumor activity of AT-LF132.  $5 \times 10^6$  KB cells were injected into the flank of NMRI-nu mice (Janvier Labs). 50  $\mu$ l of solution containing 10  $\mu$ g of either AT-LF132, 10  $\mu$ g of AU-LF132 or 2 % sucrose were injected intratumorally on days 9, 11, 13 and 18 after injection of tumor cells. (d) Tumor volume was measured *in vivo* throughout the experiment using a caliper applying the formula  $a \times b^2/2$ , with  $a$  indicating the length of the tumor and  $b$  the width. Arrows display days of treatment. Data represent means  $\pm$  SEM. (e) Tumor volume was determined *ex vivo* on day 21 after injection of tumor cells using the formula  $a \times b \times c/2$ . Data represent means  $\pm$  SEM. ns: not significant. Statistical significance was assessed by Kruskal-Wallis test adjusted for multiple comparisons, with \*:  $p < 0.05$ , \*\*\*:  $p < 0.001$ .  $N = 7$  for AT-LF132,  $N = 10$  for AU-LF132 and 2 % sucrose.

In addition, a hematoxylin-eosin staining of the tumor sections was performed (fig. 23). In case of one animal of the AT-LF132 group, two animals of the AU-LF132 group and five animals of the 2 % sucrose group, reduced tissue preservation and variable staining characteristics inhibited proper evaluations. However, tissue sampling in processing did not differ compared to the other KB tumor samples taken. Those samples were excluded from further analysis.

### 3 Results

The tumors formed from injected KB cells were surrounded by a fibrous capsule, as can be seen in figure 23a (black arrow). In the center of the tumors, extended necrosis was present (fig. 23b, lower left corner). The fractions of necrotic area in relation to the complete tumor area in one slide were estimated for the different groups and are presented in figure 23c. For the AT-LF132 group, the percentages of necrotic area were distributed evenly and ranged from 30 % to 80 %. One part of tumors treated with AU-LF132 showed small necrotic areas (25 %), while the fraction of necrotic area for the other four tumors was between 50 % and 70 %. The tumors of 2 % sucrose treated mice displayed necrotic areas of 40-70 %. With 45.0 %, 47.5 % and 50.0 % for AT-LF132, AU-LF132 and 2 % sucrose, respectively, the mean percentages of necrotic area were similar for the three groups.

Next, the number of degenerating (fig. 23d, blue arrows) as well as of mitotic (fig. 23d, black arrows) cells was counted and shown in figure 23e and 23f, respectively. Degeneration of cells includes both main types of cellular death, namely necrosis and apoptosis. With means of 16 (AT-LF132), 17 (AU-LF132) or 14 (2 % sucrose) cells in average per picture, there was no substantial difference in the number of degenerating cells between the groups. Apart from one tumor of the AU-LF132 treated group with 45 degenerated cells, 7-26 cells in average per picture were dying in all groups. The number of mitotic cells was generally lower than the number of dying cells. In case of cmRNA-LF132 treated tumors 6 and for 2 % sucrose injected tumors 7 cells in average were observed in the mitotic phase per picture. With 4 to 10 cells in average per picture, divergence was greatest for the AU-LF132 group.

### 3 Results

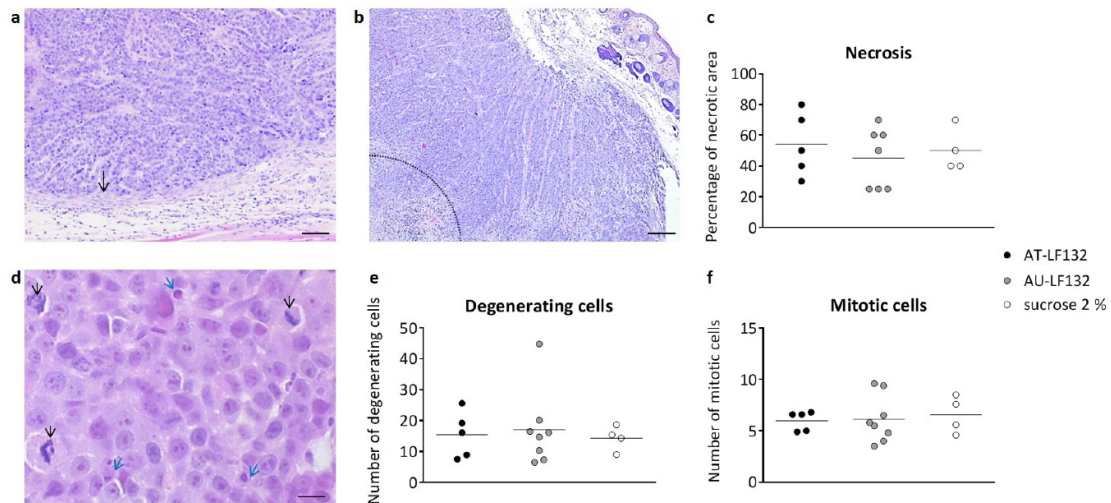


**Figure 23: KB tumor histology after treatment with AT-LF132.**  $5 \times 10^6$  KB cells were injected into the flank of NMRI-nu mice (Janvier Labs).  $50 \mu\text{l}$  of solution containing  $10 \mu\text{g}$  of either AT-LF132,  $10 \mu\text{g}$  of AU-LF132 or 2 % sucrose were injected intratumorally on days 9, 11, 13 and 18 after injection of tumor cells. On day 21 after injection of the cells, mice were sacrificed, tumors explanted and tumor sections were stained with hematoxylin and eosin (H&E). a), b), d) Representative images of tumors treated six times (a,b)) or four times (d)) with sucrose 2 % are shown. a) Arrow depicts the fibrous capsule surrounding the tumor. Scale bar represents  $50 \mu\text{m}$ . b) Necrotic area (lower left corner) in the center of the tumor is shown. Scale bar represents  $200 \mu\text{m}$ . c) Estimated percentages of necrotic area to the total tumor area in one slide. Data is presented as mean and as individual values. d-f) Degenerating cells (blue arrows) and cells in mitosis (black arrows) were counted in 11 pictures per tumor and averaged (see material and methods). d) Scale bar represents  $25 \mu\text{m}$ . e), f) Data is presented as mean and as individual values.

Further morphological observations were for one the infiltration of cells of the immune system into the tumor tissue which occurred equally for LF132-AT and LF132-AU treated mice but not in case of tumors treated with 2 % sucrose. Likewise, granulation and the formation of edema and acute hemorrhage were noticed only in case of cmRNA treated groups. Extended necrosis of the surrounding tissue and inflammation of the subcutis were observed in case of the AT-LF132 treated tumors while this was not present in the 2 % sucrose treated animals. Mice treated with AU-LF132 showed similar findings as AT-LF132 treated animals. As already depicted clinically, microscopically ulcerations were only present in AT-LF132 treated animals. However, due to the low number of samples, no further conclusions were drawn.

This experiment clearly demonstrates the potential of complexed cmRNAs coding for toxic proteins to reduce tumor growth *in vivo*.

### 4 Discussion

Employment of mRNA coding for different cellular and viral proteins for cancer treatment was investigated in previous studies. Research focused primarily on the area of cancer immunotherapy, where preclinical and clinical studies were performed [9]. Anti-tumor immunity was achieved mainly by activation of the immune system with mRNA-encoded stimulating agents or by transfecting dendritic cells with mRNA tumor antigens for vaccination [9]. Van der Jeught *et al.*, for instance, delivered mRNA coding for interferon  $\beta$  fused to the transforming growth factor  $\beta$  (TGF  $\beta$ ) receptor II intratumorally to enhance tumor-specific immunity [159]. Treatment of tumors with so-called TriMix mRNA, coding for CD70, CD40 ligand and constitutively active TLR 4, induced systemic anti-tumor immunity [30]. Also, an mRNA-encoded herpes simplex virus-thymidine kinase/ganciclovir (TK/GCV) suicide system was applied intravenously to suppress tumor growth [55]. In all studies, reduction of tumor growth was observed. The present study aimed to investigate whether protein toxins are suitable for employment as mRNA cancer therapeutics. For this purpose, chemically modified mRNAs (cmRNAs) coding for the catalytic A-chain of three AB-toxins, namely subtilase cytotoxin (SubA), diphtheria toxin (DTA) and abrin-a (AA), were employed.

#### 4.1 Mechanisms of toxicity

##### 4.1.1 Nonfunctional and untranslatable control cmRNAs

Depending on the dose, transfections with mRNA may induce adverse effects independently of the encoded protein due to cytotoxicity of the transfection reagent, the mRNA or the produced protein. In order to ensure that the observed toxicity was specific to the encoded proteins, two control cmRNAs were employed for each toxin. The untranslatable cmRNAs display the same sequence as the corresponding toxins but show a scrambled Kozak element [1] and the start as well as all in frame downstream ATGs were mutated to TAGs [65]. Prior to translation, the 40 S ribosome scans the mRNA sequence, starting at the 5' end, and initiates translation when it reaches the first AUG codon [1]. Binding to this first AUG by the ribosome is strongly supported by a consensus sequence (Kozak element [1]) directly upstream. Accordingly, as could be asserted in this study, the introduced alterations result in prevention of translation [65]. Exemplary, in contrast to toxin AA cmRNA, no expression of AA protein could be detected in KB cells even at high doses of untranslatable AA cmRNA. The minor toxicities associated with higher doses of untranslatable cmRNA are assumedly due to either the toxicity of the

## 4 Discussion

transfection reagent or the high amount of introduced cmRNA. A blockage of ribosomes through the untranslatable cmRNA is supposedly the cause for the small reduction in luc activity by AU cmRNA observed in reticulocyte lysate. Consequently, the observed effects induced by the toxin-encoding cmRNAs have to be viewed in this context. As expected, the detected toxicities of the untranslatable control cmRNAs of the three different toxins were comparable.

As second control, cmRNAs coding for reportedly nonfunctional forms of the toxins, attained by introducing point mutations, were utilized. In case of DTA, Glycin-52 was changed to a glutamic acid according to the discovery of Giannini in 1984 [148]. The so-called CRM197 mutant lost the ability of diphtheria toxin to bind to NAD<sup>+</sup>, a necessary step prior to adenylation of eEF-2, and thereby its toxicity [148, 160]. Recently, it was detected that this mutation causes a conformational change which in turn leads to blockage of the NAD binding pocket [143]. As it is suitable for vaccination purposes [143], this mutant has been studied extensively. In the current study, while no influence on protein synthesis could be discerned, DN (DTA nonfunctional) induced a reduction in cell viability in HuH7 and KB cells that was only slightly reduced compared to the toxin variant (DT). Though initially believed to be entirely nontoxic, several studies meanwhile reported toxicity associated with CRM197. Already in 1990 it was shown that the mutant, though incapable to reduce protein synthesis, exhibited desoxyribonuclease activity [161]. Thereof the authors deduced that the two active sites were distinct. Among others, Qiao *et al.* not only demonstrated cytotoxicity but also reduction in protein synthesis after infection with CRM197-producing viruses [162]. They argue that CRM197 was often observed to be nontoxic as treatment with CRM197 protein did not result in sufficient high amounts of its A-subunit in the cytoplasm in contrast to CRM197-expressing cells. One group employed the double mutant K51E/E148K to induce immune tolerance to DT in transgenic mice as it didn't show any signs of cytotoxicity [163].

In order to generate the nonfunctional SubA mutant, serine-272 and Histidine-89 were mutated to Alanine [145]. The first publications concerning SubAB discovered that the substitution of the mentioned serine abolishes cytotoxicity [59, 83] and prevents BiP cleavage, suggesting it as vaccine candidate [164]. Due to the similarity of SubA to the family of serine proteases, this particular serine was proposed by the authors to constitute the catalytic site. Morinaga *et al.* also observed no influence on cell cycle, cell growth or protein synthesis by the S272A mutant in opposition to the native variant [165, 166]. For this thesis a double mutant (S272A, H89A) was employed where, in addition to serine-272, histidine-89, another member

## 4 Discussion

of the catalytic triad, was also replaced by an alanine [83, 145]. Though no decrease in protein synthesis was noticeable for SN (SubA nonfunctional), slightly increased toxicity with respect to SU (SubA untranslatable) could be observed on KB and on HuH7 cells at higher doses. This stands in contrast to the findings of the aforementioned groups, where cytotoxicity was completely eliminated. Potentially, the divergence can be explained by the high translational capacity requested by the transfected mRNA molecules or by the presence of a high quantity of exogenous proteins affecting the endoplasmic reticulum (ER). Besides, as the applied SN sequence contained the ER retention signal KDEL, it is conceivable that the KDEL receptors were overloaded and vital ER resident proteins could not be retrieved from the golgi apparatus [149].

In the experiments performed in the present study, AN (AA nonfunctional) proved to be the most toxic of the three nonfunctional controls. As for DN, its influence on viability and inhibition of cell growth was merely slightly lower than for AT (AA toxin). In addition, however, substantial decrease in the intensity of EGFP fluorescence was observed, a circumstance that had not been detected for the other nonfunctional controls. Noticeably, the percentage of EGFP positive cells was unaltered. The sequence of AN differed from AT only in the substitution of arginine-167 by leucine and of glutamic acid-164 by alanine as was already done by Hung *et al.* [146]. They observed that inhibition of protein synthesis by the double mutant was 1,250-fold reduced and, while it was only decreased 25-fold by E164A, it was diminished still 625-fold by R167L. The authors concluded that R167 was essential for deadenylation of the 28 S ribosome and proposed that this arginine acts as a nucleophile to interact with the C-1 of the ribose. The importance of E164 for the catalytic reaction might have been underestimated, though, as another group detected that the protein synthesis inhibitory capacity was lessened 1,600 times if the glutamic acid-164 was replaced by a glutamine [167]. They explained this discrepancy by the assumption that, in case of mutation to alanine, the loss of E164 was partly compensated by the rotation of E195 into the active site. This event would not be feasible in case of a mutation to the bulky glutamine. The double mutant E164A/R167L was successfully employed to vaccinate mice against abrin [147]. According to Gadadhar and Karande, substituting E164 by alanine blocked inhibition of protein synthesis but had no influence on the induction of cell death [63]. However, after mutating glutamic acid-164 to alanine, Mishra *et al.* observed that not the inhibition of protein synthesis in general was diminished but its kinetics [107].

## 4 Discussion

Summarizing, the untranslatable controls and SN displayed no cytotoxicity except at higher doses while AN and DN demonstrated considerable, though reduced, influence on cell viability. In addition, AN inhibited protein synthesis in HuH7 and in KB cells.

### 4.1.2 Inhibition of protein synthesis

Fluorescence inhibition of co-transfected EGFP mRNA confirmed that the transfected toxin mRNAs were translated into active proteins [65]. The observed dose dependency of translational inhibition by the three toxins was shown before [107, 166, 168, 169]. Strikingly, at 0.05 ng or 0.04 ng dose, reduction of the mean fluorescence intensity (MFI) exceeded the decrease in EGFP positive cells considerably [65]. In those EGFP positive cells, the comparably low amount of toxin mRNA presumably was not able to inactivate protein synthesis before enough EGFP molecules for fluorescence detection had been synthesized [65]. In contrast, none of the cells transfected with 5 ng DT or AT mRNA showed detectable EGFP fluorescence [65]. These results demonstrate that the two toxins exert their influence shortly after the start of translation [65]. This is substantiated by the almost complete prevention of luc mRNA translation by AT mRNA observed in reticulocyte lysate [65]. As was shown by previous studies, DT as well as AT directly inhibit protein synthesis, either by blocking eEF-2 by ribosylation (DT) [79, 80] or by cleaving an adenine from the 28 S rRNA (AT) [103]. In consequence, such immediate effects on translation are conceivable [65]. Also, Hung *et al.* detected depurination of isolated rat liver ribosomes already 15 min after treatment with the A-chain of the protein abrin-a [65, 146]. Likewise, ADP-ribosylation of eEF-2 by diphtheria toxin in a cell free system was observed after an incubation time of 15 min [169].

At 5 ng ST mRNA, the percentage of EGFP positive cells was still considerably high while the MFI of EGFP was reduced markedly, as was observed for the lower dose. This stands in opposition to the findings for DT and AT mRNA. SubA mediated cleavage of GRP78 blocks translation indirectly by inducing the unfolded protein response (UPR), which causes a general stop of protein synthesis. According to Morinaga *et al.*, this is asserted by phosphorylation of eIF2 $\alpha$  (eukaryotic initiation factor 2 $\alpha$ ) which is indispensable for the initiation of translation [165]. Due to this detoured mode of action, it seems plausible that even at high concentrations of ST mRNA a certain amount of EGFP protein is produced before translation ceases. Also, cleavage of GRP78, the first step of the induced cascade, was only detected 30 min after treatment with SubAB [165].

## 4 Discussion

### 4.1.3 Cell death, influence on proliferation and on cell cycle

Translation of EGFP cmRNA was inhibited substantially at low doses (5 ng/100  $\mu$ l) of any of the three cmRNAs, while cell death and a reduction in cell viability was only detected at higher doses. This discrepancy indicates that higher amounts of toxin are needed to disturb protein metabolism to such an extent that it results in cell death [65]. Furthermore, it has been assumed that abrin-a can induce cell death independent of inhibition of protein synthesis [65, 104, 170]. Potentially, higher concentrations of abrin-a are necessary for this toxicity enhancing effect [65]. The same reasoning applies to SubA, where cell death ensues in consequence of the activated UPR [59, 90]. Also, the need for higher concentrations of SubAB or diphtheria toxin to induce cell death in contrast to a stop in protein synthesis was demonstrated before [166, 168]. Chang *et al.*, however, showed similar dose response for diphtheria toxin-mediated translational inhibition as for cell death and also, depending on the cell line, a considerable reduction in protein synthesis without ensuing cell death [171]. The authors also suggested that cell death following DT treatment can be triggered by other factors than inhibition of protein synthesis (refer to section 4.1.4).

As viability measurements are based on determining changes in cell metabolism, impedance measurements were performed as an additional, metabolism independent investigation method. It must be remembered, though, that changes in the determined cell viability can be influenced by the death of cells as well as by a stop in cell proliferation. The same accounts for the conducted impedance measurements. The experiments performed in this study, though, clearly demonstrated reduced cell proliferation after transfection with toxin cmRNA in addition to cell death. Impedance measurements performed on HuH7 cells displayed a reduction in cell confluency in comparison to the time point of transfection with ST or DT cmRNA, indicating cell death. In case of KB cells transfected with AT cmRNA, the occurrence of cell death was demonstrated directly by staining with propidiumiodide. This was further confirmed by growth inhibition (GI) analysis of viability measurements after transfecting KB cells with DT or AT cmRNA. A considerable decline in cell proliferation after transfection with each of the three toxin cmRNAs could likewise be ascertained employing a scratch assay. This experiment is typically performed to examine the wound healing properties of cells under varying conditions [152, 153] but also conveys indications about the proliferating potential of the investigated cells. However, no influence on the cell cycle of transfected cells was observed for any of the tested cmRNAs. Decreased cell proliferation [169], e. g. by analysis of the DNA synthesis rate

## 4 Discussion

[172], and cell death, for instance attested by trypan blue uptake [168, 171], after treatment with DT was shown before. Next to establishing SubA-induced cell cycle arrest in G<sub>0</sub>/G<sub>1</sub> phase in Vero cells via downregulation of cyclin D1 [165], Morinaga *et al.* detected cell death ensuing SubAB treatment by trypan blue dye exclusion [166] as was already demonstrated by Paton *et al.* [83]. In accordance to these findings concerning the cell cycle, a EGF-SubA immunotoxin inhibited cell proliferation in glioma cells [173]. Likewise, inhibition of HeLa cell proliferation [174] and induction of cell death in HepG2 cells [63] was demonstrated following treatment with abrin-a.

### 4.1.4 Apoptotic characteristics of induced cell death

Having established that all three toxin cmRNAs reduce cell proliferation as well as prompt cell death, the characteristics of cell death were investigated by diverse assays.

In case of DT cmRNA, only a limited number of treated HuH7 cells displayed apoptotic characteristics, namely exposure of phosphatidylserine (PS) and DNA fragmentation. Fragmentation of DNA after DT treatment was observed before in different studies [168, 171]. In contrast, the exposure of phosphatidylserine, generally observed as one characteristic of apoptotic cells, was perceived only to a low degree in this study after treatment with DT-encoding cmRNA and has very rarely been investigated previously. Also, induction of caspase-3 and -7 activity was not detected in the present study, although caspase-3 activity has been demonstrated after treatment of U937 cells with DT [175]. The decreased activity of caspase-3 measured in comparison to the untransfected control (UT) cells might be a consequence of the reduced cell number. For KB as wells as for HuH7 cells, rounding and detachment after treatment, markers of apoptotic cell death [114], were noticed.

Research over the last decades has shown that DT dependent toxicity varies between cell types. Some cell lines show resistance to cell death despite a translational stop after DT treatment, suggesting that inhibition of protein synthesis is not sufficient for the induction of cell death [171, 176]. An analogous induction of translational stop by other methods was found to cause cell death considerably delayed in comparison to DT treatment [171]. However, inhibition of the ADP-ribosyltransferase activity of DT and thereby of its capability to block protein synthesis also prevented cell death [176], demonstrating the requirement of protein synthesis inhibition for DNA fragmentation and cell death. Cell-free assays conducted by Chang *et al.* showed direct cleavage of DNA by DT [177] and further studies showed that its nuclease activity is associated

## 4 Discussion

with the A-fragment of DT [178]. Bruce *et al.*, moreover, demonstrated that not only DT itself displays nuclease activity but also the mutant CMR197 that contains a mutation in the active site for ADP-ribosylation [161]. The authors concluded that nuclease activity and ADP-ribosylation present two distinct catalytic sites and presumed that the higher cytotoxicity of the native toxin compared to the mutant is a consequence of decreased amounts of DNA repair enzymes due to the block in translation. Besides, inhibition of the cellular apoptosis susceptibility (CAS) protein by an antisense method resulted in resistance to cell death induced by DT, by further ADP-ribosylating toxins or by TNF [179]. In combination with the finding that, next to playing an important role in mitosis [180], CAS was demonstrated to support the formation of the apoptosome [181], this implies involvement of apoptosis in DT-induced cell death. Also, DT was found to depolymerize the actin cytoskeleton to a higher extent than can be explained by the obstruction of protein synthesis [182]. In U937 cells, Thorburn *et al.* discovered FADD-dependent activation of caspases-3, 8 and 9, indicating that components of the intrinsic as well as of the extrinsic pathway of initiation are involved in DT-mediated apoptosis [183]. Taken together, it can be said that cytotoxicity of DT is a result of various factors and the contribution of each one appears to be cell type dependent. Though DT was studied extensively in the past, its method to trigger cell death has not yet been completely understood.

SubA-induced protein synthesis inhibition and cell death were demonstrated in this study. However, only minor caspase-3/7 activity, 18 % Annexin V+/PI- cells and 42 % of cells in SubG<sub>1</sub> phase were detected 72 after transfection in HuH7 cells. The occurrence of apoptosis after treatment with SubAB is generally accepted. Activation of caspase-3 in response to SubA or SubAB treatment was shown before by various groups [62, 173, 184]. Likewise, a comparable percentage of cells (around 20 %) was found to be Annexin V+/PI- in a caspase dependent manner [184] and DNA fragmentation was observed before [184, 185].

Several studies showed that cell death after SubAB treatment is not merely the result of inhibited protein synthesis but induced by the UPR. This would also account for the discrepancy observed in the current study in case of HuH7 cells; namely that, though reduction in cell viability was comparable, decrease in protein synthesis by SubA was lower than by AA or DTA. An important hint in that direction is the transient nature of the translational stop. Decrease in protein synthesis is at a maximum 1 h after treatment as is the phosphorylation of eIF2 $\alpha$  (p-eIF2 $\alpha$ ), the mediator of protein synthesis inhibition, which was not discovered any more

## 4 Discussion

after 6 h [185]. Furthermore, p-eIF2 $\alpha$  was not detected after treatment with a SubAB protein mutated in the catalytic triad responsible for BiP cleavage (A272) and in cells deleted of PERK [185]. This indicates the dependence of eIF2 $\alpha$  phosphorylation on BiP cleavage and on the activity of the UPR sensor PERK which is causal for translational inhibition during UPR [92]. In accordance, Wolfson *et al.* also found that inhibition of protein synthesis is maximal 1 h after treatment and dependent on PERK [185]. Besides, phosphorylated and hence active PERK was mainly observed 0.5 h and 1 h after treatment [165]. Novoa *et al.* established that the UPR stimulated GADD (growth arrest and DNA damage gene) 34 protein dephosphorylates eIF2 $\alpha$  in a feedback mechanism and thereby allows the resumption of protein synthesis [186]. The authors assume that this might be a necessary step to enable the enhanced production of important UPR proteins like BiP itself.

In contrast to the transient inhibition of protein synthesis, however, newly produced BiP mRNA continued to be cleaved by SubA or SubAB [62, 165, 185] and therefore UPR endured even after re-establishment of protein synthesis. In case of prolonged UPR, cell death is achieved by the induction of apoptosis. Accordingly, the employment of the mRNA-encoded toxin instead of the protein toxin itself, connected with prolonged presence of SubA in the cytosol, comprises the benefit of a substantially lengthened period of ER stress which consequently most certainly results in cell death. Highly important in the triggering of cell death after ER stress is the transcriptional factor CHOP whose expression is increased by different arms of the UPR signaling path [94]. CHOP, also named GADD153, was found to be increased in cells treated with SubAB [185]. Regarding CHOP and other factors of significance in UPR, increased RNA levels were noticed after treatment with SubAB but not after treatment with the mutant A272, asserting BiP cleavage as starting point of subtilase cytotoxin induced UPR. Apart from increasing the expression of GADD34, thereby reversing the translational stop and allowing the expression of pro-apoptotic proteins, CHOP also induces apoptosis by inhibiting expression of the anti-apoptotic Bcl-2 and by stimulating Ca<sup>2+</sup> transport from the ER to the mitochondria [187]. This is also supported by the finding of cytochrome c release from mitochondria after treatment with SubAB [165], a central part of the intrinsic apoptotic pathway [110]. The reduction in protein expression and enhanced degradation of proteins as part of the UPR and consequent downregulation of cyclin D1 might also contribute to the SubAB induced cell cycle arrest as observed by Morinaga *et al.* [165]. The involvement of the UPR in SubA caused signaling implicates a diverse range of possible pathways leading to cell death or to cell survival.

## 4 Discussion

In accordance with what has been reported by different groups [108, 170], this study clearly demonstrated that abrin-a induces apoptotic cell death in KB cells by detecting caspase-3 activation, phosphatidylserine exposure and nuclear fragmentation [65]. In HuH7 cells, in contrast, indications observed for apoptotic cell death were only small; aside from DNA fragmentation analysis which revealed 55 % of cells in apoptosis at 72 h after transfection. Though caspase-3 activation was shown to be a key component of abrin induced apoptosis with peak activation ranging from 10 h to 48 h [107, 108, 170, 188] [65] it could not be detected in HuH7 cells after treatment with abrin a. Qu and Qing showed Annexin V positive but PI negative cells at 8-36 h post treatment with abrin while starting at 40 h the Annexin V positive cells became permeable for PI [170] [65]. They also detected nuclear fragmentation 15 h after exposure of cells to abrin as was likewise shown by other groups at 12 h and 24 h [65, 108, 189]. After staining with Hoechst, chromatin condensation was observed in previous studies [65, 170]. Rounding and detachment of cells, as hallmark of apoptotic cell death [114], were observed in the present study after transfecting KB or HuH7 cells with abrin-a encoding mRNA. While it is established that cells treated with abrin-a undergo apoptosis, different pathways have been proposed [65]. According to Gadadhar and Karande, substituting E164 by alanine blocked inhibition of protein synthesis but had no influence on the induction of cell death [63]. From this they deduced that cell death after abrin exposure can occur independently of its protein synthesis inhibitory capacity. Likewise, Qu and Qing suggest that the inhibition of protein synthesis and mitochondrial membrane damage after ROS (reactive oxygen species) production present two independent pathways [65, 170]. Along the same line, Shih *et al.* found that the AOP-1 (anti-oxidant protein) is bound by abrin, leading to its inhibition and subsequently to the induction of ROS and the release of cytochrome c independently of the *N*-glycosidase activity of abrin [190]. However, after mutating glutamic acid-164 to alanine, Mishra *et al.* observed that the occurrence of cell death was delayed in a manner comparable to the delay in inhibition of protein synthesis and thereof deduced that stop of translation is the main factor in abrin induced cell death [107]. The intrinsic mitochondrial pathway following abrin treatment was confirmed by various groups [65, 108, 189]. In cells overexpressing the anti-apoptotic Bcl-2, apoptotic cell death after abrin treatment was absent while inhibition of protein synthesis occurred [108]. The same group also detected mitochondrial membrane permeabilization, ROS production and DNA fragmentation after abrin treatment in a Fas receptor independent manner. Saxena *et al.*, in contrast, showed the involvement of the Fas

## 4 Discussion

ligand and thereby of the extrinsic pathway after exposure to abrin [65] and that blockage of the Fas receptor considerably reduced apoptosis in Jurkat cells [188].

The differences observed between KB and HuH7 cells are in accordance with what was discovered by Bora *et al.* While they detected caspase dependent apoptotic cell death after treatment with abrin in Jurkat cells, cells underwent programmed necrosis in the B cell line U266B1 [191]. Though neither exposure of phosphatidylserine, fragmentation of DNA nor activation of caspase-3 was perceived in U266B1 cells, they nevertheless underwent depolarization of the mitochondrial membrane and produced ROS in a caspase independent manner after treatment with abrin. In this case, cell death in form of programmed necrosis might result from ROS-mediated modifications of the plasma membrane leading to membrane permeabilization or from ROS-induced lysosomal membrane permeabilization (LMP) [191, 192]. In accordance, it was discovered that apoptosis after abrin treatment could not be completely abolished by inhibition of caspases [170], suggesting a caspase independent pathway also involved in abrin induced apoptosis.

The results obtained for the induction of apoptosis in HuH7 cells after treatment with any of the three mRNA-encoded toxins does not meet with the findings of previous studies. As abrin, however, could be shown to distinctly induce apoptosis in KB cells, it cannot be excluded that the outcome for DTA and SubA might as well be different in another cell line. The interactions of different factors in addition to or caused by the inhibition of protein synthesis makes it likely that considerable differences between the cell lines in regard to the means of cell death appear. Also, great variations in kinetics between the single cells might be expected after transfection which would explain that only a small fraction of cells is presently in the particular apoptotic phase at the time point of analysis. This is corroborated by the fact that the percentage of Annexin V+/PI- (early apoptotic) cells is not exceeded by the number of Annexin V+/PI+ (necrotic or secondary necrotic) cells. Due to the lack of phagocytic cells, cells undergoing apoptosis *in vitro* will eventually die by secondary necrosis, signified amongst others by permeabilization of the cell membrane [193]. Further studies are necessary to clarify the apoptotic features of the ensuing cell death in regard to the selected cell line and toxin, taking into account also experiments concerning the mitochondria, oxidative cell stress and ER stress. Increasing the transfection efficiency, e. g. by magnetofection, might enhance the number of transfected cells without intensifying unspecific toxicity and thereby facilitating investigations regarding the induced cell death.

## 4 Discussion

### 4.1.5 Comparison of toxins

Cell viability assays performed on the cell lines HuH7 and KB accentuated the distinction between the degrees of toxicity caused by the three toxins. Concerning HuH7 cells, the decline in cell viability 48 h after transfection was comparably high for all three toxins. While SubA cmRNA showed a similar effect on KB cells, AT and DTA cmRNA showed stronger toxicity compared to HuH7 cells [65]. Because of differences in cell number and cell size, a direct comparison between the two cell lines regarding their sensitivity to toxin mediated cell death is limited [65]. As DTA inactivates eEF-2 by ADP-ribosylation [58, 194] and AT blocks the binding of eEF-2 to the ribosome by cleaving an adenine from the rRNA [103], the two toxins show a similar and irreversible mode of action [65]. The activation of the unfolded protein response (UPR), as cause for cell death by SubA [59], distinguishes it clearly from the other toxins [65]. As the induction of the UPR also increases the expression of GRP78 [195], the substrate of SubA [59], it seems possible that UPR induced apoptosis can be evaded [65]. Along this line, the UPR was found to be negatively regulated in HuH7 cells due to the high expression of miR-122, giving another potential reason for the increased susceptibility of HuH7 cells to the UPR-inducing subtilase cytotoxin [196]. Interestingly, though the reduction of cell viability was equal for all toxin cmRNAs in case of HuH7 cells, the efficacy regarding inhibition of protein synthesis is reduced for ST compared to DT and AT. As was elucidated in the foregoing section, translational stop is the main reason for cell death in case of DT and abrin. After treatment with SubA, in contrast, reduced protein expression is solely part of the response. Morinaga *et al.* demonstrated that, after treatment with SubAB, UPR persists after recommencement of protein synthesis [165].

As the molecular weight of AT compared to DTA cmRNA is higher (AT: 1.0 kb versus DTA: 0.8 kb), AT was more effective than DTA when considering molecular toxicity [65]. As one challenge of successful mRNA-based therapy is transfection efficiency, high effectivity per mRNA molecule is desirable [65]. Moreover, with high molecular toxicity, comparably lower doses of AT are sufficient, thereby reducing potential toxic side effects of mRNA delivery [65].

## 4 Discussion

### 4.2 Clinical application

The main part of the present thesis was concerned with investigating cell toxicity following transfections with toxin-encoding cmRNAs on human cell lines *in vitro*. However, first attempts towards a more practical evaluation were performed as well.

#### 4.2.1 *In vivo* tumor experiments

As one of the first steps towards a clinical application, the capability of the approach to reduce tumor growth was tested by intratumoral application of AT-encoding cmRNA in a KB xenograft tumor model in immunosuppressed mice. Due to the high toxicity of the examined toxin it had to be ascertained first that the applied complexes were restrained to the tumor tissue and did not reach the blood circulation. KB tumors are well-suited for this purpose. Smrekar *et al.* investigated the cause for the reduced uptake of systemically employed plasmid DNA by KB tumors and discovered its comparatively low vascularization [197]. In addition, leakage of the cmRNA complexes into the system is prevented by the formation of a fibrous capsule surrounding the tumor as was observed as well in the present as in further studies [198, 199]. In addition, treatment of KB tumors with mRNA-encoded firefly luciferase in the present study demonstrated the locally confined expression of the intratumorally delivered complexes. In spite of these precautions, three out of ten mice of the LF132-AT treated group had to be euthanized in advance due to bad health condition. Possibly, some of the tumors were too small to completely absorb the injection volume or had not formed a capsule yet at the first application of the complexed cmRNA, resulting in leakage of the formulation into the blood stream. The observed systemic toxicity might also result from an accidental puncturing of a blood vessel during intratumoral injection.

Tumor growth in mice could be diminished considerably by four intratumoral injections of 10 µg formulated AT cmRNA compared to the AU control cmRNA [65]. Foregoing *in vitro* experiments had demonstrated the necessity for repeated applications. The size of the tumors was determined *ex vivo* to exclude errors of measurements resulting from inflammatory processes causing swelling of the surrounding tissue. Twelve days after start of the treatment, the volume of tumors treated with AT-LF132 was significantly reduced by 89 % compared to tumors that had been injected with AU-LF132 [65]. In comparison, in a previous study plasmid DNA coding for the A-chain of diphtheria toxin under a target cell specific double promoter could diminish tumor size in bladder cancer by 68 % compared to the luc-expressing control plasmid group

## 4 Discussion

[65, 200]. To achieve these effects, three injections, each with 25 µg plasmid, were employed [65]. Ramnath *et al.* showed a reduction in volume of transplanted tumors in mice up to 62 % compared to the control group after five intralesional treatments with the protein abrin-a [201] [65]. In the mentioned study, depending on the chosen cell line, simultaneous application of the protein while injecting the tumor cells resulted in complete inhibition of tumor growth. Another group could show that by single injection of 9 µg of an immunotoxin containing the A-chain of abrin-a, tumor growth in mice could be delayed by seven to ten days in human small cell lung cancer [64, 65]. Five intravenous applications of nanoparticles containing 10 µg herpes simplex virus-thymidine kinase-encoding mRNA on alternating days combined with semi-daily treatments with ganciclovir of athymic mice with a xenograft tumor resulted in significantly reduced tumor growth [55]. Notably, in this study the employment of mRNA proved to be substantially more effective than pDNA. In comparison to those studies, the present study demonstrated an equal or in part considerably heightened inhibitory effect on tumor growth.

In the current study, necrosis in the center of the tumors was observed for all mice of each group. The estimated percentages of necrotic tissue were vastly distributed. However, neither distinct variations between the groups nor an obvious relation to the tumor size was noticed. Presence of necrotic intratumoral regions in KB tumors was perceived before [198, 199] and Smrekar *et al.* assumed that this ensued in consequence to their low vascularization [197]. The preceding *in vitro* experiments of the present study had shown that cells transfected with AT cmRNA were reduced in proliferation and underwent cell death. Accordingly, a diminished number of cells in mitosis along with an increase in degenerating cells would be expected for AT cmRNA treated tumors in comparison to the control groups. The number of degenerating cells was distinctive and substantially higher than the number of cells in mitosis. Nevertheless, no noteworthy differences between the respective means of the individual groups were found. The mRNA-encoded herpes simplex virus-thymidine kinase/ganciclovir (TK/GCV) system, which induced apoptosis *in vitro*, was also attested to cause apoptosis in treated tumors [55]. As euthanasia in the present study was conducted three days after the last and eight days after the penultimate injection, it is conceivable that the proliferation inhibiting effect of abrin-a was no longer observable. However, the absence of dying or degenerating cells indicates that the principal part of the observed reduction in tumor growth was due to a decrease in proliferation. Histological analysis also demonstrated necrosis in the peripheral tissue of the tumors and local immunologic effects caused by the cationic lipid formulated

## 4 Discussion

cmRNA that were not present in 2 % sucrose treated tumors. Nonetheless, injections with AU-LF132 did not result in reduced tumor growth compared to treatment with 2 % sucrose.

The conducted experiment in mice clearly demonstrated the potential of toxin-encoding cmRNAs to reduce tumor growth.

### 4.2.2 Cell-specificity of cmRNA translation

As described in the introduction section, various methods exist to enable cell-specific toxicity in gene or transcript therapy and are necessary to implement for prospective clinical applications. Primarily, these methods comprise linkage of the transfection reagent to a ligand whose receptor is overexpressed on the target cell and utilization of cell-specific promoters. Equivalent to the employment of cell-specific promoters for gene therapy, microRNAs (miRNAs) can be exploited to confine expression of the encoded protein to the target cell. In the present study, the employment of three miRNAs was envisaged with the aim of preventing translation in healthy liver tissue and hematopoietic cells without disturbing translation in the target tissue liver cancer. Brown *et al.* established the concept by including four repeats of the binding site of miR-142-3p in the 3' UTR of the expression vector [202]. As the corresponding miRNA is predominantly present in hematopoietic cells, like antigen presenting cells (APCs), expression of the transgene could be blocked in those cells without affecting expression in the target cells. Avoiding expression of the transgene in APCs is of importance in order to diminish stimulation of the immune system [202, 203]. The miRNA-122-5p is abundantly expressed in the liver, downregulated in many liver cancer types like HCC (hepatocellular carcinoma) and rarely found in other tissues [142, 204, 205]. Suzuki *et al.* implemented four binding sites of miR-122-5p in an adenoviral vector in order to protect the liver from expression of the encoded protein after systemic administration [206]. In doing so they could reduce firefly luciferase activity in the liver up to 1,500 fold after intratumoral injection. Combining the binding sites for miR-142-3p and miR-122-5p in one vector allowed inhibition of transgene expression as well in the miR-142-3p expressing monocyte cell line U937 as in the hepatocyte cell line HuH7 [142]. Though originally established from a hepatocarcinoma, HuH7 cells present several features of a well-differentiated liver tissue [207], like high expression of miR-122-5p [142, 206]. Next to HuH7 and U937 cells, further applied cell lines in the current study are the hepatocarcinoma cell line HepG2 and the embryonal kidney cell line HEK293. HepG2 cells were intended to represent HCC tissue as the expression of miR-122 as well as of miR-142-3p was detected to be

## 4 Discussion

diminished [208, 209], the same applying for HEK293 cells [208]. Wu *et al.* demonstrated that through combination of binding sites of different miRNAs highly expressed in the non-target tissue, prevention of transgene expression could be improved compared to multiple deployment of one type of miRNA binding site [210]. Therefore, with miR-125-5p another miRNA whose expression profile resembles that of miR-122-5p, implying expression in liver tissue and HuH7 cells but downregulation in HCC and HepG2 cells, was employed [211]. The results of the qPCR experiments conducted in the present study regarding the expression of the chosen miRNAs in the four cell lines match the expectations formed according to the literature. As it was furthermore established by other groups that the success of miRNA-deploying targeting increased with the number of repeats of miRNA binding sites [212], varying numbers of miRNA binding sites were employed to test this proposition.

The setup was designed to potentially give answers to the following questions:

- Can the cytotoxicity of the toxin-encoding cmRNAs be reduced in liver or haematopoietic cells by incorporation of appropriate miRNA binding sites?
- Can cytotoxicity be reduced simultaneously in liver and hematopoietic cells?
- Which compilation of different miRNA binding sites (regarding type and number of repeats) yields the best results?
- Is cytotoxicity in the target cells affected by the integration of miRNA binding sites?
- Does this concept also work in animal tumor models in case of intratumoral as well as systemic application?

So far, eight out of nine constructs were cloned successfully. Apart from the performed qPCR experiments, no further assays to address the presented questions could be conducted due to shortage of time.

### 4.2.3 Combination therapies and immunotherapy

Experiments performed in the present study demonstrated the likelihood of a so-called bystander effect after treatment with the toxin-encoding cmRNAs. The occurrence of a bystander effect is defined by an indirect cytotoxicity mediated through transfected neighboring cells. Clearly, no toxic impact of DT or AT cmRNA-transfected cells on untransfected cells was observed. In contrast, treatment of untransfected cells with the supernatant or with the lysate of cells transfected with ST cmRNA resulted in a statistically

## 4 Discussion

significant reduction in cell viability. The occurrence of a bystander effect is double-edged. For one, it considerably increases the risk that in case of tumor treatment healthy tissue might be affected as well. On the other hand, treatment efficiency augments as also non-transfected cancer cells are killed. Freeman *et al.*, for instance, observed that for tumor regression it was sufficient when one half of the tumor cells expressed the herpes simplex virus thymidine kinase (HSV-TK) which activates the toxin ganciclovir [213]. In case of ganciclovir treatment, cells expressing the HSV-TK were lethal to non-expressing cells.

Considering the specific properties of toxicity induced by the toxins, various combination strategies can be envisaged. A previous study showed that the employment of a protein synthesis inhibitory immunotoxin, in this case DT, diminished the chemoresistance of acute myeloid leukemia cells by blocking the expression of multidrug resistance (MDR) proteins [214]. Also, the efficacy of ER stress stimulating drugs like bortezomib on melanoma cells was demonstrated to be enhanced after downregulation of GRP78 by subtilase cytotoxin or GRP78 siRNA [215]. Possibly, by combining chemotherapy with toxin-encoding mRNA treatment, the therapeutic dose of both could be reduced and side effects minimized while increasing the therapeutic effect.

Another very promising approach that opens various possibilities and was investigated vastly is cancer immunotherapy. Increased anti-tumoral immune response is achieved either by inhibiting the immunosuppressive function of the tumor by blocking molecules inhibiting T cell differentiation or function, e. g. PD-1 [216], or by directly stimulating the immune system through the inclusion of chemokines, cytokines or tumor associated antigens [65, 217]. In regard to the first strategy, Ghiringhelli *et al.* found that by cyclophosphamide mediated reduction of circulating regulatory T cells and thereby of their repressive influence on conventional T cells and NK (natural killer) cells, tumor growth could be decelerated [218, 219]. Combination with a subsequent immunostimulatory therapy achieved complete regression of pre-developed tumors in rats [218]. Analogous to the employment of immunosuppressive or immunostimulatory agents like the CD40 ligand [220] in armed oncolytic viruses [221], co-administration with a toxin-encoding mRNA can be envisaged [65]. It has been observed that the anti-tumor immune response initiated by oncolytic viruses displays an important component of their efficiency. As the immunogenic progression of cell death is crucial for the outcome, oncolytic viruses were engineered to modulate the type of cell death, for instance by deleting genes coding for anti-apoptotic proteins [217]. Due to its immunological properties,

## 4 Discussion

the mRNA molecule itself might serve as adjuvant [27, 65]. As the anti-tumor effect of an abrin-containing immunotoxin was increased by combination with the cytokine IL-12 [222], it can be assumed that the toxin abrin-a is in general suitable for immunotherapy. Conceivably, such approaches might be applicable to reduce tumor growth prior to surgery as was repeatedly done applying chemotherapy [223] and to induce a systemic immune response to disseminated tumor cells [65].

### 4.3 Conclusion and outlook

The present study could show that chemically modified mRNAs encoding the A-chain of diphtheria toxin, subtilase cytotoxin or abrin-a display effective anti-tumor properties *in vitro* or *in vivo* [65]. By repeated injections of complexed AT cmRNA into tumors in mice, tumor growth could be inhibited in a manner comparable to previous *in vivo* studies applying abrin-a or toxin-encoding plasmids [65]. The employment of mRNA is very attractive as it shows various safety-relevant benefits compared to pDNA and limited toxicity has been associated with immunotoxins [65]. The type of induced cell death is of relevance for the induction of an anti-tumor immune response and hence for a potential combination with anti-cancer immunotherapy. Accordingly, since the conducted experiments demonstrated cell dependency regarding the form of the induced cell death, appropriate evaluations of the suitability of the particular toxins with respect to the intended tumor tissue have to be performed. The promising results obtained with AT, however, prompt further studies using different tumor models to fully appreciate the anti-tumor efficacies of toxin-encoding cmRNAs [65].

## References

1. Kozak, M., *Initiation of translation in prokaryotes and eukaryotes*. Gene, 1999. **234**(2): p. 187-208.
2. Spriggs, K.A., M. Bushell, and A.E. Willis, *Translational regulation of gene expression during conditions of cell stress*. Molecular cell, 2010. **40**(2): p. 228-237.
3. Li, Y. and M. Kiledjian, *Regulation of mRNA decapping*. Wiley Interdiscip Rev RNA, 2010. **1**(2): p. 253-65.
4. Martin, S.A., E. Paoletti, and B. Moss, *Purification of mRNA guanylyltransferase and mRNA (guanine-7-) methyltransferase from vaccinia virions*. J Biol Chem, 1975. **250**(24): p. 9322-9.
5. Wilkie, G.S., K.S. Dickson, and N.K. Gray, *Regulation of mRNA translation by 5'- and 3'-UTR-binding factors*. Trends Biochem Sci, 2003. **28**(4): p. 182-8.
6. Ferizi, M., et al., *Human cellular CYBA UTR sequences increase mRNA translation without affecting the half-life of recombinant RNA transcripts*. Sci Rep, 2016. **6**: p. 39149.
7. Gustafsson, C., S. Govindarajan, and J. Minshull, *Codon bias and heterologous protein expression*. Trends Biotechnol, 2004. **22**(7): p. 346-53.
8. Brawerman, G., *The Role of the poly(A) sequence in mammalian messenger RNA*. CRC Crit Rev Biochem, 1981. **10**(1): p. 1-38.
9. Sahin, U., K. Kariko, and O. Tureci, *mRNA-based therapeutics--developing a new class of drugs*. Nat Rev Drug Discov, 2014. **13**(10): p. 759-80.
10. Holcik, M. and N. Sonenberg, *Translational control in stress and apoptosis*. Nat Rev Mol Cell Biol, 2005. **6**(4): p. 318-27.
11. Kaul, G., G. Pattan, and T. Rafeequi, *Eukaryotic elongation factor-2 (eEF2): its regulation and peptide chain elongation*. Cell biochemistry and function, 2011. **29**(3): p. 227-234.
12. Michel, Y.M., et al., *Cap-Poly(A) synergy in mammalian cell-free extracts. Investigation of the requirements for poly(A)-mediated stimulation of translation initiation*. J Biol Chem, 2000. **275**(41): p. 32268-76.
13. Wolff, J.A., et al., *Direct gene transfer into mouse muscle in vivo*. Science, 1990. **247**(4949 Pt 1): p. 1465-8.
14. Medzhitov, R., *Toll-like receptors and innate immunity*. Nat Rev Immunol, 2001. **1**(2): p. 135-45.
15. Nallagatla, S.R. and P.C. Bevilacqua, *Nucleoside modifications modulate activation of the protein kinase PKR in an RNA structure-specific manner*. RNA, 2008. **14**(6): p. 1201-13.
16. Hornung, V., et al., *5'-Triphosphate RNA is the ligand for RIG-I*. Science, 2006. **314**(5801): p. 994-7.
17. Bokar, J.A. and F.M. Rottman, *Biosynthesis and functions of modified nucleosides in eukaryotic mRNA*. ASM Press, Washington, D. C., 1998: p. 183-200.
18. Kariko, K., et al., *Suppression of RNA recognition by Toll-like receptors: the impact of nucleoside modification and the evolutionary origin of RNA*. Immunity, 2005. **23**(2): p. 165-75.
19. Kariko, K., et al., *Incorporation of pseudouridine into mRNA yields superior nonimmunogenic vector with increased translational capacity and biological stability*. Mol Ther, 2008. **16**(11): p. 1833-40.
20. Kormann, M.S., et al., *Expression of therapeutic proteins after delivery of chemically modified mRNA in mice*. Nat Biotechnol, 2011. **29**(2): p. 154-7.
21. Anderson, B.R., et al., *Incorporation of pseudouridine into mRNA enhances translation by diminishing PKR activation*. Nucleic Acids Res, 2010. **38**(17): p. 5884-92.
22. Warren, L., et al., *Highly efficient reprogramming to pluripotency and directed differentiation of human cells with synthetic modified mRNA*. Cell Stem Cell, 2010. **7**(5): p. 618-30.
23. Furuichi, Y. and A.J. Shatkin, *Viral and cellular mRNA capping: past and prospects*. Adv Virus Res, 2000. **55**: p. 135-84.
24. Peng, J., E.L. Murray, and D.R. Schoenberg, *In vivo and in vitro analysis of poly(A) length effects on mRNA translation*. Methods Mol Biol, 2008. **419**: p. 215-30.

## References

25. Phua, K.K., K.W. Leong, and S.K. Nair, *Transfection efficiency and transgene expression kinetics of mRNA delivered in naked and nanoparticle format*. J Control Release, 2013. **166**(3): p. 227-33.
26. Agapov, E.V., et al., *Noncytopathic Sindbis virus RNA vectors for heterologous gene expression*. Proc Natl Acad Sci U S A, 1998. **95**(22): p. 12989-94.
27. Tavernier, G., et al., *mRNA as gene therapeutic: How to control protein expression*. Journal of Controlled Release 2011. **150**: p. 238-247.
28. Kim, T.K. and J.H. Eberwine, *Mammalian cell transfection: the present and the future*. Analytical and bioanalytical chemistry, 2010. **397**(8): p. 3173-3178.
29. Plank, C., O. Zelphati, and O. Mykhaylyk, *Magnetically enhanced nucleic acid delivery. Ten years of magnetofection-progress and prospects*. Adv Drug Deliv Rev, 2011. **63**(14-15): p. 1300-31.
30. Van Lint, S., et al., *Intratumoral Delivery of TriMix mRNA Results in T-cell Activation by Cross-Presenting Dendritic Cells*. Cancer Immunol Res, 2016. **4**(2): p. 146-56.
31. Sharom, F.J., *ABC multidrug transporters: structure, function and role in chemoresistance*. Pharmacogenomics, 2008. **9**(1): p. 105-27.
32. Rich, J.N., *Cancer stem cells in radiation resistance*. Cancer Res, 2007. **67**(19): p. 8980-4.
33. Monsuez, J.J., et al., *Cardiac side-effects of cancer chemotherapy*. Int J Cardiol, 2010. **144**(1): p. 3-15.
34. Monje, M. and J. Dietrich, *Cognitive side effects of cancer therapy demonstrate a functional role for adult neurogenesis*. Behav Brain Res, 2012. **227**(2): p. 376-9.
35. Holohan, C., et al., *Cancer drug resistance: an evolving paradigm*. Nat Rev Cancer, 2013. **13**(10): p. 714-26.
36. Scott, A.M., J.D. Wolchok, and L.J. Old, *Antibody therapy of cancer*. Nat Rev Cancer, 2012. **12**(4): p. 278-87.
37. Kreitman, R.J., et al., *Phase II trial of recombinant immunotoxin RFB4(dsFv)-PE38 (BL22) in patients with hairy cell leukemia*. J Clin Oncol, 2009. **27**(18): p. 2983-90.
38. Eklund, J.W. and T.M. Kuzel, *Denileukin diftitox: a concise clinical review*. Expert Rev Anticancer Ther, 2005. **5**(1): p. 33-8.
39. Kreitman, R.J., *Immunotoxins for targeted cancer therapy*. AAPS J, 2006. **8**(3): p. E532-51.
40. Pastan, I., *Targeted therapy of cancer with recombinant immunotoxins*. Biochim Biophys Acta, 1997. **1333**(2): p. C1-6.
41. Potala, S., S.K. Sahoo, and R.S. Verma, *Targeted therapy of cancer using diphtheria toxin-derived immunotoxins*. Drug Discov Today, 2008. **13**(17-18): p. 807-15.
42. Pai-Scherf, L.H., et al., *Hepatotoxicity in cancer patients receiving erb-38, a recombinant immunotoxin that targets the erbB2 receptor*. Clin Cancer Res, 1999. **5**(9): p. 2311-5.
43. Pastan, I., et al., *Immunotoxin treatment of cancer*. Annu Rev Med, 2007. **58**: p. 221-37.
44. Gofrit, O.N., et al., *DNA based therapy with diphtheria toxin-A BC-819: a phase 2b marker lesion trial in patients with intermediate risk nonmuscle invasive bladder cancer*. J Urol, 2014. **191**(6): p. 1697-702.
45. Mizrahi, A., et al., *Development of targeted therapy for ovarian cancer mediated by a plasmid expressing diphtheria toxin under the control of H19 regulatory sequences*. J Transl Med, 2009. **7**: p. 69.
46. Qu, L., et al., *Suicide gene therapy for hepatocellular carcinoma cells by survivin promoter-driven expression of the herpes simplex virus thymidine kinase gene*. Oncol Rep, 2013. **29**(4): p. 1435-40.
47. Altieri, D.C., *Survivin, versatile modulation of cell division and apoptosis in cancer*. Oncogene, 2003. **22**(53): p. 8581-9.
48. Boulaiz, H., et al., *A novel double-enhanced suicide gene therapy in a colon cancer cell line mediated by gef and apoptin*. BioDrugs, 2014. **28**(1): p. 63-74.
49. Vago, R., et al., *Nanoparticle-mediated delivery of suicide genes in cancer therapy*. Pharmacol Res, 2016. **111**: p. 619-41.
50. Hacein-Bey-Abina, S., et al., *LMO2-associated clonal T cell proliferation in two patients after gene therapy for SCID-X1*. Science, 2003. **302**(5644): p. 415-9.

## References

51. Hackett, P.B., et al., *Evaluating risks of insertional mutagenesis by DNA transposons in gene therapy*. *Transl Res*, 2013. **161**(4): p. 265-83.
52. Yamamoto, A., et al., *Current prospects for mRNA gene delivery*. *Eur J Pharm Biopharm*, 2009. **71**(3): p. 484-9.
53. Rejman, J., et al., *mRNA transfection of cervical carcinoma and mesenchymal stem cells mediated by cationic carriers*. *J. Control. Release*, 2010. **147**: p. 385–391.
54. Pearson, H., *Human genetics: One gene, twenty years*. *Nature*, 2009. **460**(7252): p. 164-9.
55. Wang, Y., et al., *Systemic delivery of modified mRNA encoding herpes simplex virus 1 thymidine kinase for targeted cancer gene therapy*. *Mol Ther*, 2013. **21**(2): p. 358-67.
56. Bennett, M.J., S. Choe, and D. Eisenberg, *Domain swapping: entangling alliances between proteins*. *Proc Natl Acad Sci U S A*, 1994. **91**(8): p. 3127-31.
57. Gill, D.M., *Seven toxic peptides that cross cell membranes*. Academic Press, Inc., New York, 1978: p. 291-322.
58. Frankel, A.E., et al., *Diphtheria fusion protein therapy of chemoresistant malignancies*. *Curr Cancer Drug Targets*, 2002. **2**(1): p. 19-36.
59. Paton, A.W., et al., *AB5 subtilase cytotoxin inactivates the endoplasmic reticulum chaperone BiP*. *Nature*, 2006. **443**(7111): p. 548-52.
60. Endo, Y., et al., *The mechanism of action of ricin and related toxic lectins on eukaryotic ribosomes. The site and the characteristics of the modification in 28 S ribosomal RNA caused by the toxins*. *J Biol Chem*, 1987. **262**(12): p. 5908-12.
61. Alouf, J.E. and J.H. Freer, *The Comprehensive Sourcebook of Bacterial Toxins*. Academic Press, London, 1999.
62. Backer, J.M., et al., *Chaperone-targeting cytotoxin and endoplasmic reticulum stress-inducing drug synergize to kill cancer cells*. *Neoplasia*, 2009. **11**(11): p. 1165-73.
63. Gadadhar, S. and A.A. Karande, *Abrin immunotoxin: targeted cytotoxicity and intracellular trafficking pathway*. *PLoS One*, 2013. **8**(3): p. e58304.
64. Wawrzynczak, E.J., et al., *Molecular and biological properties of an abrin A chain immunotoxin designed for therapy of human small cell lung cancer*. *Br J Cancer*, 1992. **66**(2): p. 361-6.
65. Hirschberger K., Jarzebinska, A., Kessel E., Kretzschmann V., Aneja M. K., Dohmen C., Hermann-Janson A., Wagner E., Plank C., Rudolph C., *Exploring Cytotoxic mRNAs as a Novel Class of Anti-cancer Biotherapeutics*. *Molecular Therapy-Methods & Clinical Development*, 2018. **8**: p. 141-151.
66. Frankel, A.E., et al., *Phase I trial of a novel diphtheria toxin/granulocyte macrophage colony-stimulating factor fusion protein (DT388GMCSF) for refractory or relapsed acute myeloid leukemia*. *Clin Cancer Res*, 2002. **8**(5): p. 1004-13.
67. Roux Jr., E. and A. Yersin, *contribution a l'etude de la diphtherie*. *Ann. Inst. Pasteur*, 1888. **2**: p. 620-629.
68. Control, C.f.D. and Prevention, *Epidemiology and prevention of vaccine-preventable diseases Public Health Foundation*. Washington, DC, 2015: p. 231-246.
69. Collier, R.J., *Understanding the mode of action of diphtheria toxin: a perspective on progress during the 20th century*. *Toxicon*, 2001. **39**(11): p. 1793-803.
70. Collier, R.J. and H.A. Cole, *Diphtheria toxin subunit active in vitro*. *Science*, 1969. **164**(3884): p. 1179-81.
71. Gill, D.M. and A.M. Pappenheimer, Jr., *Structure-activity relationships in diphtheria toxin*. *J Biol Chem*, 1971. **246**(5): p. 1492-5.
72. Murphy, J.R., *Mechanism of diphtheria toxin catalytic domain delivery to the eukaryotic cell cytosol and the cellular factors that directly participate in the process*. *Toxins (Basel)*, 2011. **3**(3): p. 294-308.
73. Gordon, V.M., et al., *Proteolytic activation of bacterial toxins by eukaryotic cells is performed by furin and by additional cellular proteases*. *Infection and immunity*, 1995. **63**(1): p. 82-87.
74. Naglich, J.G., et al., *Expression cloning of a diphtheria toxin receptor: identity with a heparin-binding EGF-like growth factor precursor*. *Cell*, 1992. **69**(6): p. 1051-61.

## References

75. Boquet, P. and A.M. Pappenheimer, Jr., *Interaction of diphtheria toxin with mammalian cell membranes*. J Biol Chem, 1976. **251**(18): p. 5770-8.
76. Donovan, J.J., et al., *Diphtheria toxin forms transmembrane channels in planar lipid bilayers*. Proc Natl Acad Sci U S A, 1981. **78**(1): p. 172-6.
77. Kagan, B.L., A. Finkelstein, and M. Colombini, *Diphtheria toxin fragment forms large pores in phospholipid bilayer membranes*. Proc Natl Acad Sci U S A, 1981. **78**(8): p. 4950-4.
78. Olsnes, S., J. Wesche, and P. Falnes, *Uptake of protein toxins acting inside cells*, in *Bacterial protein toxins*. 2000, Springer. p. 1-19.
79. Collier, R.J., *Effect of diphtheria toxin on protein synthesis: inactivation of one of the transfer factors*. J Mol Biol, 1967. **25**(1): p. 83-98.
80. Honjo, T., Y. Nishizuka, and O. Hayaishi, *Diphtheria toxin-dependent adenosine diphosphate ribosylation of aminoacyl transferase II and inhibition of protein synthesis*. J Biol Chem, 1968. **243**(12): p. 3553-5.
81. Van Ness, B.G., J.B. Howard, and J.W. Bodley, *ADP-ribosylation of elongation factor 2 by diphtheria toxin. Isolation and properties of the novel ribosyl-amino acid and its hydrolysis products*. J Biol Chem, 1980. **255**(22): p. 10717-20.
82. Van Ness, B.G., J.B. Howard, and J.W. Bodley, *ADP-ribosylation of elongation factor 2 by diphtheria toxin. NMR spectra and proposed structures of ribosyl-diphthamide and its hydrolysis products*. J Biol Chem, 1980. **255**(22): p. 10710-6.
83. Paton, A.W., et al., *A new family of potent AB(5) cytotoxins produced by Shiga toxigenic Escherichia coli*. J Exp Med, 2004. **200**(1): p. 35-46.
84. Corrigan, J.J., Jr. and F.G. Boineau, *Hemolytic-uremic syndrome*. Pediatr Rev, 2001. **22**(11): p. 365-9.
85. Amaral, M.M., et al., *Action of shiga toxin type-2 and subtilase cytotoxin on human microvascular endothelial cells*. PLoS One, 2013. **8**(7): p. e70431.
86. Plaut, R.D. and N.H. Carbonetti, *Retrograde transport of pertussis toxin in the mammalian cell*. Cell Microbiol, 2008. **10**(5): p. 1130-9.
87. Paton, A.W. and J.C. Paton, *Escherichia coli Subtilase Cytotoxin*. Toxins (Basel), 2010. **2**(2): p. 215-228.
88. Le Nours, J., et al., *Structural basis of subtilase cytotoxin SubAB assembly*. J Biol Chem, 2013. **288**(38): p. 27505-16.
89. Hendershot, L.M., *The ER function BiP is a master regulator of ER function*. Mt Sinai J Med, 2004. **71**(5): p. 289-97.
90. Logue, S.E., et al., *New directions in ER stress-induced cell death*. Apoptosis, 2013. **18**(5): p. 537-46.
91. Hollien, J. and J.S. Weissman, *Decay of endoplasmic reticulum-localized mRNAs during the unfolded protein response*. Science, 2006. **313**(5783): p. 104-7.
92. Harding, H.P., Y. Zhang, and D. Ron, *Protein translation and folding are coupled by an endoplasmic-reticulum-resident kinase*. Nature, 1999. **397**(6716): p. 271-4.
93. Adachi, Y., et al., *ATF6 is a transcription factor specializing in the regulation of quality control proteins in the endoplasmic reticulum*. Cell Struct Funct, 2008. **33**(1): p. 75-89.
94. Oyadomari, S. and M. Mori, *Roles of CHOP/GADD153 in endoplasmic reticulum stress*. Cell Death Differ, 2004. **11**(4): p. 381-9.
95. Li, J. and A.S. Lee, *Stress induction of GRP78/BiP and its role in cancer*. Curr Mol Med, 2006. **6**(1): p. 45-54.
96. Harama, D., et al., *A subcytotoxic dose of subtilase cytotoxin prevents lipopolysaccharide-induced inflammatory responses, depending on its capacity to induce the unfolded protein response*. J Immunol, 2009. **183**(2): p. 1368-74.
97. Tahirov, T.H., et al., *Crystal structure of abrin-a at 2.14 Å*. J Mol Biol, 1995. **250**(3): p. 354-67.
98. Olsnes, S., *The history of ricin, abrin and related toxins*. Toxicon, 2004. **44**(4): p. 361-70.
99. Ehrlich, P., *Experimentelle untersuchungen über immunität. II. Ueber abrin*. DMW-Deutsche Medizinische Wochenschrift, 1891. **17**(44): p. 1218-1219.

## References

100. Fernando, C., *Poisoning due to Abrus precatorius (jequirity bean)*. *Anaesthesia*, 2001. **56**(12): p. 1178-80.
101. Dickers, K.J., et al., *Abrin poisoning*. *Toxicol Rev*, 2003. **22**(3): p. 137-42.
102. Reddy, V.V. and M. Sirsi, *Effect of Abrus precatorius L. on experimental tumors*. *Cancer Res*, 1969. **29**(7): p. 1447-51.
103. Endo, Y., A. Gluck, and I.G. Wool, *Ribosomal RNA identity elements for ricin A-chain recognition and catalysis*. *J Mol Biol*, 1991. **221**(1): p. 193-207.
104. Narayanan, S., et al., *Ribosome inactivating proteins and apoptosis*. *FEBS Lett*, 2005. **579**(6): p. 1324-31.
105. Wang, L.C., et al., *Abrin-a A chain expressed as soluble form in Escherichia coli from a PCR-synthesized gene is catalytically and functionally active*. *Biochimie*, 2004. **86**(4-5): p. 327-33.
106. Lord, J.M. and L.M. Roberts, *Toxin entry: retrograde transport through the secretory pathway*. *J Cell Biol*, 1998. **140**(4): p. 733-6.
107. Mishra, R., M.S. Kumar, and A.A. Karande, *Inhibition of protein synthesis leading to unfolded protein response is the major event in abrin-mediated apoptosis*. *Mol Cell Biochem*, 2015. **403**(1-2): p. 255-65.
108. Narayanan, S., A. Surolia, and A.A. Karande, *Ribosome-inactivating protein and apoptosis: abrin causes cell death via mitochondrial pathway in Jurkat cells*. *Biochem J*, 2004. **377**(Pt 1): p. 233-40.
109. Debatin, K.M. and P.H. Krammer, *Death receptors in chemotherapy and cancer*. *Oncogene*, 2004. **23**(16): p. 2950-66.
110. Kroemer, G. and J.C. Reed, *Mitochondrial control of cell death*. *Nat Med*, 2000. **6**(5): p. 513-9.
111. Elmore, S., *Apoptosis: a review of programmed cell death*. *Toxicol Pathol*, 2007. **35**(4): p. 495-516.
112. Wyllie, A.H., "Where, O death, is thy sting?" *A brief review of apoptosis biology*. *Mol Neurobiol*, 2010. **42**(1): p. 4-9.
113. Slee, E.A., C. Adrain, and S.J. Martin, *Executioner caspase-3, -6, and -7 perform distinct, non-redundant roles during the demolition phase of apoptosis*. *J Biol Chem*, 2001. **276**(10): p. 7320-6.
114. Kothakota, S., et al., *Caspase-3-generated fragment of gelsolin: effector of morphological change in apoptosis*. *Science*, 1997. **278**(5336): p. 294-8.
115. Segawa, K., et al., *Caspase-mediated cleavage of phospholipid flippase for apoptotic phosphatidylserine exposure*. *Science*, 2014. **344**(6188): p. 1164-1168.
116. Li, L.Y., X. Luo, and X. Wang, *Endonuclease G is an apoptotic DNase when released from mitochondria*. *Nature*, 2001. **412**(6842): p. 95-99.
117. Joza, N., et al., *Essential role of the mitochondrial apoptosis-inducing factor in programmed cell death*. *Nature*, 2001. **410**(6828): p. 549-554.
118. Cho, K., et al., *Therapeutic nanoparticles for drug delivery in cancer*. *Clin Cancer Res*, 2008. **14**(5): p. 1310-6.
119. Fire, A., et al., *Potent and specific genetic interference by double-stranded RNA in Caenorhabditis elegans*. *nature*, 1998. **391**(6669): p. 806-811.
120. Marquez, R.T. and A.P. McCaffrey, *Advances in microRNAs: implications for gene therapeutics*. *Hum Gene Ther*, 2008. **19**(1): p. 27-38.
121. Doench, J.G., C.P. Petersen, and P.A. Sharp, *siRNAs can function as miRNAs*. *Genes Dev*, 2003. **17**(4): p. 438-42.
122. Lai, E.C., *Micro RNAs are complementary to 3' UTR sequence motifs that mediate negative post-transcriptional regulation*. *Nat Genet*, 2002. **30**(4): p. 363-4.
123. Lee, R.C., R.L. Feinbaum, and V. Ambros, *The C. elegans heterochronic gene lin-4 encodes small RNAs with antisense complementarity to lin-14*. *Cell*, 1993. **75**(5): p. 843-854.
124. Reinhart, B.J., et al., *The 21-nucleotide let-7 RNA regulates developmental timing in Caenorhabditis elegans*. *nature*, 2000. **403**(6772): p. 901-906.
125. Cai, Y., et al., *A brief review on the mechanisms of miRNA regulation*. *Genomics, proteomics & bioinformatics*, 2009. **7**(4): p. 147-154.

## References

126. Lewis, B.P., C.B. Burge, and D.P. Bartel, *Conserved seed pairing, often flanked by adenosines, indicates that thousands of human genes are microRNA targets*. Cell, 2005. **120**(1): p. 15-20.
127. Cho, W.C., *OncomiRs: the discovery and progress of microRNAs in cancers*. Mol Cancer, 2007. **6**: p. 60.
128. Drakaki, A. and D. Iliopoulos, *MicroRNA Gene Networks in Oncogenesis*. Curr Genomics, 2009. **10**(1): p. 35-41.
129. Tzur, G., et al., *Comprehensive gene and microRNA expression profiling reveals a role for microRNAs in human liver development*. PLoS One, 2009. **4**(10): p. e7511.
130. Vasudevan, S., Y. Tong, and J.A. Steitz, *Switching from repression to activation: microRNAs can up-regulate translation*. Science, 2007. **318**(5858): p. 1931-4.
131. Leung, A.K. and P.A. Sharp, *microRNAs: a safeguard against turmoil?* Cell, 2007. **130**(4): p. 581-5.
132. Humphreys, D.T., et al., *MicroRNAs control translation initiation by inhibiting eukaryotic initiation factor 4E/cap and poly(A) tail function*. Proc Natl Acad Sci U S A, 2005. **102**(47): p. 16961-6.
133. Liu, X., et al., *Structurally flexible triethanolamine-core poly(amidoamine) dendrimers as effective nanovectors to deliver RNAi-based therapeutics*. Biotechnol Adv, 2014. **32**(4): p. 844-52.
134. Thai, T.-H., P.A. Christiansen, and G.C. Tsokos, *Is there a link between dysregulated miRNA expression and disease?* Discovery medicine, 2010. **10**(52): p. 184-194.
135. Xia, H., et al., *siRNA-mediated gene silencing in vitro and in vivo*. Nat Biotechnol, 2002. **20**(10): p. 1006-10.
136. Lee, S.K., et al., *Effective gene silencing by multilayered siRNA-coated gold nanoparticles*. Small, 2011. **7**(3): p. 364-70.
137. Mok, H., et al., *Multimeric small interfering ribonucleic acid for highly efficient sequence-specific gene silencing*. Nat Mater, 2010. **9**(3): p. 272-8.
138. Kim, S.S., et al., *Targeted delivery of siRNA to macrophages for anti-inflammatory treatment*. Mol Ther, 2010. **18**(5): p. 993-1001.
139. Tekedereli, I., et al., *Therapeutic Silencing of Bcl-2 by Systemically Administered siRNA Nanotherapeutics Inhibits Tumor Growth by Autophagy and Apoptosis and Enhances the Efficacy of Chemotherapy in Orthotopic Xenograft Models of ER (-) and ER (+) Breast Cancer*. Mol Ther Nucleic Acids, 2013. **2**: p. e121.
140. Ebert, M.S., J.R. Neilson, and P.A. Sharp, *MicroRNA sponges: competitive inhibitors of small RNAs in mammalian cells*. Nat Methods, 2007. **4**(9): p. 721-6.
141. Kelly, E.J., et al., *Engineering microRNA responsiveness to decrease virus pathogenicity*. Nat Med, 2008. **14**(11): p. 1278-83.
142. Brown, B.D., et al., *Endogenous microRNA can be broadly exploited to regulate transgene expression according to tissue, lineage and differentiation state*. Nat Biotechnol, 2007. **25**(12): p. 1457-67.
143. Malito, E., et al., *Structural basis for lack of toxicity of the diphtheria toxin mutant CRM197*. Proc Natl Acad Sci U S A, 2012. **109**(14): p. 5229-34.
144. Bagaria, A., et al., *Structure-function analysis and insights into the reduced toxicity of Abrus precatorius agglutinin I in relation to abrin*. J Biol Chem, 2006. **281**(45): p. 34465-74.
145. Furukawa, T., et al., *Fatal hemorrhage induced by subtilase cytotoxin from Shiga-toxicogenic Escherichia coli*. Microb Pathog, 2011. **50**(3-4): p. 159-67.
146. Hung, C.H., et al., *Cloning and expression of three abrin A-chains and their mutants derived by site-specific mutagenesis in Escherichia coli*. Eur J Biochem, 1994. **219**(1-2): p. 83-7.
147. Han, Y.H., et al., *A recombinant mutant abrin A chain expressed in Escherichia coli can be used as an effective vaccine candidate*. Hum Vaccin, 2011. **7**(8): p. 838-44.
148. Giannini, G., R. Rappuoli, and G. Ratti, *The amino-acid sequence of two non-toxic mutants of diphtheria toxin: CRM45 and CRM197*. Nucleic Acids Res, 1984. **12**(10): p. 4063-9.
149. Cooper, G., *The Cell: A Molecular Approach, 2nd edn. The Cell: A Molecular Approach*. Sunderland, MA. 2000, USA: Sinauer Associates.

## References

150. Munro, S. and H.R. Pelham, *A C-terminal signal prevents secretion of luminal ER proteins*. Cell, 1987. **48**(5): p. 899-907.
151. Buonocore, L. and J.K. Rose, *Prevention of HIV-1 glycoprotein transport by soluble CD4 retained in the endoplasmic reticulum*. Nature, 1990. **345**(6276): p. 625-8.
152. Matthay, M.A., et al., *Transient effect of epidermal growth factor on the motility of an immortalized mammary epithelial cell line*. Journal of cell science, 1993. **106**(3): p. 869-878.
153. Cha, D., et al., *Enhanced modulation of keratinocyte motility by transforming growth factor- $\alpha$  (TGF- $\alpha$ ) relative to epidermal growth factor (EGF)*. Journal of Investigative Dermatology, 1996. **106**(4): p. 590-597.
154. Koopman, G., et al., *Annexin V for flow cytometric detection of phosphatidylserine expression on B cells undergoing apoptosis*. Blood, 1994. **84**(5): p. 1415-20.
155. Riccardi, C. and I. Nicoletti, *Analysis of apoptosis by propidium iodide staining and flow cytometry*. Nat Protoc, 2006. **1**(3): p. 1458-61.
156. Mykhaylyk, O., et al., *Silica-iron oxide magnetic nanoparticles modified for gene delivery: a search for optimum and quantitative criteria*. Pharm Res, 2012. **29**(5): p. 1344-65.
157. Jarzebinska, A., et al., *A Single Methylene Group in Oligoalkylamine-Based Cationic Polymers and Lipids Promotes Enhanced mRNA Delivery*. Angew Chem Int Ed Engl, 2016. **55**(33): p. 9591-5.
158. Nicoletti, I., et al., *A rapid and simple method for measuring thymocyte apoptosis by propidium iodide staining and flow cytometry*. J Immunol Methods, 1991. **139**(2): p. 271-9.
159. Van der Jeught, K., et al., *Intratumoral administration of mRNA encoding a fusokine consisting of IFN-beta and the ectodomain of the TGF-beta receptor II potentiates antitumor immunity*. Oncotarget, 2014. **5**(20): p. 10100-13.
160. Lory, S., S. Carroll, and R. Collier, *Ligand interactions of diphtheria toxin. II. Relationships between the NAD site and the P site*. Journal of Biological Chemistry, 1980. **255**(24): p. 12016-12019.
161. Bruce, C., et al., *Diphtheria toxin and its ADP-ribosyltransferase-defective homologue CRM197 possess deoxyribonuclease activity*. Proc Natl Acad Sci U S A, 1990. **87**(8): p. 2995-8.
162. Qiao, J., K. Ghani, and M. Caruso, *Diphtheria toxin mutant CRM197 is an inhibitor of protein synthesis that induces cellular toxicity*. Toxicon, 2008. **51**(3): p. 473-7.
163. Kimura, Y., et al., *Transgenic mice expressing a fully nontoxic diphtheria toxin mutant, not CRM197 mutant, acquire immune tolerance against diphtheria toxin*. J Biochem, 2007. **142**(1): p. 105-12.
164. Talbot, U.M., J.C. Paton, and A.W. Paton, *Protective immunization of mice with an active-site mutant of subtilase cytotoxin of Shiga toxin-producing Escherichia coli*. Infect Immun, 2005. **73**(7): p. 4432-6.
165. Morinaga, N., et al., *Subtilase cytotoxin, produced by Shiga-toxigenic Escherichia coli, transiently inhibits protein synthesis of Vero cells via degradation of BiP and induces cell cycle arrest at G1 by downregulation of cyclin D1*. Cell Microbiol, 2008. **10**(4): p. 921-9.
166. Morinaga, N., et al., *Two distinct cytotoxic activities of subtilase cytotoxin produced by shiga-toxigenic Escherichia coli*. Infect Immun, 2007. **75**(1): p. 488-96.
167. Chen, J.K., et al., *Identification of amino acid residues of abrin-a A chain is essential for catalysis and reassociation with abrin-a B chain by site-directed mutagenesis*. Protein Eng, 1997. **10**(7): p. 827-33.
168. Kochi, S.K. and R.J. Collier, *DNA fragmentation and cytolysis in U937 cells treated with diphtheria toxin or other inhibitors of protein synthesis*. Exp Cell Res, 1993. **208**(1): p. 296-302.
169. Kageyama, T., et al., *Diphtheria toxin mutant CRM197 possesses weak EF2-ADP-ribosyl activity that potentiates its anti-tumorigenic activity*. J Biochem, 2007. **142**(1): p. 95-104.
170. Qu, X. and L. Qing, *Abrin induces HeLa cell apoptosis by cytochrome c release and caspase activation*. J Biochem Mol Biol, 2004. **37**(4): p. 445-53.
171. Chang, M.P., et al., *Internucleosomal DNA cleavage precedes diphtheria toxin-induced cytolysis. Evidence that cell lysis is not a simple consequence of translation inhibition*. J Biol Chem, 1989. **264**(26): p. 15261-7.

## References

172. Ramakrishnan, S., et al., *Vascular endothelial growth factor-toxin conjugate specifically inhibits KDR/flk-1-positive endothelial cell proliferation in vitro and angiogenesis in vivo*. *Cancer Res*, 1996. **56**(6): p. 1324-30.
173. Prabhu, A., et al., *Targeting the unfolded protein response in glioblastoma cells with the fusion protein EGF-SubA*. *PLoS One*, 2012. **7**(12): p. e52265.
174. Bhutia, S.K., et al., *Abrus abrin derived peptides induce apoptosis by targeting mitochondria in HeLa cells*. *Cell Biol Int*, 2009. **33**(7): p. 720-7.
175. Komatsu, N., T. Oda, and T. Muramatsu, *Involvement of both caspase-like proteases and serine proteases in apoptotic cell death induced by ricin, modeccin, diphtheria toxin, and pseudomonas toxin*. *J Biochem*, 1998. **124**(5): p. 1038-44.
176. Morimoto, H. and B. Bonavida, *Diphtheria toxin- and Pseudomonas A toxin-mediated apoptosis. ADP ribosylation of elongation factor-2 is required for DNA fragmentation and cell lysis and synergy with tumor necrosis factor-alpha*. *J Immunol*, 1992. **149**(6): p. 2089-94.
177. Chang, M.P., et al., *Second cytotoxic pathway of diphtheria toxin suggested by nuclease activity*. *Science*, 1989. **246**(4934): p. 1165-8.
178. Lessnick, S.L., et al., *Localization of diphtheria toxin nuclease activity to fragment A*. *J Bacteriol*, 1992. **174**(6): p. 2032-8.
179. Brinkmann, U., et al., *Role of CAS, a human homologue to the yeast chromosome segregation gene CSE1, in toxin and tumor necrosis factor mediated apoptosis*. *Biochemistry*, 1996. **35**(21): p. 6891-9.
180. Ogryzko, V.V., et al., *Antisense inhibition of CAS, the human homologue of the yeast chromosome segregation gene CSE1, interferes with mitosis in HeLa cells*. *Biochemistry*, 1997. **36**(31): p. 9493-500.
181. Kim, H.E., et al., *PHAPI, CAS, and Hsp70 promote apoptosome formation by preventing Apaf-1 aggregation and enhancing nucleotide exchange on Apaf-1*. *Mol Cell*, 2008. **30**(2): p. 239-47.
182. Varol, B., et al., *The cytotoxic effect of diphtheria toxin on the actin cytoskeleton*. *Cell Mol Biol Lett*, 2012. **17**(1): p. 49-61.
183. Thorburn, J., A.E. Frankel, and A. Thorburn, *Apoptosis by leukemia cell-targeted diphtheria toxin occurs via receptor-independent activation of Fas-associated death domain protein*. *Clin Cancer Res*, 2003. **9**(2): p. 861-5.
184. Matsuura, G., et al., *Novel subtilase cytotoxin produced by Shiga-toxigenic Escherichia coli induces apoptosis in vero cells via mitochondrial membrane damage*. *Infect Immun*, 2009. **77**(7): p. 2919-24.
185. Wolfson, J.J., et al., *Subtilase cytotoxin activates PERK, IRE1 and ATF6 endoplasmic reticulum stress-signalling pathways*. *Cell Microbiol*, 2008. **10**(9): p. 1775-86.
186. Novoa, I., et al., *Feedback inhibition of the unfolded protein response by GADD34-mediated dephosphorylation of eIF2alpha*. *J Cell Biol*, 2001. **153**(5): p. 1011-22.
187. Sano, R. and J.C. Reed, *ER stress-induced cell death mechanisms*. *Biochim Biophys Acta*, 2013. **1833**(12): p. 3460-70.
188. Saxena, N., P. Yadav, and O. Kumar, *The Fas/Fas ligand apoptotic pathway is involved in abrin-induced apoptosis*. *Toxicol Sci*, 2013. **135**(1): p. 103-18.
189. Bhutia, S.K., et al., *Inhibitory effect of Abrus abrin-derived peptide fraction against Dalton's lymphoma ascites model*. *Phytomedicine*, 2009. **16**(4): p. 377-85.
190. Shih, S.F., et al., *Abrin triggers cell death by inactivating a thiol-specific antioxidant protein*. *J Biol Chem*, 2001. **276**(24): p. 21870-7.
191. Bora, N., S. Gadadhar, and A.A. Karande, *Signaling different pathways of cell death: Abrin induced programmed necrosis in U266B1 cells*. *Int J Biochem Cell Biol*, 2010. **42**(12): p. 1993-2003.
192. Zong, W.X. and C.B. Thompson, *Necrotic death as a cell fate*. *Genes Dev*, 2006. **20**(1): p. 1-15.
193. Silva, M.T., *Secondary necrosis: the natural outcome of the complete apoptotic program*. *FEBS Lett*, 2010. **584**(22): p. 4491-9.
194. Pappenheimer, A.M., Jr., *Diphtheria toxin*. *Annu Rev Biochem*, 1977. **46**: p. 69-94.

## References

195. Ye, J., et al., *ER stress induces cleavage of membrane-bound ATF6 by the same proteases that process SREBPs*. Mol Cell, 2000. **6**(6): p. 1355-64.
196. Yang, F., et al., *Modulation of the unfolded protein response is the core of microRNA-122-involved sensitivity to chemotherapy in hepatocellular carcinoma*. Neoplasia, 2011. **13**(7): p. 590-600.
197. Smrekar, B., et al., *Tissue-dependent factors affect gene delivery to tumors in vivo*. Gene Ther, 2003. **10**(13): p. 1079-88.
198. Yamate, J., et al., *Establishment and characterization of transplantable tumor line (KB) and cell lines (KB-P and KB-D8) from a rat thymus-derived dendritic cell sarcoma*. Virchows Arch, 2002. **440**(6): p. 616-26.
199. Rossin, R., et al., *<sup>64</sup>Cu-labeled folate-conjugated shell cross-linked nanoparticles for tumor imaging and radiotherapy: synthesis, radiolabeling, and biologic evaluation*. J Nucl Med, 2005. **46**(7): p. 1210-8.
200. Amit, D., et al., *Development of targeted therapy for bladder cancer mediated by a double promoter plasmid expressing diphtheria toxin under the control of IGF2-P3 and IGF2-P4 regulatory sequences*. Int J Clin Exp Med, 2011. **4**(2): p. 91-102.
201. Ramnath, V., G. Kuttan, and R. Kuttan, *Antitumour effect of abrin on transplanted tumours in mice*. Indian J Physiol Pharmacol, 2002. **46**(1): p. 69-77.
202. Brown, B.D., et al., *Endogenous microRNA regulation suppresses transgene expression in hematopoietic lineages and enables stable gene transfer*. Nat Med, 2006. **12**(5): p. 585-91.
203. De Geest, B.R., S.A. Van Linthout, and D. Collen, *Humoral immune response in mice against a circulating antigen induced by adenoviral transfer is strictly dependent on expression in antigen-presenting cells*. Blood, 2003. **101**(7): p. 2551-6.
204. Lagos-Quintana, M., et al., *Identification of tissue-specific microRNAs from mouse*. Curr Biol., 2002. **12**(9): p. 735-739.
205. Tsai, W.C., et al., *MicroRNA-122 plays a critical role in liver homeostasis and hepatocarcinogenesis*. J Clin Invest, 2012. **122**(8): p. 2884-97.
206. Suzuki, T., et al., *miR-122a-regulated expression of a suicide gene prevents hepatotoxicity without altering antitumor effects in suicide gene therapy*. Mol Ther, 2008. **16**(10): p. 1719-26.
207. Nakabayashi, H., et al., *Growth of human hepatoma cells lines with differentiated functions in chemically defined medium*. Cancer Res, 1982. **42**(9): p. 3858-63.
208. Tian, W., et al., *High-throughput functional microRNAs profiling by recombinant AAV-based microRNA sensor arrays*. PLoS One, 2012. **7**(1): p. e29551.
209. Chai, S., et al., *Regulatory role of miR-142-3p on the functional hepatic cancer stem cell marker CD133*. Oncotarget, 2014. **5**(14): p. 5725-35.
210. Wu, C., et al., *Combinatorial control of suicide gene expression by tissue-specific promoter and microRNA regulation for cancer therapy*. Mol Ther, 2009. **17**(12): p. 2058-66.
211. Harel, L., et al., *Novel expression vectors enabling induction of gene expression by small-interfering RNAs and microRNAs*. PLoS One, 2014. **9**(12): p. e115327.
212. Cawood, R., et al., *Use of tissue-specific microRNA to control pathology of wild-type adenovirus without attenuation of its ability to kill cancer cells*. PLoS Pathog, 2009. **5**(5): p. e1000440.
213. Freeman, S.M., et al., *The "bystander effect": tumor regression when a fraction of the tumor mass is genetically modified*. Cancer Res, 1993. **53**(21): p. 5274-83.
214. Frankel, A.E., et al., *Cell-specific modulation of drug resistance in acute myeloid leukemic blasts by diphtheria fusion toxin, DT388-GMCSF*. Bioconjug Chem, 1998. **9**(4): p. 490-6.
215. Martin, S., et al., *Targeting GRP78 to enhance melanoma cell death*. Pigment Cell Melanoma Res, 2010. **23**(5): p. 675-82.
216. Palucka, A.K. and L.M. Coussens, *The Basis of Oncoimmunology*. Cell, 2016. **164**(6): p. 1233-47.
217. Guo, Z.S., Z. Liu, and D.L. Bartlett, *Oncolytic Immunotherapy: Dying the Right Way is a Key to Eliciting Potent Antitumor Immunity*. Front Oncol, 2014. **4**: p. 74.
218. Ghiringhelli, F., et al., *CD4+CD25+ regulatory T cells suppress tumor immunity but are sensitive to cyclophosphamide which allows immunotherapy of established tumors to be curative*. Eur J Immunol, 2004. **34**(2): p. 336-44.

## References

219. Ghiringhelli, F., et al., *Metronomic cyclophosphamide regimen selectively depletes CD4+CD25+ regulatory T cells and restores T and NK effector functions in end stage cancer patients*. *Cancer Immunol Immunother*, 2007. **56**(5): p. 641-8.
220. Pesonen, S., et al., *Oncolytic immunotherapy of advanced solid tumors with a CD40L-expressing replicating adenovirus: assessment of safety and immunologic responses in patients*. *Cancer Res*, 2012. **72**(7): p. 1621-31.
221. Cattaneo, R., et al., *Reprogrammed viruses as cancer therapeutics: targeted, armed and shielded*. *Nat Rev Microbiol*, 2008. **6**(7): p. 529-40.
222. Ciomber, A., et al., *Antitumor effects of recombinant antivascular protein ABRaA-VEGF121 combined with IL-12 gene therapy*. *Archivum immunologiae et therapiae experimentalis*, 2014. **62**(2): p. 161-168.
223. Cunningham, D., et al., *Perioperative chemotherapy versus surgery alone for resectable gastroesophageal cancer*. *New England Journal of Medicine*, 2006. **355**(1): p. 11-20.

## Supplements

**Table S 1: Toxin and control sequences ordered by GeneArt®.** Sequences for the three toxin constructs SubA, DTA and AA (ST, DT, AT) and their corresponding nonfunctional (SN, DN, AN) and untranslatable (SU, DU, AU) controls were produced by GeneArt as DNA strings in two parts. The nucleotide sequences were optimized for expression in *homo sapiens* by GeneArt. The nonfunctional constructs show the same sequence as the toxin constructs but for one or two point mutations (small letters) were introduced in order to completely inhibit or to reduce the proteins capability to block translation [83, 145, 146, 148]. The untranslatable constructs show the same sequence as the toxin constructs, but the Kozak element [1] was scrambled (**bold**) and the start as well as all in frame downstream ATGs mutated into TAGs. Sequences were cloned into a pVAX1-A120 [20] backbone at the *KpnI* site (see table S2) by seamless cloning (homologous recombination). Underlined parts represent homology regions between part 1 and part 2. Italic parts represent homology regions between insert (part 1 or part 2) and the backbone. Bold and underlined sequences represent the KDEL amino acid sequence (compare section 2.2.2).

	Sequence ordered by GeneArt	NCBI GenBank
ST, part 1	TAAACTTAAGCTTGGTACGCCACCATGCTGAAGATCCTGTGGACCTACATCCTGTTTCTGCTGTTCA TCAGCGCCAGCGCCAGAGCCGAGAAGCCCTGGTACTTTGACGCCATCGGCCTGACCGAGACAACC ATGTCCCTGACCGACAAGAACACCCCGTGGTGGTGTCCGTGGTGGATAGCGGCGTGGCCTTTAT CGGCGGCTGAGCGATAGCGAGTTCGCCAAGTTCAGCTTACCCAGGACGGCAGCCATTCCCCG TGAAGAAGTCCGAGGCCCTGTACATCCACGGCACCGCCATGGCTAGCCTGATCGCCAGCAGATAC GGCATCTACGGCGTGTACCCACGCCCTGATCAGCAGCAGAAGAGTGATCCCCGACGGCGTGCA GGACAGCTGGATCAGAGCCATCGAGTCTATTATGAGCAACGTGTTCTGGCCCTGGCGAGGAAA AGATCATCAACATCTCTGGCGGCCAGAAAGCGTGGCCAGCGCTTCTGTGTGGACCGAGCTGCTG AGCCGGATGGGCCGGAACAACGACAGACTGATTGTGGCCCGTGGGCAACGACGGCGCCGACA TTAGAAAGCTGAGCGCCAGCAGCGGATCTGGCCTGCCGCTTATACCCTGTGTCAGCGTGAAC AAAAAGCAGGACCCCGTATCCGGGTGGCCGCCCTGGCCAGTAT	AF399919.3
ST, part 2	CCGGGTGGCCCGCTGGCCAGTATAGAAAGGGCGAGACACCCGTGCTGCACGGCGGAGGAATC ACCGCAGCAGATTTGGCAACAACCTGGGTGGACATTGCCGCCCTGGCCAGAATATCACCTTCT GAGGCCCGACGCCAAGACCGGCACAGGCTCTGGAACATCTGAGGCCACCGCCATCGTGTCTGGC GTGCTGGCCGCTATGACCAGCTGCAACCCTAGAGCCACAGCCACCGAGCTGAAGCGGACCCGTCT GGAAAGCGCCGACAAGTACCCAGCCTGGTGGACAAAGTGACCGAGGGCAGAGTCTGAACGCC GAGAAGGCCATCAGCATGTTCTGCAAGAAAACTACATCCCCGTGCGGCAGGGCCGGATGAGCG AGGAACTG <b>AAGGACGAGCTG</b> TGACGAGCTCGGATCCACTAG	AF399919.3
SN, part 1	TAAACTTAAGCTTGGTACGCCACCATGCTGAAGATCCTGTGGACCTACATCCTGTTTCTGCTGTTCA TCAGCGCCAGCGCCAGAGCCGAGAAGCCCTGGTACTTTGACGCCATCGGCCTGACCGAGACAACC ATGTCCCTGACCGACAAGAACACCCCGTGGTGGTGTCCGTGGTGGATAGCGGCGTGGCCTTTAT CGGCGGCTGAGCGATAGCGAGTTCGCCAAGTTCAGCTTACCCAGGACGGCAGCCATTCCCCG TGAAGAAGTCCGAGGCCCTGTACATCgcccGACCGCCATGGCTAGCCTGATCGCCAGCAGATAC GGCATCTACGGCGTGTACCCACGCCCTGATCAGCAGCAGAAGAGTGATCCCCGACGGCGTGCA GGACAGCTGGATCAGAGCCATCGAGTCTATTATGAGCAACGTGTTCTGGCCCTGGCGAGGAAA AGATCATCAACATCTCTGGCGGCCAGAAAGCGTGGCCAGCGCTTCTGTGTGGACCGAGCTGCTG AGCCGGATGGGCCGGAACAACGACAGACTGATTGTGGCCCGTGGGCAACGACGGCGCCGACA TTAGAAAGCTGAGCGCCAGCAGCGGATCTGGCCTGCCGCTTATACCCTGTGTCAGCGTGAAC AAAAAGCAGGACCCCGTATCCGGGTGGCCGCCCTGGCCAGTAT	Altered [83, 145] from AF399919.3
SN, part 2	CCGGGTGGCCCGCTGGCCAGTATAGAAAGGGCGAGACACCCGTGCTGCACGGCGGAGGAATC ACCGCAGCAGATTTGGCAACAACCTGGGTGGACATTGCCGCCCTGGCCAGAATATCACCTTCT GAGGCCCGACGCCAAGACCGGCACAGGCTCTGGAACAgcccGAGGCCACCGCCATCGTGTCTGGCG TGCTGGCCGCTATGACCAGCTGCAACCCTAGAGCCACAGCCACCGAGCTGAAGCGGACCCGTCTG GAAAGCGCCGACAAGTACCCAGCCTGGTGGACAAAGTGACCGAGGGCAGAGTCTGAACGCCG AGAAGGCCATCAGCATGTTCTGCAAGAAAACTACATCCCCGTGCGGCAGGGCCGGATGAGCGA GAAACTG <b>AAGGACGAGCTG</b> TGACGAGCTCGGATCCACTAG	Altered from AF399919.3

Supplements

	Sequence ordered by GeneArt	NCBI GenBank
SU, part 1	TAAACTTAAGCTTGGTAC <b>CCGCACT</b> AGCTGAAGATCCTGTGGACCTACATCCTGTTTCTGCTGTTCA TCAGCGCCAGCGCCAGAGCCGAGAAGCCCTGGTACTTTGACGCCATCGGCCTGACCGAGACAACC TAGTCCCTGACCGACAAGAACACCCCGTGGTGGTGTCCGTGGTGGATAGCGGCCTGGCCTTTAT CGCGCGCTGAGCGATAGCGAGTTCGCCAAGTTCAGCTTCACCCAGGACGGCAGCCATTCCCGG TGAAGAAGTCCGAGGCCCTGTACATCCACGGCACCGCCTAGGCTAGCCTGATCGCCAGCAGATAC GGCATCTACGGCGTGTACCCACGCGCCTGATCAGCAGCAGAAGAGTGATCCCGACGGCGTGCA GGACAGCTGGATCAGAGCCATCGAGTCTATTTAGAGCAACGTGTTCTGGCCCTGGCGAGGAAA AGATCATCAACATCTCTGGCGGCCAGAAAGCGTGGCCAGCGCTTCTGTGTGGACCGAGCTGCTG AGCCGGTAGGGCCGAACAACGACAGACTGATTGTGGCCCGTGGGCAACGACGGCGCCGACA TTAGAAAGCTGAGCGCCAGCAGCGGATCTGCCTGCCGTTATCACCTGTGTCAGCGTGAAC AAAAAGCAGGACCCCGTAT <u>CCGGGTGGCCCGCTGGCCAGTAT</u>	Altered from AF399919.3
SU, part 2	<u>CCGGGTGGCCCGCTGGCCAGTATAGAAAGGGCGAGACACCCGTGTCACGCGGGAGGAATC</u> ACCGCAGCAGATTTGGCAACAACCTGGGTGGACATTGCCCGCCCTGGCCAGAATATCACCTTCT GAGGCCCGACGCCAAGACCGGCACAGGCTCTGGAACATCTGAGGCCACCGCCATCGTGTCTGGC GTGCTGGCCGCTTAGACCAGCTGCAACCTAGAGCCACAGCCACCGAGCTGAAGCGGACCCGTCT GGAAAGCGCCGACAAGTACCCAGCCTGGTGGACAAAGTGACCGAGGGCAGAGTGCTGAACGCC GAGAAGGCCATCAGCTAGTTCTGCAAGAAAACTACATCCCGTGCGGCAGGGCCGGTAGAGCG AGGAAGTGAAGGACGAGCTGTGACGAGCTCGGATCCACTAG	Altered from AF399919.3
DT, part 1	TAAACTTAAGCTTGGTACGCCACCATGGGCGCCGACGACGTGGTGGACAGCAGCAAGAGCTTCGT GATGGAAAACTCAGCAGCTACCACGGCACCAAGCCGGCTACGTGGACTCCATCCAGAAGGGAA TCCAGAAGCCCAAGAGCGGCACCCAGGGCAACTACGACGACACTGGAAGGGCTTCTACAGCAC CGACAACAATACGACGCCGCTGCTACAGCGTGGACAACGAGAATCCCTGAGCGGCAAAGCC GGCGGAGTCGTGAAAGTGACCTACCCCGCCTGACCAAGGTGCTGG	K01722.1
DT, part 2	<u>CCCCGGCCTGACCAAGGTGCTGGCCCTGAAGGTGGACAATGCCGAGACAATCAAGAAAGAGCTG</u> GGCCTGAGCCTGACCGAGCCCTGATGGAACAAGTGGGCACCGAAGAGTTCATCAAGAGATTCTG GCGACGGCCAGCCGGTGGTGTCTCTGCTTTTGGCAGGGCAGCAGCAGCGTGGAGTA CATCAACAACCTGGGAGCAGGCCAAGCCCTGAGCGTGGAACTGGAATCAACTTCGAGACACGG GGCAAGCGGGGCCAGGACGCTATGTACGAGTATATGGCCAGGCCTGCGCCGGCAACAGAGTGC GGAGATAACGAGCTCGGATCCACTAG	K01722.1
DN, part 1	TAAACTTAAGCTTGGTACGCCACCATGGGCGCCGACGACGTGGTGGACAGCAGCAAGAGCTTCGT GATGGAAAACTCAGCAGCTACCACGGCACCAAGCCGGCTACGTGGACTCCATCCAGAAGGGAA TCCAGAAGCCCAAGAGCGGCACCCAGGGCAACTACGACGACACTGGAAGgagTTCTACAGCACC GACAACAATACGACGCCGCTGGCTACAGCGTGGACAACGAGAATCCCTGAGCGGCAAAGCCG GCGGAGTCGTGAAAGTGACCTA <u>CCCCGGCCTGACCAAGGTGCTGG</u>	Altered [148] from K01722.1
DN, part 2	<u>CCCCGGCCTGACCAAGGTGCTGGCCCTGAAGGTGGACAATGCCGAGACAATCAAGAAAGAGCTG</u> GGCCTGAGCCTGACCGAGCCCTGATGGAACAAGTGGGCACCGAAGAGTTCATCAAGAGATTCTG GCGACGGCCAGCCGGTGGTGTCTCTGCTTTTGGCAGGGCAGCAGCAGCGTGGAGTA CATCAACAACCTGGGAGCAGGCCAAGCCCTGAGCGTGGAACTGGAATCAACTTCGAGACACGG GGCAAGCGGGGCCAGGACGCTATGTACGAGTATATGGCCAGGCCTGCGCCGGCAACAGAGTGC GGAGATAACGAGCTCGGATCCACTAG	K01722.1
DU, part 1	TAAACTTAAGCTTGGTAC <b>CCGCACT</b> AGGGCGCCGACGACGTGGTGGACAGCAGCAAGAGCTTCGT GTAGGAAAACTCAGCAGCTACCACGGCACCAAGCCGGCTACGTGGACTCCATCCAGAAGGGAA TCCAGAAGCCCAAGAGCGGCACCCAGGGCAACTACGACGACACTGGAAGGGCTTCTACAGCAC CGACAACAATACGACGCCGCTGGCTACAGCGTGGACAACGAGAATCCCTGAGCGGCAAAGCC GGCGGAGTCGTGAAAGTGACCTA <u>CCCCGGCCTGACCAAGGTGCTGG</u>	Altered from K01722.1

Supplements

	Sequence ordered by GeneArt	NCBI GenBank
DU, part 2	<u>CCCCGGCCTGACCAAGGTGCTGGCCCTGAAGGTGGACATAGCCGAGACAATCAAGAAAGAGCTGGCCTGAGCCTGACCGAGCCCTGTAGGAACAAGTGGGCACCGAAGAGTTCATCAAGAGATTGCGCGACGGCGCCAGCCGGTGGTGTCTCTGCTTTTGCCGAGGGCAGCAGCAGCGTGGAGTACATCAACAACCTGGGAGCAGGCCAAGGCCCTGAGCGTGGAACTGGAAATCAACTTCGAGACACGGGGCAAGCGGGCCAGGACGCTTAGTACGAGTATTAGGCCAGGCCTGCGCCGGCAACAGAGTGGGAGATAACGAGCTCGGATCCACTAG</u>	Altered from K01722.1
AT, part 1	<u>TAAACTTAAGCTTGGTACGCCACCATGGAAGATCGGCCATCAAGTTCAGCACCGAGGGCGCCAC AAGCCAGAGCTACAAGCAGTTCATCGAGGCCCTGAGAGAGCGGCTGAGAGGCGGCCTGATCCAC GACATTCCTGCTGCCTGACCCACACCTGCAGGAACGGAACCGGTACATCACCGTGGAACT GAGCAACAGCGACACCGAGAGCATCGAAGTGGGCATCGACGTGACCAACGCCTACGTGGTGGCC TACAGAGCCGGAACCCAGTCTACTTCTGAGGGACGCCCTAGCAGCGCCAGCGACTATCTGTTC ACCGGCACCGACCAGCACAGCCTGCCTTTCTACGGCACCTACGGCGACCTGGAAGATGGGCCCA CCAGA</u>	AY458627.1
AT, part 2	<u>AAAGATGGGCCACCAGAGCAGACAGCAGATCCCACTGGGACTGCAGGCCCTGACACACGGCAT CAGCTTTTTCAGAAGCGGCGGCAACGACAACGAGGAAAAGGCCCGACCTGATCGTGATCATCC AGATGGTGGCCGAGGCCCGCAGATTCGTTACATCTCCAACAGAGTGCGGGTGCCATCCAGACA GGCACCGCCTTTAGCCCGACGCCCATGATCAGCCTGAAAAACAACCTGGGACAACCTGAGCAG AGGCGTGCAGGAATCCGTGCAGGACACATTCGGAACCAAGTGACCCTGACCAACATCCGGAACG AGCCCGTATCGTGGACAGCCTGAGCCACCCTACAGTGGCCGTGCTGGCCCTGATGCTGTTGCTG TGCAACCCCCCAACTGACGAGCTCGGATCCACTAG</u>	AY458627.1
AN, part 1	<u>TAAACTTAAGCTTGGTACGCCACCATGGAAGATCGGCCATCAAGTTCAGCACCGAGGGCGCCAC AAGCCAGAGCTACAAGCAGTTCATCGAGGCCCTGAGAGAGCGGCTGAGAGGCGGCCTGATCCAC GACATTCCTGCTGCCTGACCCACACCTGCAGGAACGGAACCGGTACATCACCGTGGAACT GAGCAACAGCGACACCGAGAGCATCGAAGTGGGCATCGACGTGACCAACGCCTACGTGGTGGCC TACAGAGCCGGAACCCAGTCTACTTCTGAGGGACGCCCTAGCAGCGCCAGCGACTATCTGTTC ACCGGCACCGACCAGCACAGCCTGCCTTTCTACGGCACCTACGGCGACCTGGAAGATGGGCCCA CCAGA</u>	AY458627.1
AN, part 2	<u>AAAGATGGGCCACCAGAGCAGACAGCAGATCCCACTGGGACTGCAGGCCCTGACACACGGCAT CAGCTTTTTCAGAAGCGGCGGCAACGACAACGAGGAAAAGGCCCGACCTGATCGTGATCATCC AGATGGTGGCCGcGCGCCctgTTTCGGTACATCTCCAACAGAGTGCGGGTGCCATCCAGACAG GCACCGCCTTTAGCCCGACGCCCATGATCAGCCTGAAAAACAACCTGGGACAACCTGAGCAGA GCGTGCAGGAATCCGTGCAGGACACATTCGGAACCAAGTGACCCTGACCAACATCCGGAACGA GCCCGTATCGTGGACAGCCTGAGCCACCCTACAGTGGCCGTGCTGGCCCTGATGCTGTTGCTGT GCAACCCCCCAACTGACGAGCTCGGATCCACTAG</u>	Altered [146] from AY458627.1
AU, part 1	<u>TAAACTTAAGCTTGGTACCCGCACTAGGAAGATCGGCCATCAAGTTCAGCACCGAGGGCGCCAC AAGCCAGAGCTACAAGCAGTTCATCGAGGCCCTGAGAGAGCGGCTGAGAGGCGGCCTGATCCAC GACATTCCTGCTGCCTGACCCACACCTGCAGGAACGGAACCGGTACATCACCGTGGAACT GAGCAACAGCGACACCGAGAGCATCGAAGTGGGCATCGACGTGACCAACGCCTACGTGGTGGCC TACAGAGCCGGAACCCAGTCTACTTCTGAGGGACGCCCTAGCAGCGCCAGCGACTATCTGTTC ACCGGCACCGACCAGCACAGCCTGCCTTTCTACGGCACCTACGGCGACCTGGAAGTAGGGCCCA CCAGA</u>	Altered from AY458627.1
AU, part 2	<u>AAAGTAGGGGCCACCAGAGCAGACAGCAGATCCCACTGGGACTGCAGGCCCTGACACACGGCAT CAGCTTTTTCAGAAGCGGCGGCAACGACAACGAGGAAAAGGCCCGACCTGATCGTGATCATCC AGTAGGTGGCCGAGGCCCGCAGATTCGTTACATCTCCAACAGAGTGCGGGTGCCATCCAGACA GGCACCGCCTTTAGCCCGACGCCCATGATCAGCCTGAAAAACAACCTGGGACAACCTGAGCAG AGGCGTGCAGGAATCCGTGCAGGACACATTCGGAACCAAGTGACCCTGACCAACATCCGGAACG AGCCCGTATCGTGGACAGCCTGAGCCACCCTACAGTGGCCGTGCTGGCCCTGATGCTGTTGCTG TGCAACCCCCCAACTGACGAGCTCGGATCCACTAG</u>	Altered from AY458627.1

## Supplements

**Table S 2: Sequence of the vector pVAX1-A120.** The sequence is cut at the NotI site (as was done for linearization prior cmRNA production). Bold letters indicate the KpnI digestion site where the sequences from table S1 were incorporated by seamless cloning. The underlined part represents the homology region between the backbone and part 1. *Italic parts* represent homology regions between part 2 and the backbone. Small letters indicate the T7 promoter.

<p>pVAX1-A120 [20]</p>	<pre> GGCCGCTCGAGTCTAGAGGGCCCGTTAAACCCGCTGATCAGCCTCGACTGTGCCTTCTAGTTGCCAGCCATCT GTTGTTTGCCCTCCCCCGTGCCTTCTTGACCCTGGAAGGTGCCACTCCACTGTCTTTCTAATAAAAATGAG GAAATTGCATCGCATTGTCTGAGTAGGTGTCATTCTATTCTGGGGGTGGGGTGGGGCAGGACAGCAAGGGG GAGGATTGGGAAGACAATAGCAGGCATGCTGGGGATGCGGTGGGCTCTATGGCTTCTACTGGCGGTTTTAT GGACAGCAAGCGAACCGAATTGCCAGCTGGGGCGCCCTCTGGTAAGTTGGGAAGCCCTGCAAAGTAAACT GGATGGCTTTCTCGCCCAAGGATCTGATGGCGCAGGGGATCAAGCTCTGATCAAGAGACAGGATGAGGAT CGTTTCGCATGATTGAACAAGATGGATTGCACGCAGGTTCTCCGGCCGCTTGGGTGGAGAGGCTATTCGGCTA TGACTGGGCACAACAGACAATCGGCTGCTCTGATGCCGCCGTGTTCCGGCTGTCAGCGCAGGGGGCGCCCGTT CTTTTTGTCAAGACCGACTGTCCGGTGCCCTGAATGAACTGCAAGACGAGGCAGCGCGGCTATCGTGGCTGG CCACGACGGGGCTTCTTGCGCAGCTGTGCTCGACGTTGCTACTGAAGCGGGAAGGGACTGGCTGCTATTGGG CGAAGTGCCGGGGCAGGATCTCTGTCACTCACCTTGCTCTGCCGAGAAGTATCCATCATGCGGATGGCAA TGCGGGGCTGCATACGCTTGATCCGGCTACCTGCCATTGACCAACGAAACATCGCATCGAGCGAGC ACGTA CTGGATGGAAGCCGGTCTTGTCGATCAGGATGATCTGGACGAAGAGCATCAGGGGCTCGGCCAGC CGAACTGTTCCGAGGCTCAAGGGCAGCATGCCGACGGCGAGGATCTCGTCTGACCCATGGCGATGCTGCTG TTGCCGAATATCATGGTGGAAAATGGCCGTTTTCTGGATTTCGACTGTGGCCGGCTGGGTGTGGCGGACC GCTATCAGGACATAGCGTTGGCTACCCGTGATATTGCTGAAGAGCTTGGCGGCGAATGGGCTGACCGCTTCT CGTGCTTTACGGTATCGCCGCTCCCGATTGCGAGCGCATCGCTTCTATCGCTTCTTGACGAGTTCTTCTGAAT TATTAACGCTTACAATTTCTGATGCGGATTTTTCTCCTTACGCATCTGTGCGGATTTTACACCCGCATACAGTG GCACTTTTCGGGGAAATGTGCGCGGAACCCCTATTTGTTTTATTTTTCTAAATACATTCAAATATGTATCCGCTCAT GAGACAATAACCCGTATAAATGCTTCAATAATAGCACGTGCTAAACTTCATTTTTAATTTAAAGGATCTAGGT GAAGATCCTTTTTGATAATCTCATGACCAAAATCCCTAACGTGAGTTTTCGTTCCACTGAGCGTCAGACCCCGT AGAAAAGATCAAAGGATCTTCTTGAGATCCTTTTTCTGCGGTAATCTGCTGCTGCAAAACAAAAAACACC GCTACCAGCGGTGTTTTGTTGGCGGATCAAGAGCTACCAACTCTTTTTCCGAAGGTAAGTGGCTTCAAGCAGAG CGCAGATACCAAACTGTCCTTCTAGTGTAGCCGTAGTTAGGCCACCACTCAAGAACTCTGTAGCACCAGCCTA TACCTCGCTCTGCTAATCCTGTTACCAGTGGCTGCTGCCAGTGGCGATAAGTCGTCTTACCGGGTTGGAG TCAAGACGATAGTTACCGGATAAAGCGCAGCGGTCGGGCTGAACGGGGGTTCTGTCACACAGCCAGCTTG GAGCGAACGACCTACACCGAACTGAGATACCTACAGCGTGAGCTATGAGAAAGCGCCACGCTTCCGAAGGGA GAAAGGCGGACAGGTATCCGGTAAGCGGCAGGGTCGGAACAGGAGAGCGCAGGGAGCTTCCAGGGGG AAACGCCTGGTATCTTTATAGTCTGTGCGGTTTCGCCACCTGACTTGAGCGTCAATTTTGTGATGCTCGTC AGGGGGGGCGGAGCCTATGGAAAAACGCCAGCAACGCGCCCTTTTTACGGTTCTGGGCTTTTGTGCGCCTTT GCTCACATGTTCTTGACTCTTCGCGATGTACGGGCCAGATATACGCGTTGACATTGATTATTGACTAGTTATTA TAGTAATCAATTACGGGGTCATTAGTTCATAGCCCATATATGGAGTTCCGCGTTACATAACTACGGTAAATGGC CCGCTGGCTGACCGCCCAACGACCCCGCCATTGACGTCATAAATGACGTATGTTCCCATAGTAACGCCAAT AGGGACTTTCCATTGACGTC AATGGGTGGACTATTTACGGTAAACTGCCACTTGGCAGTACATCAAGTGTATC ATATGCCAAGTACGCCCTATTGACGTCAATGACGGTAAATGGCCCGCTGGCATTATGCCAGTACATGACC TTATGGGACTTTCTACTTGGCAGTACATCTACGTATTAGTCATCGCTATTACCATGGTGATGGGTTTTGGCAG TACATCAATGGGCGTGATAGCGTTTTGACTCACGGGATTTCCAAGTCTCCACCCATTGACGTCAATGGGAG TTGTTTTGGCACCAAAATCAACGGGACTTTCCAAAATGTCGTAACAACCTCCGCCCATTTGACGCAAAATGGGCG GTAGGCGGTACGGTGGGAGGTCTATATAAGCAGAGCTCTCTGGCTAACTAGAGAACCCACTGCTTACTGGCTT ATCGAAAATaatacgactcactatagggAGACCCAAGCTGGCTAGCGTTTAAACTTAAGCTTGGT<b>ACC</b>GAGCTCGGATC CACTAGTCCAGTGTGGTGAAATTCGCAGAA AA AAAAGC </pre>
----------------------------	--

Publication

## Publication

Parts of this thesis have already been published as listed below:

Hirschberger K., Jarzebinska, A., Kessel E., Kretschmann V., Aneja M. K., Dohmen C., Hermann-Janson A., Wagner E., Plank C., Rudolph C., *Exploring Cytotoxic mRNAs as a Novel Class of Anti-cancer Biotherapeutics*. Molecular Therapy-Methods & Clinical Development, 2018. **8**: p. 141-151.

## Acknowledgements

### Acknowledgements

The work presented in this thesis would not have been possible without the support of many people.

First of all I want to thank my first supervisor Prof. Dr. Christian Plank and my mentor PD Dr. Carsten Rudolph for the opportunity to perform the work at Ethris GmbH. It was great to be part of the company and to gain insight into non-academical research.

Moreover, I am grateful to Christian for supervising me as a doctoral student and for his support through-out the time of my studies, including the planning and discussion of experiments. Likewise, I owe thanks to Carsten for his help and contribution, not least for the publication of the paper.

Also, I am grateful to my second supervisor, Prof. Dr. Michael W. Pfaffl, for his input regarding the progress and the results of my work.

My thanks furthermore go to Prof. Dr. Percy A. Knolle for the opportunity to join in his weekly research seminar at the Institute of Molecular Immunology and Experimental Oncology at TU Munich.

I am particularly grateful to Dr. Verena Kretschmann. In addition to our weekly meetings she was at any time supportive and ready to give advice while encouraging my independence and enabling me to learn as much as possible. Especially, I want to thank her for her help and input regarding the design and analysis of experiments, the detailed discussion of results and their implications for future work and the writing of the paper.

Special thanks also go to Dr. Manish K. Aneja. Having supervised my master thesis and the beginning of my doctoral thesis, he continued his support through-out my entire work. Most of all, I am grateful for his help concerning the design and the cloning of the mRNA constructs and his input to the paper.

Furthermore, I want to thank Prof. Dr. Ernst Wagner, Dr. Daniela Emrich, Dr. Anita Jarzebinska, Dr. Eva Kessel, Dr. Christian Dohmen, Dr. Annika Hermann-Janson and Katrin Lindner for the cooperative work regarding the *in vivo* experiment. I especially thank Dani for her input to and proof-reading of the paper and Christian in addition for his help concerning the design of the miRNA constructs.

## Acknowledgements

Moreover, I want to thank the whole RNA Immunology group (Verena, Dani, Simone, Katrin, Selia and Tobi), always kind, supportive and patiently listening to and joining in the discussions regarding my project.

Similarly, I am grateful to the entire Ethris team, in particular for the great and friendly atmosphere. Everyone was always more than willing to share his or her knowledge and experience, inside and outside of the lab, and thereby supported me in my progress. Besides, I want to thank Dr. Olga Mykhailyk for providing me with magnetic nanoparticles.

Also, I thank Dr. Nina Böttinger for her help regarding the xCELLigence experiment.

Last, but of course most importantly, I want to thank my family and friends for their help and support in numerous ways.



# Eidesstattliche Erklärung

Ich erkläre an Eides statt, dass ich die bei der promotionsführenden Einrichtung  
Fakultät für Medizin

der TUM zur Promotionsprüfung vorgelegte Arbeit mit dem Titel:  
Development of cytotoxic mRNAs as a new class of anti-cancer biotherapeutics

in

Fakultät, Institut, Lehrstuhl, Klinik, Krankenhaus, Abteilung

unter der Anleitung und Betreuung durch: Prof. Dr. Christian Plank ohne sonstige Hilfe erstellt und bei der Abfassung nur die gemäß § 6 Ab. 6 und 7 Satz 2 angebotenen Hilfsmittel benutzt habe.

Ich habe keine Organisation eingeschaltet, die gegen Entgelt Betreuerinnen und Betreuer für die Anfertigung von Dissertationen sucht, oder die mir obliegenden Pflichten hinsichtlich der Prüfungsleistungen für mich ganz oder teilweise erledigt.

Ich habe die Dissertation in dieser oder ähnlicher Form in keinem anderen Prüfungsverfahren als Prüfungsleistung vorgelegt.

Die vollständige Dissertation wurde in \_\_\_\_\_ veröffentlicht. Die promotionsführende Einrichtung

\_\_\_\_\_ hat der Veröffentlichung zugestimmt.

Ich habe den angestrebten Doktorgrad noch nicht erworben und bin nicht in einem früheren Promotionsverfahren für den angestrebten Doktorgrad endgültig gescheitert.

Ich habe bereits am \_\_\_\_\_ bei der Fakultät für \_\_\_\_\_  
\_\_\_\_\_ der Hochschule \_\_\_\_\_  
unter Vorlage einer Dissertation mit dem Thema \_\_\_\_\_  
\_\_\_\_\_ die Zulassung zur Promotion beantragt mit dem Ergebnis: \_\_\_\_\_

Die öffentlich zugängliche Promotionsordnung der TUM ist mir bekannt, insbesondere habe ich die Bedeutung von § 28 (Nichtigkeit der Promotion) und § 29 (Entzug des Doktorgrades) zur Kenntnis genommen. Ich bin mir der Konsequenzen einer falschen Eidesstattlichen Erklärung bewusst.

Mit der Aufnahme meiner personenbezogenen Daten in die Alumni-Datei bei der TUM bin ich

einverstanden,  nicht einverstanden.

München, 11.01.2018, Kristin Hirschberger

Ort, Datum, Unterschrift